

STRUCTURAL AND KINEMATIC SYNTHESIS OF OVERCONSTRAINED MECHANISMS

**A Thesis Submitted to
the Graduate School of Engineering and Sciences of
İzmir Institute of Technology
in Partial Fulfillment of the Requirements for the Degree of**

DOCTOR OF PHILOSPHY

in Mechanical Engineering

**by
Özgün SELVİ**

**January 2012
İZMİR**

We approve the thesis of **Özgün SELVİ**

Prof. Dr. Sc. Rasim ALİZADE
Supervisor

Prof. Dr. Oktay PASHAEV
Committee Member

Assist. Prof. Dr. M. İ. Can DEDE
Committee Member

Prof. Dr. Marco CECCARELLI
Committee Member

Assist. Prof. Dr. Fatih Cemal CAN
Committee Member

18 January 2012

Prof. Dr. Metin TANOĞLU
Head of the Department of
Mechanical Engineering

Prof. Dr. R. Tuğrul SENGER
Dean of the Graduate School of
Engineering and Sciences

Learn from yesterday, live for today, hope for tomorrow.

The important thing is not to stop questioning...

Albert EINSTEIN

ACKNOWLEDGEMENTS

I would like to express my appreciation to my supervisor Prof. Dr. Sc. Rasim ALIZADE for his endless support and trust, encourage, ideas and comments throughout the all steps of this study. I would like to acknowledge to my parents for their support and patience and thanks to my dearest friends for their moral support. I would like to express my gratitude to Prof. Marco CECCARELLI for his support during my stay in Italy.

ABSTRACT

STRUCTURAL AND KINEMATIC SYNTHESIS OF OVERCONSTRAINED MECHANISMS

Investigation on overconstrained mechanisms needs attention especially in the structural synthesis. Knowing overconstrained conditions and including them in the design process will help creating manipulators with less degree of freedom (DoF) and more rigidity. Also this knowledge of overconstrained conditions will clarify concept of mobility of the parallel manipulators. Another subject, kinematic synthesis of overconstrained mechanisms, is important because it will allow describing a function, path, or motion with less DoF less number of joints. The aim of this thesis is to describe a generalized approach for structural synthesis and creation of new overconstrained manipulators and to describe a potentially generalizable approach for function and motion generation synthesis of overconstrained mechanism.

Moreover, screw theory is investigated as a mathematical base for defining kinematics of overconstrained mechanisms. Also, overconstrained mechanisms are investigated and generation of new mechanisms is introduced with examples. Some mathematical models for the subspace geometries are given. A method for defining overconstrained simple structural groups is introduced and extended to design of manipulators with examples and solid drawings. Linear approximation and least squares approximation methods are used for the function generation and motion generation of overconstrained 6R mechanisms.

A gap of describing overconstrained manipulators is filled in the area of structural synthesis. A general methodology is described for structural synthesis, mobility and motion calculations of overconstrained manipulators using simple structural groups. A potentially generalizable method for the kinematic synthesis of overconstrained manipulators is described both for function and motion generation.

ÖZET

KISITLI MEKANİZMALARIN YAPISAL VE KİNEMATİK SENTEZİ

Kısıtlı mekanizmaların özellikle yapısal sentezi için incelenme gerekliliği vardır. Kısıtlı mekanizmaların kısıtlılık koşullarını bilinmesi ve bu koşulları tasarım aşamasında kullanılması daha az serbestlikli ve daha dayanıklı manipülatörlerin tasarlanmasını sağlar. Ayrıca bu kısıtlı koşul bilgisi paralel manipulatörlerin mobilite konusunu da aydınlatacaktır. Kısıtlı mekanizmaların kinematik sentezi bu mekanizmalarla yani daha az mafsal sayısına sahip olan mekanizmalarla bir fonksiyon, yol yada hareket yaratımının sağlanabilmesine yardımcı olur.

Bu tezin amacı, kısıtlı manipulatörlerin tasarlanabilmesi için gereken genel bir yöntem tanımlamak ve ayrıca kısıtlı mekanizmalar için geliştirilebilecek bir fonksiyon ve hareket sentezi yöntemi tanımlamaktır. Bu amaca yönelik olarak kısıtlı mekanizmaların kinematik olarak incelenmesi için vida teorisi kullanılmış ve birim vida dönüşüm matrisi yöntemi geliştirilmiştir. Ayrıca bilinen kısıtlı mekanizmalar incelenmiş ve bu mekanizmalar kullanılarak yeni kısıtlı mekanizmalar yaratmak için bir yöntem verilmiş ve uygulanmıştır. Kısıtlı manipulatörlerin yapısal sentezi için gereken basit yapısal grupların tanımlanması için gerekli formüller verilmiş ve örneklendirilmiştir. Kinematik sentez için ise interpolasyon yaklaşımı ve en küçük karaler yaklaşımı altı mafsalı kısıtlı mekanizmaların fonksiyon ve hareket sentezlerine uygulanmıştır.

Böylelikle kısıtlı mekanizmaların yapısal sentezi, mobilite ve hareket hesapları için vida teorisi ve basit yapısal gruplar kullanılarak genel bir metodoloji anlatılmıştır. Ayrıca kısıtlı mekanizmalar için hem fonksiyon yaratım sentezi hem de hareket yaratım sentezi üzerine genellenebilecek bir kinematik sentez yöntemi açıklanmıştır.

TABLE OF CONTENTS

LIST OF FIGURES	x
LIST OF TABLES	xiii
CHAPTER 1. INTRODUCTION	1
1.1. Literature Survey for Structural Synthesis of Parallel Manipulators.....	2
1.2. Literature Survey for Kinematic Synthesis of Parallel Mechanisms.....	5
1.3. Kinematic Bonding and Representation of Joints.....	7
1.4. Research on Structural and Kinematic Synthesis of Parallel Mechanisms	8
CHAPTER 2. THEORY OF SCREWS	10
2.1. Screw Coordinates	11
2.2. Method of Unit Transformation Matrix for the Calculations of Recurrent Screws	12
2.2.1. Recurrent Unit Vectors	13
2.2.2. Transformation of Screw Systems in Space	15
2.2.3. Transformation Matrix of Screw Systems	16
2.2.4. Transformation Screw Matrix Position Analysis.....	17
2.2.5. Screw Matrix Velocity and Acceleration Analyses	19
2.2.6. Robot Actuator Force Analysis.....	24
2.3. Reciprocity and Virtual Work.....	26
2.4. Screw Systems	27
2.4.1. Operation on Screw Systems	28
2.5. Structural Analysis of Parallel Mechanisms with Theory of Screws	28
CHAPTER 3. GEOMETRY ANALYSIS OF SUBSPACES.....	31
3.1. Generation of Overconstrained Mechanisms by Using Mechanisms in Lower Subspaces	33
3.1.1. Overconstrained Mechanisms in Subspace $\lambda=2$	34
3.1.2. Overconstrained Mechanisms in Subspace $\lambda=3$	36

3.1.3. Overconstrained Mechanisms in Subspace $\lambda=4$	37
3.2. Combination of Subspaces.....	38
3.2.1. Combined Overconstrained Mechanisms in Subspace $\lambda=3$	39
3.2.2. Combined Overconstrained Mechanisms in Subspace $\lambda=4$	41
3.2.3. Combined Overconstrained Mechanisms in Subspace $\lambda=5$	44
3.3. Mathematical Models of Overconstrained Subspaces	50
3.3.1. Intersection of Two Non-Parallel Planes with Sphere.....	50
3.3.2. Intersection of Two Spheres with a Plane	53
3.3.3. Intersection of Three Spheres	54
3.3.4. Intersection of Plane and Sphere	55
CHAPTER 4. STRUCTURAL SYNTHESIS OF OVERCONSTRAINED MANIPULATORS	57
4.1. Degree of Screw and Mathematical Models of Kinematic Pairs.....	57
4.2. Novel Mobility Equation of Mechanisms.....	62
4.3. Simple Overconstrained Structural Groups	63
4.4. Simple Overconstrained Structural Groups with General Constraint One.....	64
4.5. Simple Overconstrained Structural Groups with General Constraint Two	69
4.6. Structural Design of Overconstrained Parallel Manipulators	72
CHAPTER 5. KINEMATIC SYNTHESIS OF PARALEL MECHANISMS	76
5.1. Kinematic Synthesis of Overconstrained Mechanisms	76
5.1.1. Function Generation Synthesis with Double Spherical Mechanism.....	77
5.1.2. Function Generation Synthesis with Planar Spherical Mechanism.....	85
5.1.3. Motion Generation Synthesis of Planar Spherical Mechanism	93
5.2. Kinematic Synthesis of Multi Loop Platform Mechanisms.....	97

CHAPTER 6. AN EXPERIMENTAL CHARACTERIZATION OF EARTHQUAKE EFFECTS ON MECHANISM OPERATION BY USING A PARALLEL MANIPULATOR	107
6.1. Earthquake Motion Characteristics.....	108
6.2. Operation of Mechanisms	110
6.2.1. An Example with A Slider Crank Mechanism	111
6.2.2. An Example with A Leg Mechanism	112
6.3. An Experimental Evaluation.....	114
6.4. Experimental Tests with Prototypes	119
6.4.1. Slider Crank Actuated with Dc Motor.....	120
6.4.2. Slider Crank Actuated by Servo Motor	121
6.4.3. Leg Mechanism.....	122
6.4.4. LARM Hand	123
6.4.5. Vehicle Model.....	124
6.5. Results of Tests and Considerations for Characterization	125
6.5.1. Slider Crank	126
6.5.1.1. Actuation by Dc Motor.....	126
6.5.1.2. Actuation by Servo Motor	127
6.5.2. LARM Hand	128
6.5.3. Leg Mechanism.....	129
6.5.4. Vehicle Model.....	130
 CHAPTER 7. CONCLUSION	 132
 REFERENCES	 133

LIST OF FIGURES

<u>Figure</u>	<u>Page</u>
Figure 1.1. Kinematic bonding for mechanisms.....	8
Figure 2.1. Line coordinates of a screw	11
Figure 2.2. Three recurrent unit vectors in space.	13
Figure 2.3. Four recurrent unit screws in space	15
Figure 2.4. Link and joint parameters.....	19
Figure 2.5. 7R spatial linkage	22
Figure 2.6. Wrench and twist acting on a rigid body.....	27
Figure 2.7. Twist system for one leg of a parallel manipulator	29
Figure 2.8. Screw systems of a manipulator.....	30
Figure 3.1. Combined six-bar mechanisms; a) Planar-planar, b) Planar-spherical	34
Figure 3.2. Combination of two spherical four bar mechanism.	39
Figure 3.3. Intersection of two non-parallel planes with sphere.....	51
Figure 3.4. Intersection of two spheres and a plane.....	53
Figure 3.5. Intersection of three spheres.....	54
Figure 3.6. Intersection of plane and sphere	56
Figure 4.1. Simple structural group with one platform and three legs in $\lambda=5$	68
Figure 4.2. Simple structural group with two platform and four legs in $\lambda=5$	69
Figure 4.3. Two platform structural group with general constraint two.....	71
Figure 4.4. Simple structural group with one platform and three legs in $\lambda=4$	71
Figure 4.5. Three DoF manipulator with one platform in $\lambda=5$	73
Figure 4.6. Four DoF manipulator with two platforms in $\lambda=5$	74
Figure 4.7. Three DoF manipulator with one platform in $\lambda=4$	74
Figure 4.8. Four DoF manipulator with two platforms in $\lambda=4$	75
Figure 5.1. Double spherical six bar linkage	78
Figure 5.2. Double spherical mechanism as two spherical four bar linkages with unit vector axes.	78
Figure 5.3. Designed double spherical six bar mechanism.....	84
Figure 5.4. a) Designed and desired functions of first spherical linkage, b) Error of first spherical linkage.....	85
Figure 5.5. a) Designed and desired functions of 6R linkage, b) Error of 6R linkage ...	85

Figure 5.6. Planar-spherical six bar linkage.	86
Figure 5.7. Planar-spherical mechanism shown as a planar and a spherical four bar linkages with screw axes.....	86
Figure 5.8. Designed planar-spherical six bar mechanism	92
Figure 5.9. a) Designed and desired function of planar linkage, b) Error of planar linkage.....	92
Figure 5.10. a) Designed and desired output functions of spherical linkage, b) Error of spherical linkage.....	93
Figure 5.11. Screw placement for the planar-spherical mechanism.	94
Figure 5.12. Three desired positions for the designed planar-spherical manipulator.....	97
Figure 5.13. Parameters of RS-RS-CS parallel mechanism	98
Figure 5.14. Designed parallel mechanism with three objective points	106
Figure 6.1. Basic characteristics of seismic waves; a) Compression and expansion waves, b) Transversal waves, c) Types of seismograms	109
Figure 6.2. A test-bed slider-crank mechanism; a) Kinematic parameters, b) Slider accelerations with stationary frame (43 rpm)	112
Figure 6.3. Leg mechanism; a) Kinematic parameters, b) Rickshaw robot.....	113
Figure 6.4. Acceleration of point A along x direction with stationary frame; a) 150 rpm, b) 257 rpm	114
Figure 6.5. An experimental setup at LARM with the slider-crank mechanism	114
Figure 6.6. CaPaMan platform with accelerometer sensors; a) Scheme, b) Sensor locations, c) Sensor installation, d) Test lay-out.....	115
Figure 6.7. Control system layout for CaPaMan as an earthquake simulator.	116
Figure 6.8. Typical characteristics of simulate earthquake	117
Figure 6.9. Accelerometer data during earthquake simulation.....	118
Figure 6.10. An example of acceleration data during earthquake simulation; a) For platform center H, b) Angular platform velocity, c) Angular platform acceleration	119
Figure 6.11. A test-bed slider-crank mechanism at LARM; a) An experimental set up with accelerometer and weight on the slider, b) Sensing axes of the accelerometer.....	120
Figure 6.12. An experimental measure of the typical accelerations of the slider crank with stationary frame; a) Crank rotation 32 rpm, b) Crank rotation 43 rpm.....	120

Figure 6.13. A test-bed slider-crank mechanism with servo motor at LARM; a) An experimental set up with accelerometer on the slider, b) Sensing axes of the accelerometer	121
Figure 6.14. Experimental measures of slider crank with servo motor without earthquake effect; Torque data of the motor, acceleration of the slider with crank rotation; a) 90 rpm, b) 180rpm.....	122
Figure 6.15. A test-bed pantograph-chebyshev mechanism at LARM; a) An experimental set up with an accelerometer, b) Sensing axes of the accelerometer	122
Figure 6.16. An experimental measure of the typical accelerations of the leg mechanism without earthquake effect; a) Crank rotation 150 rpm, b) Crank rotation 257 rpm	123
Figure 6.17. LARM Hand; a) Prototype, b) Sensor locations	124
Figure 6.18. Model car with force and accelerometer sensors; a) Experimental setup with prototype b) Sensors and directions.....	125
Figure 6.19. An experimental measure of the typical forces on the model car without earthquake effect; a) Applied voltage 7v, b) Applied voltage 9v.....	125
Figure 6.20. An experimental measure of the typical accelerations with horizontal slider under earthquake effect (type 1); a) Crank rotation 32 rpm, b) Crank rotation 43 rpm	127
Figure 6.21. An experimental measure of the typical accelerations with vertical slider under earthquake effect (type 1); a) Crank rotation 32 rpm, b) Crank rotation 43 rpm	127
Figure 6.22. An experimental measure of slider crank with servo motor with earthquake effect (type 1), Torque data of the motor, acceleration of the slider with crank rotation; a) 90 rpm, b) 180 rpm	128
Figure. 6.23. Force data of LARM Hand during earthquake type 1.....	129
Figure 6.24. An experimental measure of the typical accelerations of the leg mechanism without earthquake effect; a) Crank rotation 150 rpm, b) Crank rotation 257 rpm	130
Figure 6.25. An experimental measure of forces on the model car with earthquake effect; a) Applied voltage 7v, b) Applied voltage 9v	130
Figure 6.26. Detailed view of the experimental measure of forces on the model car with earthquake effect; a) Applied voltage 7v, b) Applied voltage 9v.....	131

LIST OF TABLES

<u>Table</u>	<u>Page</u>
Table 1.1. Representation of joints and their connections	7
Table 3.1. Summary of rigid body motions in subspace $\lambda = 5$	32
Table 3.2. Summary of rigid body motions in subspace $\lambda = 4$	32
Table 3.3. Summary of rigid body motions in subspace $\lambda = 3$	33
Table 3.4. Summary of rigid body motions in subspace $\lambda = 2$	33
Table 3.5. Overconstrained mechanisms in $\lambda = 2$	35
Table 3.6. Overconstrained mechanisms in $\lambda = 3$	36
Table 3.7. Overconstrained mechanisms in $\lambda = 4$	38
Table 3.8. Combined overconstrained mechanisms in $\lambda = 3$	40
Table 3.9. Combined overconstrained mechanisms in $\lambda = 4$	41
Table 3.10. Combined overconstrained mechanisms in $\lambda = 5$	44
Table 4.1. Kinematic representations of kinematic pairs.....	59
Table 4.2. Distribution of conditions to joints of simple structural groups in $\lambda = 5$	65
Table 4.3. Simple structural groups with general constraint one.....	66
Table 4.4. Simple structural groups with multiple platforms	67
Table 4.5. Number of simple structural groups of $\lambda = 5$	68
Table 4.6. Distribution of conditions to joints of simple structural groups in $\lambda = 4$	69
Table 4.7. Simple structural groups with general constraint two	70
Table 4.8. Number of simple structural groups of $\lambda = 4$	71
Table 5.1. Design ranges of input output parameters	83
Table 5.2. Precision points used in the synthesis.....	84
Table 5.3. Ranges of parameters.....	91
Table 5.4. Precision points for the first linkage	91
Table 5.5. Precision points of the second linkage.....	91
Table 5.6. Parameters of the synthesis and construction	106
Table 6.1. The characteristics of simulated earthquakes	116
Table 6.2. Force data of the sensors on LARM hand while the platform is stable.....	124
Table 6.3. Experimental data from experimental tests with test-bed mechanisms.....	126

CHAPTER 1

INTRODUCTION

A robotic system can be defined as a re-programmable multi-functional manipulator that is designed to move materials, parts, tools or devices through variable programmed motions for desired tasks. Similar to machines, a robotic system is an assembly of one or more mechanisms with other electrical, hydraulic or pneumatic components. Mechanisms, which are vital parts of machines, are the combination of gears, cams, linkages, springs etc. Linkage systems are elementary subject in design of manipulators and can be defined as a collection of links that are connected with actuated free joints.

When a constraint is imposed in a space then movements of rigid body in this space are restricted and this new restricted space of rigid body is called its subspace of. Knowing constraints imposed by the linkages subspace and the motion of mechanisms can be described easily. A mechanism is called as overconstrained when it belongs to a subspace. Noting that the sum of subspace number and constraint number for a mechanism is always being equal to motions in spatial environment definition of structural mobility can be defined as the difference between total mobility of joints and the total of subspace numbers of independent loops in the system. A mechanism must always transmit mechanical motion. If mobility of a linkage system is zero then it will be defined as a structural group. Structural groups can be divided into simple structural groups. Simple structural groups are kinematic chains with zero degree of freedom and cannot be divided into other simple structural groups.

Investigation on overconstrained mechanisms needs attention especially in the structural synthesis. Knowing overconstrained conditions and including them in the design process will help creating manipulators with less DoF and more rigidity. Also this knowledge of overconstrained conditions will clarify the concept of mobility of the parallel manipulators. Another subject kinematic synthesis of overconstrained mechanisms is important because it will allow describing a function, path, or motion with less DoF and with overconstrained mechanisms less number of joints. The aim of this thesis is to describe a generalized approach for the structural synthesis and creation

of new overconstrained manipulators and to describe a potentially generalizable approach for the function and motion generation synthesis of overconstrained mechanism.

1.1. Literature Survey of Structural Synthesis of Parallel Manipulators

Studies of lower mobility parallel manipulators draw attention of both industry and academia in last two decades due to the fact that six motions in space are not always needed. Overconstrained manipulators have fewer links and joints and reduced complexity with higher stiffness properties. Because of overconstrained parallel manipulators' having lower mobility and being in lower subspaces task orientated design must be utilized which requires structural design.

Structural design of a parallel manipulator can be defined by determination of the specifications of the manipulator (number and type of joints, link and joint parameters and, mobility), intended to acquire end-effector motions, in space or subspaces and by using a synthesis method, fulfilling the conversion of input actuator motions to desired end-effector motions with least-singularity, sufficient workspace and minimum number of joints that supply with constraints of design as productibility, assemblability, redundancy and placement of actuators.

In the last decades, synthesis methods for structural design are interpreted such as screw theory, group theory, velocity loop equations, linear transformations theory and theory of structural groups. Screw theory uses six dimensional vector to describe the motion of a rigid body. In their researches Huang and Li (2002a, 2002b, 2003a, 2003b, 2003c) introduced a screw theory based method for the type synthesis of parallel manipulators. The proposed method can be summarized as finding constraints that are given to the end effector from limbs by using reciprocal screws. Lower mobility non-constrained and overconstrained manipulators are also revealed. Fang and Tsai (2002, 2004a, 2004b, 2004c) investigated 4 and 5 DoF parallel manipulators with identical limb structures and 3 DoF translational and rotational non-constrained and overconstrained manipulators by using theory of reciprocal screws. Kong and Gosselin (2001, 2004, 2006) proposed a way for the type synthesis of parallel manipulators using virtual chain approach with screw theory. In their investigations parallel manipulators with different type of motions are introduced. Jin et al. (2004) examined the structural

synthesis of parallel manipulators based on selective actuation by using screw algebra. As a result of their research, parallel manipulators with 3 DoF spherical motions, 3 DoF translational motions, 3DoF hybrid motions and 6 DoF spatial motions depending on the types of actuation are found. In the work of Frisoli et al.(2000), the results of examination of the end effector accelerations of the serial chains by means of screw algebra are applied to the synthesis of translating in-parallel actuation mechanisms. Carricato (2005) introduced a methodology that uses screw theory tools to synthesize desired forms for the direct and inverse Jacobian matrices of parallel manipulators and presented a novel family of fully isotropic parallel mechanisms with Schoenflies motion at the end effector. Glazunov (2010) described an approach for the synthesis of 6 DoF decoupled parallel manipulators based on closed screw groups which also avoid complicated equations by synthesis and singularity analysis of these mechanisms. At the end of their research decoupled manipulators with three, four and six DoF are obtained. Zhao et al. (2002a) investigated the type synthesis of spatial parallel mechanism with lower DoF based on the screw theory. Motions and constraints of mechanisms are also included in the design by the use of screw groups described in their research.

A non-empty set with a closed product operation is called a group where product operation satisfies conditions such as existence of one identity element and one inverse for any element and associativity. According to Lie's theory of continuous groups the set of rigid body motions is a six dimensional group of transformations which is represented by an operator acting on points of the three dimensional affine space. Group theory is also used by many authors for the structural design of parallel manipulators. Hervé and Sparacino (1991, 1993) investigated the type synthesis of parallel robots that generate translations by using the kinematic principle of displacement subgroups intersection of the group theory. In their study motion of the ends of the legs are assigned to same displacement groups and intersection of these sub-groups result in the end effector motion as a main displacement group. In the studies of Hervé (1999), group theory is used to define the method of composition and intersection of mechanical bonds and exemplified with 3 DoF parallel manipulators where platform has three translations and each leg is a subgroup of Schoenflies motions. Hervé (2003 2004) defined planar-spherical bond generators using these generators as legs using lie groups parallel manipulators are designed which depends on the relative positions of planes and sphere centers. Using group theory Karouia and Herve (2004a, 2004b) introduced structural synthesis of 3 DoF spherical parallel mechanisms with un-identical legs. Lee

and Hervé (2009) investigated the type synthesis of Schoenflies motion generators for future structural synthesis of parallel manipulators by using Lie groups. Also Lee and Hervé (2006) apply Lie group algebraic properties for the type synthesis of non-constrained translational parallel manipulators with limbs which generates Lie subgroup of three translations and two rotations. Refaat et al. (2006) examined one rotational two translational and one translational two rotational 3 DoF overconstrained parallel mechanisms using Lie group theory. Angeles (2002) applied the group theory algebra to the qualitative synthesis of parallel manipulators. In the research not only well known planar spherical subgroups but also cylindrical, two and three dimensional translation and Schoenflies subgroups are investigated. Π , Π^2 and Π^3 type joints are utilized for the type synthesis. A geometric theory used with group theory is proposed by Meng et al. (2005) for the analysis and synthesis of sub 6 DoF parallel manipulators and a procedure is given for the structural synthesis of parallel manipulators where desired end effector motions are in the form of Lie subgroup. In the study of Gao et al. (2002) methodology in the design of parallel manipulators based on Plücker coordinates is proposed. Rico et al. (2006) introduces a theory based on the analysis of the subsets and subgroups of the Euclidean group for type synthesis of 6 DoF and lower mobility platform manipulators.

Another method for structural synthesis of parallel manipulators is velocity loop equations. Using velocity that occurs in the loops of system and Jacobian, the mobility and singularities are defined and these are used in the synthesis of the structure of the manipulator. Gregorio and Parenti-Castelli (1999, 2002) applied this method for the analysis and synthesis of 3 DoF translational parallel manipulators. Theory of linear transformations is another method proposed by Gogu (2008). For the Structural synthesis, evolutionary morphology is used to design limbs, and platforms are designed by intersection of these limbs. The only investigations known to authors so far about structural synthesis of overconstrained parallel manipulators are done by Zhao et al. [2002b], Gogu (2008), and Kong and Gosselin (2007), Alizade et al. (2007a, 2010). An analytical method of using equivalent screw groups is proposed in the study of Zhao 3RRC, 3CPR, 3UPU/SPS and 4UPU mechanisms are exposed. The method proposed by Gogu is also applied to design overconstrained manipulators. Virtual chain approach based on screw theory is utilized in the work of Kong and Gosselin (2006).

Theory of structural groups is also a method for structural synthesis of parallel manipulators. A simple structural group is kinematic chain with zero degree of freedom

and cannot be divided into other simple structural groups. Manipulators are designed by adding actuated joints to these simple structural groups. Theory of simple structural groups is applied in the studies of Alizade et al. (2007a, 2007b, 2010). In the work of Alizade et al. (2007a, 2007b) new and revised methods for structural synthesis of serial platform manipulators, parallel Cartesian platform manipulators and Euclidean parallel manipulators are illustrated along with examples. By using simple structural groups of overconstrained subspace with general constraint one Alizade et al. (2010) researched structural design of parallel manipulators with general constraint one regarding angular and linear-angular conditions.

1.2. Literature Survey for Kinematic Synthesis of Parallel Mechanisms

During design of mechanisms for generation of a motion or obtaining a function by the input output relation kinematic synthesis problem has an important place. After a specific task is attached to a mechanism, type of the joints and geometry for the mechanism should be decided.

In the kinematic synthesis, construction parameters of the mechanism are used to define an objective such as a function or motion generation. In the function generation synthesis construction parameters builds a bridge between input and output of the mechanism.

The problem of function generation synthesis can be described as determination of construction parameters of a mechanism for a given input output relation. In literature, several methods such as algebraic complex numbers vector quaternion, bi-quaternion, matrix, screw and Cad based methods were developed for planar spherical and spatial four-bar mechanisms.

Levitskii (1946) introduced a polynomial equation which includes design parameters and input output variables. Design parameters are calculated using interpolation, least-square and Chebyshev approximation methods. Freudenstein (1954) presented the function generation of planar four-bar linkage by 3,4,5 points of exact approximation and higher order approximation. Zimmerman (1967) proposed an algorithm for the analytical function generation synthesis of spherical four-bar mechanisms for given four precision positions. Linear approximation is applied to polynomial functions for three, four and five precision positions on the spherical four-

bar mechanism in the works of Alizade (1994), Alizade and Kilit (2005), Alizade and Gezgin (2011), Farhang et al. (1988, 1999), Rao et al.(1973), Murray and McCarthy (1995).

Alizade and Kilit (2005) also developed a new methodology satisfying a specific constraint. This methodology, which has been called by the authors “MDA (minimum deviation area)” is a method for selection of the precision points on given function such that the deviation area between given and generated functions will be minimum. Alizade and Gezgin (2011) introduced a new function generation synthesis method for spherical four bar mechanism with six independent parameters. Interpolation, Chebyshev and least square approximation were used and error differences were compared with graphs. A synthesis method that uses a dimensional synthesis technique and local optimization was introduced by Sancibrian et al. (2007) and a new approach for three and four precision points exact synthesis was proposed by Cervantes-Sanchez et al. (2009) along with examples of spherical four-bar mechanism. Also Kazerounian and Solecki (1993) and Gupta and Beloiu (1998) presented additional conditions as rotability, branch and circuit defect elimination that can be controlled after the synthesis problem. Function generation of spatial mechanisms are investigated in the works of Rao et al. (1973), Wu and Chen (1997), Hartenberg and Denavit (1964), Dukkupati (2001), Sancibrian et al.(2007) and Cervantes-Sánchez et al. (2011).

Motion generation is the determination of construction parameters of a mechanism for a given link motion. Bottema and Roth (1979) used kinematic mappings to derive the kinematic constraint equations of the dyad using the components of dual quaternion. Bodduluri and McCarthy (1992) and Ravani and Roth (1983) investigated the constraint manifold of spherical RR dyad fitting for an arbitrary number of location. The branching problem in finite position synthesis of spherical four-bar mechanism was presented by McCarthy and Bodduluri (2000). On the other hand, method for approximating finite set of spatial locations with spherical orientations for spherical linkage was presented by Tse and Larochelle (2000). Additionally in this study, a new technique for approximate motion synthesis of spherical RR dyad and spherical 4R closed chains was presented. Larochelle et al. (1993) developed A CAD program, named SPHINX, for motion synthesis of spherical linkage. Larochelle (2003) investigated approximate motion synthesis for planar RR, spherical RR and spatial CC dyads and dual quaternion was used in the formulation of synthesis problem. A robust analytical solution for rigid body guidance synthesis of spherical mechanism is

presented by Al-Widyan and Angeles (2003). The motion synthesis of spherical 4R linkages for specified rigid body positions was studied by Ruth and McCarthy (1999) where spherical 4R linkage is designed by using SPHINXPC CAD program. In the study of Lee et al. (2009) the least-square method was used to solve the synthesis problem for not limited prescribed rigid-body positions for the motion generation of an adjustable spherical four-bar. The synthesis of two-phase adjustable spherical mechanism was illustrated along with a numerical example.

1.3. Representation of Joints and Kinematic Bonding

For the simplicity joint types and their relations are described as shown in Table (1.1). For example a planar four bar with prismatic joints (Figure 1.1.a) can be described by kinematic bonding as $\overline{\overline{RRRR}}$. Or a $\overline{\overline{RRRR}}\underline{\underline{RRR}}$ 7R mechanism (Figure 1.1.b) describes that four of the revolute joints are parallel to each other and the rest three is also parallel but in different direction with the first group. Moreover, if there are some intersections in the system (Figure 1.1.c), it is shown with a dot on the top or below. In a mechanism with bonding $\overline{\overline{RRRR}}\dot{\underline{\underline{RRR}}}$ have the same properties with $\overline{\overline{RRRR}}\underline{\underline{RRR}}$ mechanism but two of the recurrent revolute joints in the middle are intersecting.

Table 1.1. Representation of joints and their connections.

Symbol	Definition	Symbol	Definition	Symbol	Definition
R	Revolute joint	\overline{R}	R joints with parallel axes	$R \perp R$	Perpendicular axes
P	Prismatic Joint	\underline{R}	R joints with parallel axes	$R//P$	Parallel axes
H	Helical Joint	\overline{P}	P joints with parallel normal axes	$R = R$	Coincident axes
C	Cylindrical Joint	\underline{P}	P joints with parallel normal axes	$R \bullet R$	Intersecting axes
U	Universal Joint	\dot{R}	R joints with intersecting axes	$()_E$	Planar subspace
S	Spherical Joint	\ddot{R}	R joints with intersecting axes	$()_S$	Spherical subspace
E	Planar Joint	\hat{R}	Actuated joints	$()_{E-S}$	Planar-Spherical subspace

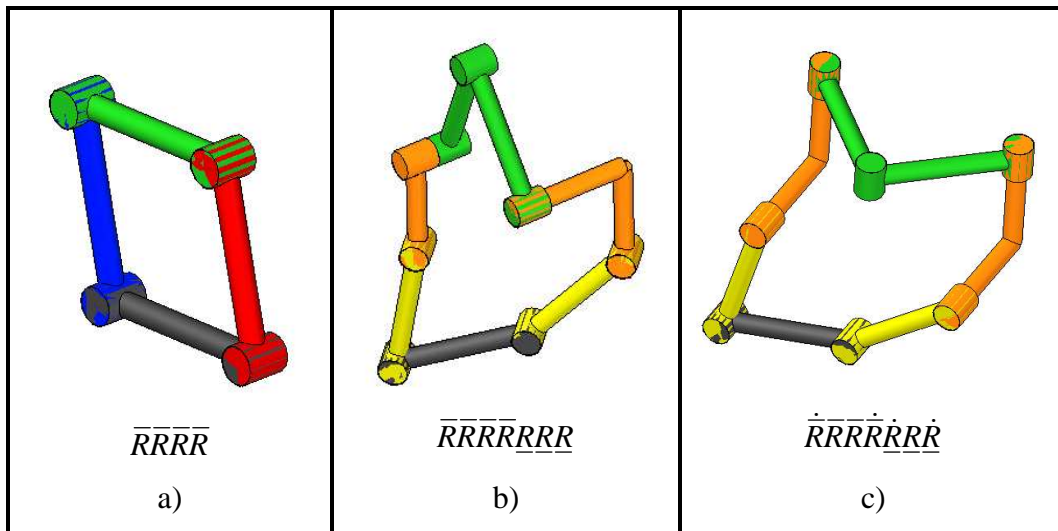


Figure 1.1. Kinematic bonding for mechanisms.

1.4. Research on Structural and Kinematic Synthesis of Parallel Mechanisms

During the investigations of this thesis, which is based on the structural and kinematic synthesis of overconstrained mechanisms, subject of structural synthesis of parallel manipulators and kinematic synthesis of mechanisms are examined. It is seen that research on structural synthesis of parallel mechanisms usually neglects overconstraint conditions of the loops of the manipulators. Including overconstrained conditions of the loops in the structural design of parallel manipulators is vital and also constraint conditions should be the basis for structural synthesis of overconstrained manipulators. For the kinematic synthesis side of the story, it is seen that in literature mostly planar, spherical or some kind of spatial mechanisms are used. To show the capabilities of overconstrained mechanism, kinematic synthesis is applied to some 6R mechanisms.

In the introduction part of this thesis, a literature survey for both structural and kinematic synthesis of mechanisms is given. Kinematic bonding of the joints, joint types and connection of links are tabulated with examples for simplicity and consistency along the thesis.

To apply kinematics and derive needed mathematical models, a tool is needed such as unit vector algebra, theory of screws, transformation matrices, quaternion, bi quaternion etc. Each method has its advantages and disadvantages. Because of the

simplicity, applicability, adaptability and improvability properties of the theory of screws is selected for kinematic calculations.

In the second Chapter of this thesis, definitions of the theory of screws are given such as twist, wrench, pitch etc. The screw and screw coordinates are defined in Cartesian space. A new method called method of unit transformation screw matrix for the calculation of recurrent screws is described. The use of this method for the position, velocity and acceleration analyses of mechanisms is shown. Also robot actuator force analysis is described. Explaining reciprocity and virtual work allowed describing screw systems. Describing operations on screw systems lead to structural analysis of parallel mechanisms using theory of screws.

After defining the rigid body motions in subspaces and their geometric relations in the third chapter, not only an intuitional method for generation of new overconstrained mechanisms in lower subspaces but also all possible mechanisms are listed. For defining the subspaces mathematically, the method to describe mathematical models of overconstrained subspaces is presented with examples.

Subsequent to the definition of all mathematical models of kinematic pairs and degree of screw, in the fourth Chapter novel mobility equation for mechanisms is given. Moreover, derivation of simple structural groups is shown with method for general constraint one and two with possible geometries. After the method for the structural synthesis of overconstrained parallel manipulators is presented along with examples for the calculation of mobility and motion of robot manipulators new formulations are given.

In Chapter five, kinematic synthesis of overconstrained mechanisms are shown for function generation of double spherical and planar spherical 6R linkages and motion generation for planar spherical 6R linkage for three positions. Also a synthesis method for a multi loop platform mechanism is shown with numerical example.

In the final section of this thesis, an experimental work on parallel manipulators is presented. Effects of earthquake disturbance on working of mechanisms are investigated by the help of a parallel robot.

CHAPTER 2

THEORY OF SCREWS

Three dimensional Euclidean space admits six motions for a rigid body with three translations and three rotations. Thus, displacement of a rigid body should be described by six independent parameters. Whatever the motion of the rigid body is according to the theorem of Chasles “any given displacement of a rigid body can be conceived by a rotation about an axis combined with a translation parallel to that axis”. Similarly, in the theorem by Poinot, any system of forces and moments applied to a rigid body can be uniquely replaced by a single force and couple in such a way that the single force is parallel to the axis of the couple. These two theorems form the basis of the theory of screws.

In the theory of screws, a screw is defined as a straight line in this rigid body whose points are displaced relative to a reference frame, and this screw will be coaxial with the line itself in any time. We denote the screw by a symbol \$ which is not an ordinary algebraic quantity; to specify it, five quantities are needed. Four of them are required to determine the position of the line and the fifth quantity is the pitch denoted by μ . The pitch of the screw is the ratio of the rotation to the translation during the displacement between two positions of the rigid body.

During an infinitesimally small displacement of the rigid body the screw remains the same as properties, but it is now referred as the instantaneous screw axis. Finite and infinitesimal displacements of rigid body are both called as twists about a screw. As the displacement of rigid body must be described by six independent parameters twist about a screw \$ is defined by five parameters from the definition of screw and a sixth quantity which is called the amplitude of the twist (α), which expresses the angle of the rotation around the line.

The definition wrench comes from the statement of Poinot. A wrench is used to describe the force and moment couple acting on the rigid body which is the simplification of all forces on the rigid body. The pitch of the wrench is taken as the ratio of the moment to the force applied to rigid body. To describe a wrench on screw \$ six parameters are needed. Five of which are required to describe the screw and sixth

where ω is the Clifford operator with property $\omega^2 = 0$.

Writing the screw in dual form, we get

$$\mathcal{S} = \begin{bmatrix} \mathbf{s} \\ \mathbf{s}_0 \end{bmatrix} = \begin{bmatrix} \mathbf{s} \\ \mathbf{r} \times \mathbf{s} + \mu \mathbf{s} \end{bmatrix}. \quad (2.2)$$

The pitch can be calculated from the parameters of the dual vector as

$$\mu = \frac{\mathbf{s} \cdot \mathbf{s}_0}{\mathbf{s} \cdot \mathbf{s}}. \quad (2.3)$$

According to this definition expanding Equation (2.2) with the components of vectors \mathbf{s} and \mathbf{u} gives the screw as

$$\mathcal{S} = [l \quad m \quad n \quad P^* \quad Q^* \quad R^*], \quad (2.4)$$

where $P^* = P + \mu l$, $Q^* = Q + \mu m$, $R^* = R + \mu n$, $P = -mz_1 + ny_1$, $Q = lz_1 - nx_1$ and $R = -ly_1 + mx_1$.

The values for the direction cosines as seen in Figure 2.1 will be $l = x_2 - x_1$, $m = y_2 - y_1$ and $n = z_2 - z_1$. The moments P^* , Q^* , R^* can be described in the form of parameters x_1, y_1, z_1 and μ with respect to direction cosines as

$$\begin{bmatrix} P^* \\ Q^* \\ R^* \end{bmatrix} = \begin{bmatrix} \mu & -z_1 & y_1 \\ z_1 & \mu & -x_1 \\ -y_1 & x_1 & \mu \end{bmatrix} \begin{bmatrix} l \\ m \\ n \end{bmatrix}. \quad (2.5)$$

2.2 Method of Unit Transformation Matrix for the Calculations of Recurrent Screws

In this section, a new method called method of unit transformation screw matrix for the calculation of recurrent screws is described. The description of the method starts

with the description of recurrent unit vectors in space. Recurrent unit vectors should be 90 degrees and consequent to each other.

2.2.1. Recurrent Unit Vectors

Three recurrent unit vectors are defined in space as shown in Figure 2.2.

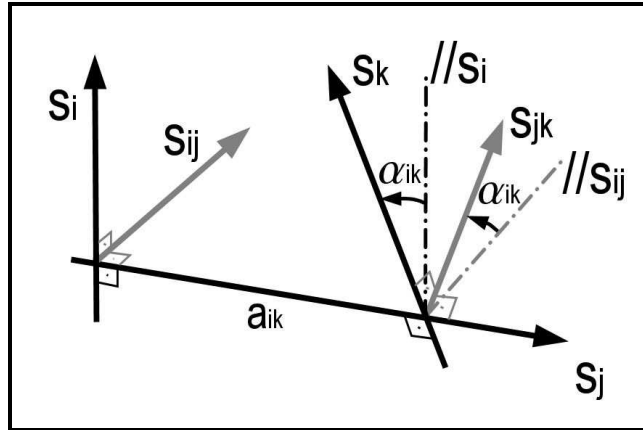


Figure 2.2. Three recurrent unit vectors in space.

Vector equations of three recurrent unit vectors s_i , s_j , s_k (Figure 2.2) can be described as

$$s_i \times s_k = s_j \sin \alpha_{ik}, \quad (2.6)$$

$$s_i \cdot s_k = \cos \alpha_{ik}, \quad (2.7)$$

$$s_j \cdot s_k = 0. \quad (2.8)$$

Multiplying both sides of Equation (2.6) with s_j we get

$$s_j \cdot (s_i \times s_k) = s_j \cdot s_j \sin \alpha_{ik}, \quad (2.9)$$

applying the rule of triple scalar product it becomes

$$(s_j \times s_i) \cdot s_k = \sin \alpha_{ik}. \quad (2.10)$$

If we define normal vector $(\mathbf{s}_j \times \mathbf{s}_i) = \mathbf{s}_{ij}$, where $\mathbf{s}_{ij} = (l_{ij}, m_{ij}, n_{ij})$ and $l_{ij} = m_j n_i - n_j m_i$, $m_{ij} = n_j l_i - l_j n_i$, $n_{ij} = l_j m_i - m_j l_i$ Equation (2.10) will be

$$\mathbf{s}_{ij} \cdot \mathbf{s}_k = \text{Sin } \alpha_{ik} . \quad (2.11)$$

Solving Equation (2.11) and Equation (2.7) with Equation (2.8) to describe vector \mathbf{s}_k we can find

$$\mathbf{s}_k = \mathbf{s}_i \text{Cos } \alpha_{ik} + \mathbf{s}_{ij} \text{Sin } \alpha_{ik} . \quad (2.12)$$

Equation (2.12) is the general equation to find the unit vector \mathbf{s}_k with given recurrent vectors \mathbf{s}_i and \mathbf{s}_j . We can write the conditions in equations (2.6-2.8) for \mathbf{s}_{jk} as $\mathbf{s}_{ij} \times \mathbf{s}_{jk} = \mathbf{s}_j \text{Sin } \alpha_{ij,jk}$, $\mathbf{s}_{ij} \cdot \mathbf{s}_{jk} = \text{Cos } \alpha_{ij,jk}$, $\mathbf{s}_j \cdot \mathbf{s}_{jk} = 0$ and write a general equation for transformation of unit vector system we can write an equation for \mathbf{s}_{jk} similar to Equation (2.12).

$$\mathbf{s}_{jk} = \mathbf{s}_{ij} \text{Cos } \alpha_{ij,jk} + \mathbf{s}_{i,j} \text{Sin } \alpha_{ij,jk} \quad (2.13)$$

The parameter $\alpha_{ij,jk} = \alpha_{ik}$ and vector $\mathbf{s}_{i,j} = -\mathbf{s}_i$ so Equation (2.13) will be

$$\mathbf{s}_{jk} = \mathbf{s}_{ij} \text{Cos } \alpha_{ik} - \mathbf{s}_i \text{Sin } \alpha_{ik} . \quad (2.14)$$

Writing Equation (2.14) and Equation (2.12) with conditions $\mathbf{s}_j = \mathbf{s}_j$ in matrix form we get the transformation matrix equation for recurrent unit vectors as

$$\begin{bmatrix} \mathbf{s}_j \\ \mathbf{s}_k \\ \mathbf{s}_{jk} \end{bmatrix} = \begin{bmatrix} 0 & 1 & 0 \\ \text{Cos } \alpha_{ik} & 0 & \text{Sin } \alpha_{ik} \\ -\text{Sin } \alpha_{ik} & 0 & \text{Cos } \alpha_{ik} \end{bmatrix} \cdot \begin{bmatrix} \mathbf{s}_i \\ \mathbf{s}_j \\ \mathbf{s}_{ij} \end{bmatrix} . \quad (2.15)$$

2.2.2. Transformation of Screw Systems in Space

Because of the analogue of vector systems to screw systems Equation (2.15) can be applied to screw systems by using dual angle formulations

$$\begin{aligned} \$ &= \mathbf{s} + \mathbf{s}_0 \omega \text{ and } \mathbf{A}_{ik} = \alpha_{ik} + \mathbf{a}_{ik} \omega, \\ \cos \mathbf{A}_{ik} &= \cos \alpha_{ik} - \omega \mathbf{a}_{ik} \sin \alpha_{ik}, \sin \mathbf{A}_{ik} = \sin \alpha_{ik} + \omega \mathbf{a}_{ik} \cos \alpha_{ik}, \end{aligned} \quad (2.16)$$

where $\omega^2 = 0$.

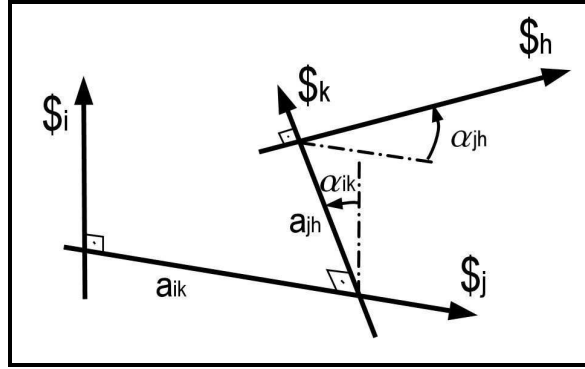


Figure 2.3. Four recurrent unit screws in space.

The screw transformation matrix equation for the unit screws as shown in Figure 2.3 is found as

$$\begin{bmatrix} \$_j \\ \$_k \\ \$_{jk} \end{bmatrix} = \begin{bmatrix} 0 & 1 & 0 \\ \cos \mathbf{A}_{ik} & 0 & \sin \mathbf{A}_{ik} \\ -\sin \mathbf{A}_{ik} & 0 & \cos \mathbf{A}_{ik} \end{bmatrix} \cdot \begin{bmatrix} \$_i \\ \$_j \\ \$_{ij} \end{bmatrix}. \quad (2.17)$$

Applying the same matrix equation for $\$_h$ with respect to $\$_j$ and $\$_k$ we get

$$\begin{bmatrix} \$_k \\ \$_h \\ \$_{kh} \end{bmatrix} = \begin{bmatrix} 0 & 1 & 0 \\ \cos \mathbf{A}_{jh} & 0 & \sin \mathbf{A}_{jh} \\ -\sin \mathbf{A}_{jh} & 0 & \cos \mathbf{A}_{jh} \end{bmatrix} \cdot \begin{bmatrix} \$_j \\ \$_k \\ \$_{jk} \end{bmatrix}. \quad (2.18)$$

Describing $[\$ _i \ \$ _j \ \$ _{ij}]^T = \mathbf{E}_i$, $[\$ _j \ \$ _k \ \$ _{jk}]^T = \mathbf{E}_j$ and $[\$ _k \ \$ _h \ \$ _{kh}]^T = \mathbf{E}_k$ and matrices for the screws as

$$\mathbf{T}_{ij} = \begin{bmatrix} 0 & 1 & 0 \\ \text{Cos } \mathbf{A}_{ik} & 0 & \text{Sin } \mathbf{A}_{ik} \\ -\text{Sin } \mathbf{A}_{ik} & 0 & \text{Cos } \mathbf{A}_{ik} \end{bmatrix} \text{ and } \mathbf{T}_{jk} = \begin{bmatrix} 0 & 1 & 0 \\ \text{Cos } \mathbf{A}_{jh} & 0 & \text{Sin } \mathbf{A}_{jh} \\ -\text{Sin } \mathbf{A}_{jh} & 0 & \text{Cos } \mathbf{A}_{jh} \end{bmatrix} .$$

The method for the calculations of screws can be defined recurrently

$$\left. \begin{array}{l} \mathbf{E}_j = \mathbf{T}_{ij} \mathbf{E}_i \\ \mathbf{E}_k = \mathbf{T}_{jk} \mathbf{E}_j \end{array} \right\} \mathbf{E}_k = \mathbf{T}_{jk} \mathbf{T}_{ij} \mathbf{E}_i \Rightarrow \mathbf{E}_k = \mathbf{T}_{ik} \mathbf{E}_i . \quad (2.19)$$

Operation shown in equations (2.18) defines the method of successive multiplications of matrices and application to screw transformations.

2.2.3. Transformation Matrix of Screw Systems

Substituting parameters of \$'s and A's from Equation (2.16) to Equation (2.17) will give us the vector matrix with parameters $\$ _k \{l_k \ m_k \ n_k \ P_k \ Q_k \ R_k \}$ as

$$\begin{aligned} \$ _k &= \$ _i \text{Cos} \mathbf{A}_{ik} + \$ _{ij} \text{Sin} \mathbf{A}_{ik} , \\ \$ _k &= (\text{Cos } \alpha_{ik} - \omega a_{ik} \text{Sin } \alpha_{ik}) (\mathbf{s}_i + \mathbf{s}_i^0 \omega) + (\text{Sin } \alpha_{ik} + \omega a_{ik} \text{Cos } \alpha_{ik}) (\mathbf{s}_{ij} + \mathbf{s}_{ij}^0 \omega) , \\ \mathbf{s}_k + \mathbf{s}_k^0 \omega &= \mathbf{s}_i \text{Cos } \alpha_{ik} + \mathbf{s}_{ij} \text{Sin } \alpha_{ik} + (\mathbf{s}_i^0 \text{Cos } \alpha_{ik} - \mathbf{s}_i a_{ik} \text{Sin } \alpha_{ik} + \mathbf{s}_{ij} a_{ik} \text{Cos } \alpha_{ik} + \mathbf{s}_{ij}^0 \text{Sin } \alpha_{ik}) \omega , \\ \mathbf{s}_k &= \mathbf{s}_i \text{Cos } \alpha_{ik} - \mathbf{s}_{ij} \text{Sin } \alpha_{ik} , \mathbf{s}_k^0 = \mathbf{s}_i^0 \text{Cos } \alpha_{ik} - \mathbf{s}_i a_{ik} \text{Sin } \alpha_{ik} + \mathbf{s}_{ij} a_{ik} \text{Cos } \alpha_{ik} + \mathbf{s}_{ij}^0 \text{Sin } \alpha_{ik} . \end{aligned}$$

Applying the same rules for $\$ _{jk}$ gives

$$\begin{aligned} \$ _{jk} &= -\$ _i \text{Sin} \mathbf{A}_{ik} + \$ _{ij} \text{Cos} \mathbf{A}_{ik} , \\ \$ _{jk} &= -(\text{Sin } \alpha_{ik} + \omega a_{ik} \text{Cos } \alpha_{ik}) (\mathbf{s}_i + \mathbf{s}_i^0 \omega) + (\text{Cos } \alpha_{ik} + \omega a_{ik} \text{Sin } \alpha_{ik}) (\mathbf{s}_{ij} + \mathbf{s}_{ij}^0 \omega) , \\ \mathbf{s}_{jk} + \mathbf{s}_{jk}^0 \omega &= -\mathbf{s}_i \text{Sin } \alpha_{ik} + \mathbf{s}_{ij} \text{Cos } \alpha_{ik} + (-\mathbf{s}_i^0 \text{Sin } \alpha_{ik} - \mathbf{s}_i a_{ik} \text{Cos } \alpha_{ik} - \mathbf{s}_{ij} a_{ik} \text{Sin } \alpha_{ik} + \mathbf{s}_{ij}^0 \text{Cos } \alpha_{ik}) \omega , \\ \mathbf{s}_{jk} &= -\mathbf{s}_i \text{Sin } \alpha_{ik} + \mathbf{s}_{ij} \text{Cos } \alpha_{ik} , \mathbf{s}_{jk}^0 = -\mathbf{s}_i^0 \text{Sin } \alpha_{ik} - \mathbf{s}_i a_{ik} \text{Cos } \alpha_{ik} - \mathbf{s}_{ij} a_{ik} \text{Sin } \alpha_{ik} + \mathbf{s}_{ij}^0 \text{Cos } \alpha_{ik} . \end{aligned}$$

Substituting parameters for $\$j$, $\$k$ and $\$jk$ in to Equation (2.17) gives us

$$\begin{bmatrix} \mathbf{s}_j \\ \mathbf{s}_j^0 \\ \mathbf{s}_k \\ \mathbf{s}_k^0 \\ \mathbf{s}_{jk} \\ \mathbf{s}_{jk}^0 \end{bmatrix} = \begin{bmatrix} 0 & 0 & 1 & 0 & 0 & 0 \\ 0 & 0 & 0 & 1 & 0 & 0 \\ C\alpha_{ik} & 0 & 0 & 0 & S\alpha_{ik} & 0 \\ -a_{ik}S\alpha_{ik} & C\alpha_{ik} & 0 & 0 & a_{ik}C\alpha_{ik} & S\alpha_{ik} \\ -S\alpha_{ik} & 0 & 0 & 0 & C\alpha_{ik} & 0 \\ -a_{ik}C\alpha_{ik} & -S\alpha_{ik} & 0 & 0 & -a_{ik}S\alpha_{ik} & C\alpha_{ik} \end{bmatrix} \cdot \begin{bmatrix} \mathbf{s}_i \\ \mathbf{s}_i^0 \\ \mathbf{s}_j \\ \mathbf{s}_j^0 \\ \mathbf{s}_{ij} \\ \mathbf{s}_{ij}^0 \end{bmatrix}, \quad (2.20)$$

where $C\alpha_{ik} = \text{Cos}(\alpha_{ik})$ and $S\alpha_{ik} = \text{Sin}(\alpha_{ik})$.

2.2.4. Transformation Screw Matrix Position Analysis

Using transformation screw matrix equations, transformations between successive screw systems can be written in a standard matrix form which includes just screw parameters. If we know the position coordinates and orientation of a screw system, \mathbf{E}_{i+1} then we can find position coordinates and orientation of the same system in the previous coordinate system \mathbf{E}_i by using a transformation screw matrix $\mathbf{T}_{i,i+1}$ as

$$\mathbf{E}_i = \mathbf{T}_{i,i+1} \mathbf{E}_{i+1}, \quad (2.21)$$

where

$$\mathbf{T}_{i,i+1} = \begin{bmatrix} 0 & 0 & 1 & 0 & 0 & 0 \\ 0 & 0 & 0 & 1 & 0 & 0 \\ C\alpha_{i,i+2} & 0 & 0 & 0 & S\alpha_{i,i+2} & 0 \\ -a_{i,i+2}S\alpha_{i,i+2} & C\alpha_{i,i+2} & 0 & 0 & a_{i,i+2}C\alpha_{i,i+2} & S\alpha_{i,i+2} \\ -S\alpha_{i,i+2} & 0 & 0 & 0 & C\alpha_{i,i+2} & 0 \\ -a_{i,i+2}C\alpha_{i,i+2} & -S\alpha_{i,i+2} & 0 & 0 & -a_{i,i+2}S\alpha_{i,i+2} & C\alpha_{i,i+2} \end{bmatrix}. \quad (2.22)$$

Furthermore, each screw vector is given by

$$\mathbf{E} = \begin{bmatrix} \mathbf{s}_i & \mathbf{s}_i^0 & \mathbf{s}_j & \mathbf{s}_j^0 & \mathbf{s}_{ij} & \mathbf{s}_{ij}^0 \end{bmatrix}^T. \quad (2.23)$$

Now by applying Equation (2.21) recursively from one link to the other we can write for an n-link single loop mechanism

$$\begin{aligned} \mathbf{E}_1 &= \mathbf{T}_{1,2} \mathbf{E}_2, \\ \mathbf{E}_1 &= \mathbf{T}_{1,2} \mathbf{T}_{2,3} \mathbf{E}_3, \\ &\dots\dots\dots \\ \mathbf{E}_1 &= \mathbf{T}_{1,2} \mathbf{T}_{2,3} \mathbf{T}_{3,4} \dots \mathbf{T}_{n-1,n} \mathbf{E}_n. \end{aligned} \quad (2.24)$$

and in general

$$\mathbf{E}_1 = \mathbf{T}_{1,2} \mathbf{T}_{2,3} \dots \mathbf{T}_{i-1,i} \mathbf{E}_i. \quad (2.25)$$

These T matrices can be denoted as a T matrix as

$$\mathbf{T}_{1,i} = \mathbf{T}_{1,2} \mathbf{T}_{2,3} \dots \mathbf{T}_{i-1,i}. \quad (2.26)$$

Then Equation (2.25) becomes

$$\mathbf{E}_1 = \mathbf{T}_{1,i} \mathbf{E}_i. \quad (2.27)$$

Because it is a close loop link 1 follows link i at the end of the loop

$$\mathbf{E}_1 = \mathbf{T}_{1,2} \mathbf{T}_{2,3} \dots \mathbf{T}_{i,i} \mathbf{E}_1. \quad (2.28)$$

From Equation (2.28) no matter which screw system is chosen, it is seen that

$$\mathbf{I} = \mathbf{T}_{1,2} \mathbf{T}_{2,3} \dots \mathbf{T}_{i-1,i} \mathbf{T}_{i,i}, \quad (2.29)$$

where, I is the 6x6 identity transformation screw matrix.

Equation (2.29) defines the loop-closure equation of mechanism in transformation screw matrix form and states that the product of transformation screw matrices around a kinematic loop must equal the identity transformation screw matrix.

2.2.5. Screw Matrix Velocity and Acceleration Analyses

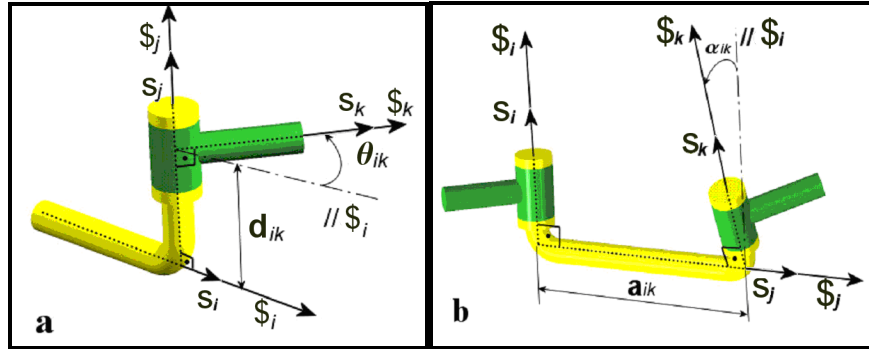


Figure 2.4. Link and joint parameters.

The link and joint parameters two of which describe the joint (Figure 2.4.a) and other two describing the link (Figure 2.4.b) are applied to the screw system (Equation 2.22) gives.

$$\mathbf{T}_{\text{joint}} = \begin{bmatrix} 0 & 0 & 1 & 0 & 0 & 0 \\ 0 & 0 & 0 & 1 & 0 & 0 \\ \cos \theta & 0 & 0 & 0 & \sin \theta & 0 \\ -d \sin \theta & \cos \theta & 0 & 0 & d \cos \theta & \sin \theta \\ -\sin \theta & 0 & 0 & 0 & \cos \theta & 0 \\ -d \cos \theta & -\sin \theta & 0 & 0 & -d \sin \theta & \cos \theta \end{bmatrix}, \quad (2.30)$$

$$\mathbf{T}_{\text{link}} = \begin{bmatrix} 0 & 0 & 1 & 0 & 0 & 0 \\ 0 & 0 & 0 & 1 & 0 & 0 \\ \cos \alpha & 0 & 0 & 0 & \sin \alpha & 0 \\ -a \sin \alpha & \cos \alpha & 0 & 0 & a \cos \alpha & \sin \alpha \\ -\sin \alpha & 0 & 0 & 0 & \cos \alpha & 0 \\ -a \cos \alpha & -\sin \alpha & 0 & 0 & -a \sin \alpha & \cos \alpha \end{bmatrix}. \quad (2.31)$$

Therefore, using equations (2.20) and (2.25) the transformation screw matrix of a link and joint can be found by multiplying the link and joint transformation screw matrices $\mathbf{T}_{\text{joint}}$ and \mathbf{T}_{link} .

$$\mathbf{T} = \mathbf{T}_i \mathbf{T}_j = \begin{bmatrix} C\alpha & 0 & 0 & 0 & S\alpha & 0 \\ -aS\alpha & C\alpha & 0 & 0 & aC\alpha & S\alpha \\ -S\alpha S\theta & 0 & C\theta & 0 & C\alpha S\theta & 0 \\ -dC\theta S\alpha - aC\alpha S\theta & -S\alpha S\theta & -dS\theta & C\theta & dC\alpha C\theta - aS\alpha S\theta & C\alpha S\theta \\ -C\theta S\alpha & 0 & -S\theta & 0 & C\alpha C\theta & 0 \\ -aC\alpha C\theta + dS\alpha S\theta & -C\theta S\alpha & -dC\theta & -S\theta & -aC\theta S\alpha - dC\alpha S\theta & C\alpha C\theta \end{bmatrix}. \quad (2.32)$$

When the joint variable is the angle θ and the derivative of \mathbf{T} with respect to this variable is

$$\frac{d\mathbf{T}}{d\theta} = \begin{bmatrix} 0 & 0 & 0 & 0 & 0 & 0 \\ 0 & 0 & 0 & 0 & 0 & 0 \\ -C\theta S\alpha & 0 & -S\theta & 0 & C\alpha C\theta & 0 \\ dS\theta S\alpha - aC\alpha C\theta & -S\alpha C\theta & -dC\theta & -S\theta & -dC\alpha S\theta - aS\alpha S\theta & C\alpha C\theta \\ S\theta S\alpha & 0 & -C\theta & 0 & -C\alpha S\theta & 0 \\ aC\alpha S\theta + dS\alpha C\theta & S\theta S\alpha & dS\theta & -C\theta & aS\theta S\alpha - dC\alpha C\theta & -C\alpha S\theta \end{bmatrix}. \quad (2.33)$$

On the other hand, if the joint is prismatic and joint variable is d , then the derivative will be

$$\frac{d\mathbf{T}}{dd} = \begin{bmatrix} 0 & 0 & 0 & 0 & 0 & 0 \\ 0 & 0 & 0 & 0 & 0 & 0 \\ 0 & 0 & 0 & 0 & 0 & 0 \\ -C\theta S\alpha & 0 & -S\theta & 0 & C\alpha C\theta & 0 \\ 0 & 0 & 0 & 0 & 0 & 0 \\ S\alpha S\theta & 0 & -C\theta & 0 & -C\alpha S\theta & 0 \end{bmatrix}. \quad (2.34)$$

These both derivatives can be described by one formula using a derivative operator Q

$$\frac{d\mathbf{T}_{i,i+1}}{d\phi_i} = Q_i \mathbf{T}_{i,i+1}. \quad (2.35)$$

Where when joint i is a revolute joint we use

$$Q_i = \begin{bmatrix} 0 & 0 & 0 & 0 & 0 & 0 \\ 0 & 0 & 0 & 0 & 0 & 0 \\ 0 & 0 & 0 & 0 & 1 & 0 \\ 0 & 0 & 0 & 0 & 0 & 1 \\ 0 & 0 & -1 & 0 & 0 & 0 \\ 0 & 0 & 0 & -1 & 0 & 0 \end{bmatrix} \quad (2.36)$$

and when that joint is a prismatic pair we use

$$Q_i = \begin{bmatrix} 0 & 0 & 0 & 0 & 0 & 0 \\ 0 & 0 & 0 & 0 & 0 & 0 \\ 0 & 0 & 0 & 0 & 1 & 0 \\ 0 & 0 & 0 & 0 & 0 & 0 \\ 0 & 0 & -1 & 0 & 0 & 0 \\ 0 & 0 & 0 & 0 & 0 & 0 \end{bmatrix} . \quad (2.37)$$

To make velocity analysis we need derivatives with respect to time instead of the joint variables. Thus, using Equation (2.35) we can find

$$\frac{d\mathbf{T}_{i,i+1}}{dt} = Q_i \mathbf{T}_{i,i+1} \dot{\phi}_i . \quad (2.38)$$

We start velocity analysis by differentiating the loop-closure conditions (Equation 2.29) with respect to time. Using the chain rule with Equation (2.38) to differentiate each factor we get

$$\sum \mathbf{T}_{1,2} \mathbf{T}_{2,3} \dots \mathbf{T}_{i-1,i} Q_i \mathbf{T}_{i,i+1} \dots \mathbf{T}_{n,1} \dot{\phi}_i = 0 . \quad (2.39)$$

Arranging Equation (2.39) in a more compact form

$$\sum \mathbf{T}_{1,i} Q_i \mathbf{T}_{i,1} \dot{\phi}_i = 0 \quad (2.40)$$

If we define the symbol D as,

$$D_i = \mathbf{T}_{1,i} Q_i \mathbf{T}_{1,i}^{-1}, \quad (2.41)$$

and take into account $\mathbf{T}_{1,1} = \mathbf{T}_{1,1}^{-1}$ Equation (2.41) can be written as

$$D_i = \mathbf{T}_{1,i} Q_i \mathbf{T}_{1,i}^{-1}. \quad (2.42)$$

Then Equation (2.40) becomes

$$\sum_{i=1}^n D_i \dot{\phi}_i = 0. \quad (2.43)$$

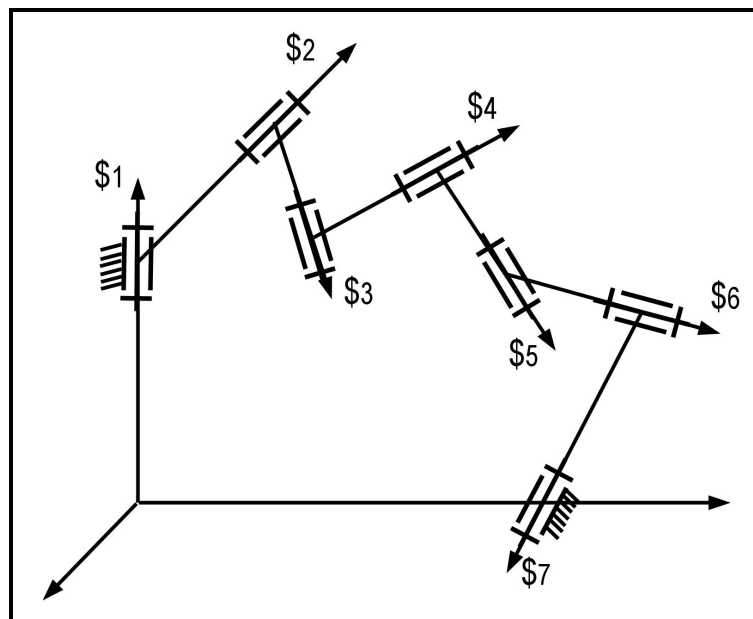


Figure 2.5. 7R spatial linkage.

To describe the concept of Jacobian Equation (2.43) will be expanded for a one degree of freedom close loop system. Let $n=7$ as shown in Figure 2.5. Thus, Equation (2.42) can be written for seven joints as

$$\begin{aligned}
D_1 &= \mathbf{T}_{1,1} Q_1 \mathbf{T}_{1,1}^{-1}, D_2 = \mathbf{T}_{1,2} Q_2 \mathbf{T}_{1,2}^{-1}, D_3 = \mathbf{T}_{1,3} Q_3 \mathbf{T}_{1,3}^{-1}, D_4 = \mathbf{T}_{1,4} Q_4 \mathbf{T}_{1,4}^{-1}, \\
D_5 &= \mathbf{T}_{1,5} Q_5 \mathbf{T}_{1,5}^{-1}, D_6 = \mathbf{T}_{1,6} Q_6 \mathbf{T}_{1,6}^{-1}, D_7 = \mathbf{T}_{1,7} Q_7 \mathbf{T}_{1,7}^{-1}.
\end{aligned} \tag{2.44}$$

Matrices D_i has the form as shown in Equation (2.45)

$$D_i = \begin{bmatrix} 0 & 0 & b & 0 & a & 0 \\ 0 & 0 & e & b & d & a \\ -b & 0 & 0 & 0 & c & 0 \\ -c & -b & 0 & 0 & f & c \\ -a & 0 & -c & 0 & 0 & 0 \\ -d & -a & -f & -c & 0 & 0 \end{bmatrix}. \tag{2.45}$$

Furthermore, using this symmetry D_i matrix can be described as vector form

$$\mathbf{D}_i = [a \ b \ c \ d \ e \ f]^T. \tag{2.46}$$

Expanding Equation (2.43) and calculating the values of \mathbf{D}_i from Equation (2.44) we get

$$\mathbf{D}_1 \dot{\phi}_1 + \mathbf{D}_2 \dot{\phi}_2 + \mathbf{D}_3 \dot{\phi}_3 + \mathbf{D}_4 \dot{\phi}_4 + \mathbf{D}_5 \dot{\phi}_5 + \mathbf{D}_6 \dot{\phi}_6 + \mathbf{D}_7 \dot{\phi}_7 = 0, \tag{2.47}$$

where $D_1 = [a_1 \ b_1 \ c_1 \ d_1 \ e_1 \ f_1]^T$, $D_2 = [a_2 \ b_2 \ c_2 \ d_2 \ e_2 \ f_2]^T$,

$D_3 = [a_3 \ b_3 \ c_3 \ d_3 \ e_3 \ f_3]^T$, $D_4 = [a_4 \ b_4 \ c_4 \ d_4 \ e_4 \ f_4]^T$,

$D_5 = [a_5 \ b_5 \ c_5 \ d_5 \ e_5 \ f_5]^T$, $D_6 = [a_6 \ b_6 \ c_6 \ d_6 \ e_6 \ f_6]^T$,

$D_7 = [a_7 \ b_7 \ c_7 \ d_7 \ e_7 \ f_7]^T$.

Taking the elements of vector Equation (2.47) as functions of input parameters ($\dot{\phi}_i$), and knowing the input velocities $\dot{\phi}_i$ and equation the sum of corresponding matrix element we can write the equations in matrix vector form as

$$J \cdot \dot{\phi} = \mathbf{V}, \tag{2.48}$$

$$\text{where } J = \begin{bmatrix} a_2 & a_3 & a_4 & a_5 & a_6 & a_7 \\ b_2 & b_3 & b_4 & b_5 & b_6 & b_7 \\ c_2 & c_3 & c_4 & c_5 & c_6 & c_7 \\ d_2 & d_3 & d_4 & d_5 & d_6 & d_7 \\ e_2 & e_3 & e_4 & e_5 & e_6 & e_7 \\ f_2 & f_3 & f_4 & f_5 & f_6 & f_7 \end{bmatrix}, \dot{\boldsymbol{\phi}} = \begin{bmatrix} \dot{\phi}_2 \\ \dot{\phi}_3 \\ \dot{\phi}_4 \\ \dot{\phi}_5 \\ \dot{\phi}_6 \\ \dot{\phi}_7 \end{bmatrix}, \mathbf{V} = \begin{bmatrix} -a_1 \dot{\phi}_1 \\ -b_1 \dot{\phi}_1 \\ -c_1 \dot{\phi}_1 \\ -d_1 \dot{\phi}_1 \\ -e_1 \dot{\phi}_1 \\ -f_1 \dot{\phi}_1 \end{bmatrix}.$$

J describes the Jacobian of the mechanism and for the inverse task of velocity analysis where the end velocities of the mechanism is given joint velocities can be found as

$$\dot{\boldsymbol{\phi}} = J^{-1} \cdot \mathbf{V}. \quad (2.49)$$

If the Jacobian is not a square matrix, then either there are less than six joint variables, other solution methods must be used or there are more than six joint variables, the problem has no unique solution.

Joint variable accelerations can be found analogously,

$$\sum_{i=1}^n D_i \ddot{\phi}_i = \mathbf{A} \quad (2.50)$$

and in the matrix vector form

$$J \cdot \ddot{\boldsymbol{\phi}} = \mathbf{A}. \quad (2.51)$$

By inverting the Jacobian in Equation (2.51) joint variable accelerations can be found.

$$\ddot{\boldsymbol{\phi}} = J^{-1} \cdot \mathbf{A}. \quad (2.52)$$

2.2.6. Robot Actuator Force Analysis

To perform a given task of the manipulator, it is important to know the forces and torques must be applied by the actuators. Contrarily, force that can be produced at

the end effector by the actuators must be known. End effector forces and moments are shown in Equation (2.53).

$$\mathbf{F}_i = [M_i^x \quad M_i^y \quad M_i^z \quad F_i^x \quad F_i^y \quad F_i^z]^T \quad (2.53)$$

If the torques of the actuators are described in a vector as

$$\boldsymbol{\tau} = [\tau_1 \quad \tau_2 \quad \dots \quad \tau_n]^T. \quad (2.54)$$

Then we define a small displacement of the tool by a six component vector

$$\delta \mathbf{R}_i = [\delta \theta_i^x \quad \delta \theta_i^y \quad \delta \theta_i^z \quad \delta R_i^x \quad \delta R_i^y \quad \delta R_i^z]^T, \quad (2.55)$$

and define the displacement of joint variables during this small displacement

$$\delta \boldsymbol{\phi}_i = [\delta \phi_1 \quad \delta \phi_2 \quad \dots \quad \delta \phi_n]^T. \quad (2.56)$$

The work done at the end effector is calculated by multiplication of the forces acting and displacement, meanwhile work done at the joints are multiplication of torques of joints with joint variable displacements and the work must be same for the conservation of energy as described in Equation (2.57).

$$\mathbf{F}^T \delta \mathbf{R} = \boldsymbol{\tau}^T \delta \boldsymbol{\phi} \quad (2.57)$$

Writing Equation (2.48) in time derivative form,

$$J \cdot \frac{d\boldsymbol{\phi}}{dt} = \frac{d\mathbf{R}}{dt}, \quad (2.58)$$

and we can write it for a short time interval δt Equation (2.58) can be written in the form

$$\delta \mathbf{R} = J \delta \boldsymbol{\phi}. \quad (2.59)$$

Substituting Equation (2.59) in Equation (2.57) and rearranging we get

$$(\boldsymbol{\tau}^T - \mathbf{F}^T J) \delta \boldsymbol{\phi} = 0. \quad (2.60)$$

The small displacement cannot be zero thus torques of the actuators can be described as

$$\boldsymbol{\tau} = J^T \mathbf{F}. \quad (2.61)$$

2.3. Reciprocity and Virtual Work

Principle of virtual work can be used to reduce a problem of kinetics at a chosen instant to one of statics. This method allows screws to be applied to a wide range of problems in kinetostatics. In kinetostatics of rigid bodies two dual vector quantities are characterized: infinitesimal displacements (twists) and force with a couple acting on rigid body (wrench). As a matter of fact twists for the rigid body defines the motion and wrench defines action, these screws are called as moment and vector or shortly motor screws.

In Figure 2.6 two screws on a rigid body of points A and B are depicted. The pitches of the screws are “ p_a ” and “ p_b ” meters/radian respectively. Minimum distance between the screws is defined with “ a ” meters and angular displacement as “ α ” radians. At point A a wrench is applied to rigid body along screw A where it is defined as $\mathbf{W} = [\mathbf{F} \quad \boldsymbol{\tau}]^T$ and at point B a twist $\mathbf{T} = [\boldsymbol{\omega} \quad \mathbf{v}]^T$. The rate of work $d\omega/dt$ of wrench acting on a rigid body while the body is going under an infinitesimal twist is the mutual moment of this wrench and twist which is

$$\mathbf{W} \circ \mathbf{T} = (\mathbf{F} \cdot \mathbf{v} + \boldsymbol{\tau} \cdot \boldsymbol{\omega}) = F\omega \left((p_a + p_b) \cos \alpha - a \sin \alpha \right). \quad (2.62)$$

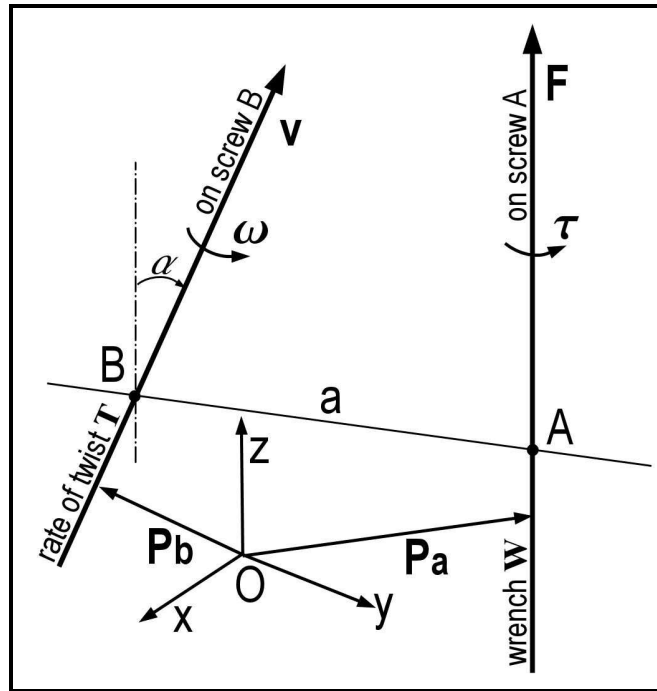


Figure 2.6. Wrench and twist acting on a rigid body.

When the wrench is unable to do any work on the body then W and T are called as reciprocal. So from Equation (2.62) it is resulted that the condition of reciprocity of a wrench and a twist is

$$(p_a + p_b) \cos \alpha - a \sin \alpha = 0. \quad (2.63)$$

2.4. Screw Systems

It is necessary to establish all the screws that the constraints will permit the body to be twisted to define the freedom of the rigid body. If there is linearly independent n screws $S_1, S_2 \dots S_n$ that the rigid body can receive a twist on each to define the freedom. So all these screws $S_1, S_2 \dots S_n$ said to form a screw system S of the n^{th} order. For the Euclidean space limits of n will be $0 \leq n \leq 6$.

For any screw system S of order n there is a reciprocal screw system S^r of order $(6-n)$. Every screw of S must be reciprocal to all screws of screw system S^r and vice versa. Reciprocity of this two screw systems can be described by above equation

$$\mathbf{S} \circ \mathbf{S}^r = 0. \quad (2.64)$$

Where “ \circ ” denotes the mutual moment or reciprocal product of two systems. This equation can be written in matrix vector form as

$$\mathbf{S}^T \Delta \mathbf{S}^r = 0 \text{ or } \mathbf{S}^T \text{NullSpace}[\mathbf{S}] = 0, \quad (2.65)$$

where $\Delta = \begin{bmatrix} 0 & \mathbf{I}_{3 \times 3} \\ \mathbf{I}_{3 \times 3} & 0 \end{bmatrix}_{6 \times 6}$.

Equation (2.65) shows us that the null space of screw system \mathbf{S} is equal to $\Delta \mathbf{S}^r$ and the relation of the dimensions of the screw system and its reciprocal is

$$\dim(\mathbf{S}) + \dim(\mathbf{S}^r) = 6. \quad (2.66)$$

2.4.1. Operation on Screw Systems

The union and intersection of two screw systems are written as $\mathbf{S}_1 \cup \mathbf{S}_2$ and $\mathbf{S}_1 \cap \mathbf{S}_2$ respectively. The dimension of union of two screw system can be given as

$$\dim(\mathbf{S}_1 \cup \mathbf{S}_2) = \dim(\mathbf{S}_1) + \dim(\mathbf{S}_2) - \dim(\mathbf{S}_1 \cap \mathbf{S}_2). \quad (2.67)$$

Screw systems also follow the conditions

$$(\mathbf{S}_1 \cup \mathbf{S}_2 \dots \cup \mathbf{S}_n)^r = (\mathbf{S}_1^r \cap \mathbf{S}_2^r \dots \cap \mathbf{S}_n^r), \quad (2.68)$$

$$(\mathbf{S}_1 \cap \mathbf{S}_2 \dots \cap \mathbf{S}_n)^r = (\mathbf{S}_1^r \cup \mathbf{S}_2^r \dots \cup \mathbf{S}_n^r). \quad (2.69)$$

2.5. Structural Analysis of Parallel Mechanisms with Theory of Screws

A parallel manipulator is composed of l serial kinematic chains connected between ground and a common moving platform. The dimension of the output twist

system of the manipulator will give us the mobility of the platform. As a first step the screws on joints in the legs are must be calculated.

In the beginning A base screw is defined for the coordinate axis on the base as $\$_{O_z} = \{0\ 0\ 1\ 0\ 0\ 0\}$, $\$_{O_y} = \{0\ 1\ 0\ 0\ 0\ 0\}$ and $\$_{O_x} = \{1\ 0\ 0\ 0\ 0\ 0\}$ then the screw parameters of each joint must be calculated using recurrent screw equations that are described before. From the screws of the joints the twists of the joint screws will be defined with respect to their joint types. If $\$ = [\mathbf{s}_i \quad \mathbf{r}_i \times \mathbf{s}_i + \mu \mathbf{s}_i]^T$ for a joint screw twist for the revolute joint will be $\$_R = [\mathbf{s}_i \quad \mathbf{r}_i \times \mathbf{s}_i]^T$ and for the prismatic joint $\$_P = [0 \quad \mathbf{s}_i]^T$.

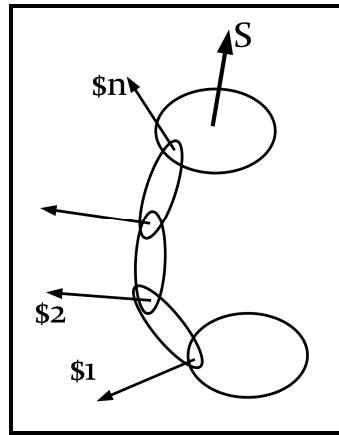


Figure 2.7. Twist system for one leg of a parallel manipulator.

After enumerating all twist for all the joints on the leg shown in Figure 2.7 the twist system of the leg must be calculated which is the union of each joint twists on that leg. If there are n joints on the leg equation of the twist of the leg will be;

$$\mathbf{S}_{mi} = \mathbf{S}_{i1} \cup \mathbf{S}_{i2} \dots \cup \mathbf{S}_{in} \quad \text{where, } i=1,2,\dots,l. \quad (2.70)$$

After describing the motion system \mathbf{S}_{mi} of the i^{th} leg the constraint screw system of the i^{th} leg \mathbf{S}_{ci} which is the reciprocal of motion system \mathbf{S}_{mi} can be found from Equation (2.71)

$$\mathbf{S}_{mi} \Delta \mathbf{S}_{ci} = 0 \quad i=1, 2, \dots, l. \quad (2.71)$$

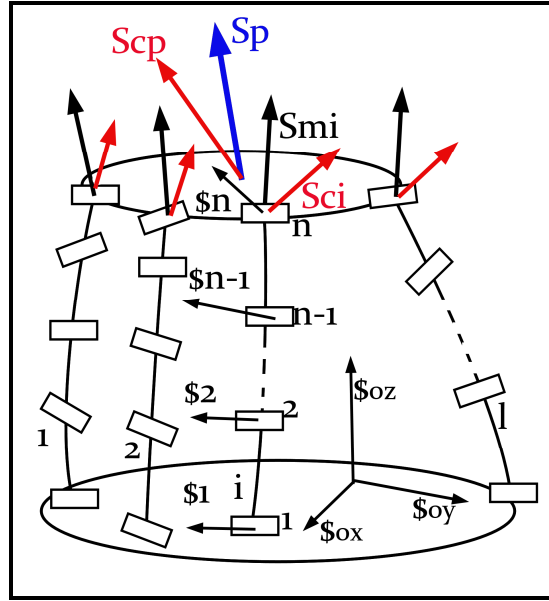


Figure 2.8. Screw systems of a manipulator.

Using equation $\Delta S_c = NullSpace[S_m]$, Equation (2.71) can be written in the form as

$$S_{ci} = \Delta NullSpace[S_{mi}]. \quad (2.72)$$

After finding all constraints imposed on the platform from all legs, the constraint system (S_{cp}) of platform that is shown in Figure 2.8 can be found by the union of all constraints effecting the platform by Equation (2.73).

$$S_{cp} = S_{c1} \cup S_{c2} \dots \dots \cup S_{cl} \quad (2.73)$$

The reciprocal of platform constraint system will give us the platform motion system (S_p) which we can interpret the motion of the platform as shown in Equation (2.74).

$$S_p = \Delta NullSpace[S_{cp}] \quad (2.74)$$

The dimension of S_p will give us the mobility of the platform,

$$M = \dim(S_p). \quad (2.75)$$

CHAPTER 3

GEOMETRY ANALYSIS OF SUBSPACES

A rigid body in space has six motions. The general constraint for a rigid body can be defined as the restrictions that are imposed by external elements. If a constraint is applied to a rigid body it can be defined that this rigid body is restricted to a subspace where the motion is less than the space. Formulation for the relation of general constraint of a rigid body can be given as

$$d = 6 - \lambda, \quad (3.1)$$

where d stands for the general constraint of the system, λ is the space or subspace number and 6 comes from the general degrees of freedom of rigid body in space.

For a manipulator, general constraint is the restrictions applied by the geometrical conditions of the linkages and joints. Thus, general constraint of a manipulator is the difference of the maximum possible motions of the end-effector in space and the maximum possible motions of the end-effector in its subspace. Six independent motions of rigid body in space consist of three translations and three rotations (PPPRRR) in Cartesian coordinate system.

The constrained motions of $\lambda=5$ can be described with the relation of two rigid body surfaces that are defined in Table 3.1. The rigid body motion PPP-RR is described by the motion of a planar surface with respect to a planar surface or a hyperbolic surface. PP-RRR motion can be described by the contact motion of a spherical surface or an elliptic toroidal surface on a planar surface. P-RRRR motion is shown by the respective motions of elliptic cylinder surface on spherical surface, hyperbolic surface on spherical surface or hyperbolic surface on elliptic toroidal surface. Finally RRRRR motion is described by the motions of a spherical surface on spherical surface or on elliptic toroidal surface and motion of elliptic toroidal surface on elliptic toroidal surface. Note that although there are more than 3 rotational motions in some examples, the excessive ones can be represented by translational motions (Table 3.1).

Table 3.1. Summary of rigid body motions in subspace $\lambda=5$.

#	Structure	Motion
1	Planar Surface - Planar Surface	PPP-RR
2	Hyperbolic Surface – Planar Surface	PPP-RR
3	Planar Surface - Spherical Surface	PP-RRR
4	Elliptic Toroidal Surface - Planar Surface	PP-RRR
5	Elliptic Cylindrical Surface - Spherical Surface	P-RRRR
6	Hyperboloid Surface - Spherical Surface	P-RRRR
7	Hyperbolic Surface - Elliptic Toroidal Surface	P-RRRR
8	Spherical Surface - Spherical Surface	RRRRR
9	Elliptic Toroidal Surface - Spherical Surface	RRRRR
10	Elliptic Toroidal Surface - Elliptic Toroidal Surface	RRRRR

The constrained motions of $\lambda=4$ can be described with the relation of one rigid body surface and a line positioned with respect to that surface. The rigid body motion PPP-R is described by the motion of a planar surface with respect to a skew line or a perpendicular line. PP-RR motion can be described by the contact motion of a Line on a planar surface. P-RRR motion is shown by the respective motions of a spherical surface with a line intersecting with the center of the sphere (Table 3.2).

Table 3.2. Summary of rigid body motions in subspace $\lambda=4$.

#	Structure	Motion
1	Planar Surface - Skew Line	PPP-R
2	Planar Surface - Perpendicular Line	PPP-R
3	Planar Surface - Parallel Line	PP-RR
4	Spherical Surface – Line	P-RRR

Motions in subspace $\lambda=3$ can be described by direct definition of surfaces. In Table 3.3 rigid body motions in subspace $\lambda=3$ are shown within four categories. In the planar motion two translations and one rotation occurs on a planar surface (Table 3.3-1). In Table 3.3-2 spherical motion is described with three rotations. In Table 3.3-3 toroidal motion is shown with also three rotations. Finally hyperbolic motion is shown with one translation and two rotations.

Table 3.3. Summary of rigid body motions in subspace $\lambda=3$.

	Structure	Motion
1	Planar	PP-R
2	Spherical	RRR
3	Toroidal	RRR
4	Hyperbolic	P-RR

In subspace $\lambda=2$ there is only two kinds of motion. First one is as shown in Table 3.4-1, a planar motion without a rotation and second one is a cylindrical motion with one translation and one rotation (PR).

Table 3.4. Summary of rigid body motions in subspace $\lambda=2$

	Structure	Motion
1	Planar	PP
2	Cylindrical	P-R

3.1. Generation of Overconstrained Mechanisms by Using Mechanisms in Lower Subspaces

Describing all subspace conditions for overconstrained mechanisms and manipulators is an important and challenging step in the design of overconstrained and non-constrained mechanical systems. In the very beginning of the design of overconstrained mechanism design integration of subspace mechanisms is used by

many designers. First time Sarrus (1853) introduced an overconstrained mechanism which is a special case of planar-hybrid linkage that has six axes intersecting by pairs of three distinct points (Figure 3.1.a). Bennett (1905) introduced spherical-hybrid linkage and plano-spherical hybrid linkage with the criteria of intersecting six axes by pairs in two different points (Figure 3.1.b).

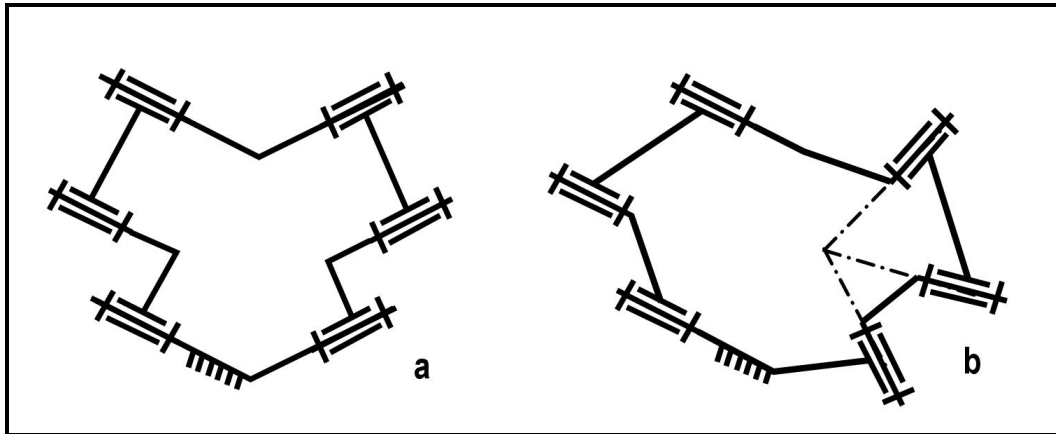


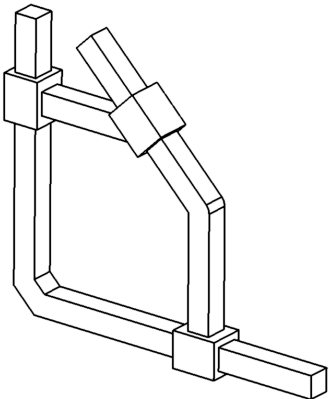
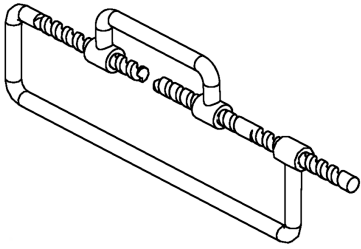
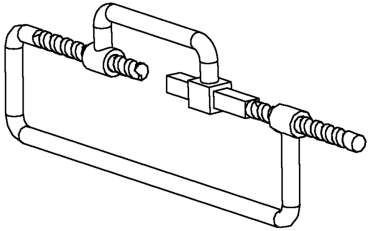
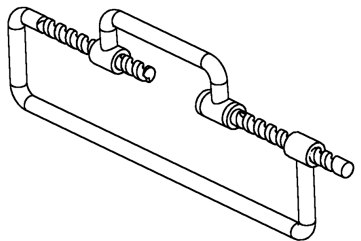
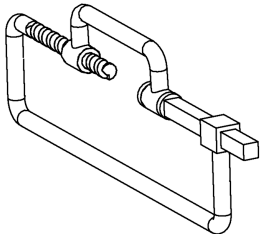
Figure 3.1. Combined six-bar mechanisms; a) Planar-planar, b) Planar-spherical.

As shown in Figure 3.1.a two slider crank mechanisms that have subspace $\lambda=3$ are used to create a six bar linkage in subspace $\lambda=5$. In Figure 3.1.b a planar and a spherical four-bar are integrated to create a six bar linkage with general constraint one. Before describing the method to create these type of subspaces in $\lambda=3, 4, 5$ the mechanisms in $\lambda=2, 3, 4$ must be listed with respect to their subspace numbers and motion types.

3.1.1. Overconstrained Mechanisms in Subspace $\lambda=2$

In subspace $\lambda=2$ there is two groups of linkages with respect to their motion types. One is a planar mechanism with only prismatic pairs where three prismatic joints connected and all three axes of joints are parallel to one plane and neither of them are parallel to each other (Table 3.5-1) and the second group of motion consist of H, P, and R pairs that are in line so that the motion of this group can be described as cylindrical. Four different types of linkage can be achieved as shown in Table 3.5-2.

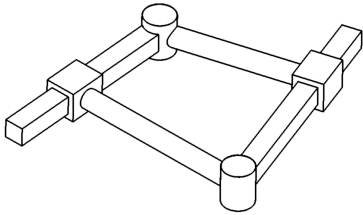
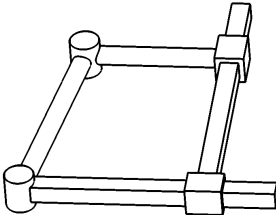
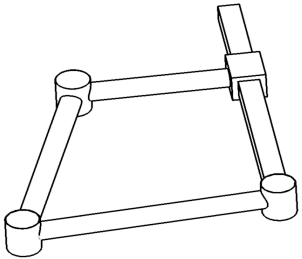
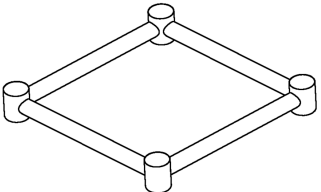
Table 3.5. Overconstrained mechanisms in $\lambda=2$.

#	Motion	Bonding	Figure
1	Planar	$(PPP)_E$	
2	Cylindrical	H=H=H	
		H//P//H	
		H=R=H	
		H=R//P	

3.1.2. Overconstrained Mechanisms in Subspace $\lambda=3$

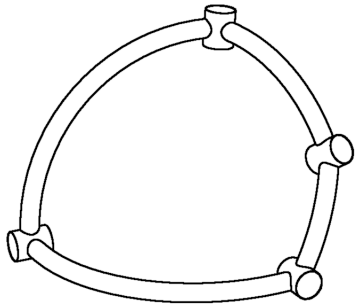
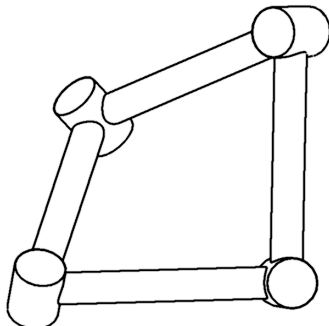
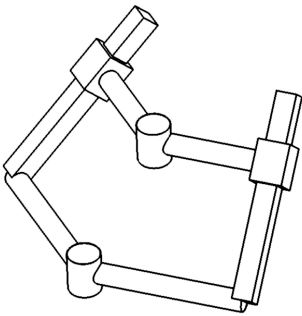
There is four groups of linkages in subspace $\lambda=3$. Mechanisms in planar motion shown in Table 3.6-1. There is only R and P joints where all axes of R joints are parallel and all axes of P joints are perpendicular to axes of R joints. Second motion group of subspaces in $\lambda=3$ is spherical where only R joints are used and all axes of R joints are intersecting in one point (Table 3.6-2). Third motion group of subspace $\lambda=3$ is Toroidal motion group (Table 3.6-3) which is well known Bennett mechanism. Last motion group of subspace $\lambda=3$ is Hyperbolic which consists of 2 R and 2P joints as shown in Table 3.6-4.

Table 3.6. Overconstrained mechanisms in $\lambda=3$.

#	Motion	Bonding	Figure
1	Planar	$(RPRP)_E$	
		$(RRPP)_E$	
		$(RRRP)_E$	
		$(RRRR)_E$	

(cont. on next page)

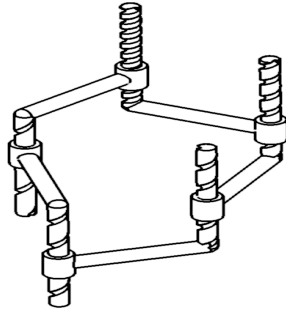
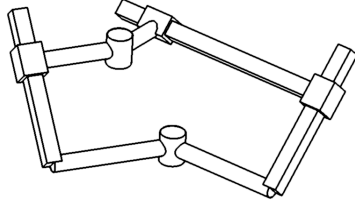
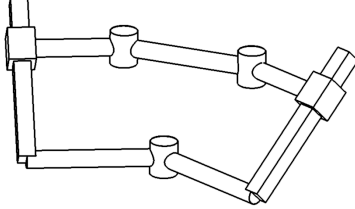
Table 3.6. (cont.)

2	Spherical	$(RRRR)_S$	
3	Toroidal	$(RRRR)_T$	
4	Hyperbolical	$(RRRR)_H$	

3.1.3. Overconstrained Mechanisms in Subspace $\lambda=4$

Two groups of mechanisms in subspace $\lambda=4$ can be defined. First one is the linkage consist of 5 parallel H pairs where pitches of helical joints are different (Table 3.7-1) which describes a special type of motion called as Schoenflies that can be defined as a motion of plane along a line. Second group is similar to first one with a skew line with respect to plane. It consists of prismatic and revolute pairs only (Table 3.7-2) where revolute joints are parallel and prismatic joints are arbitrary.

Table 3.7. Overconstrained mechanisms in $\lambda=4$.

#	Motion	Bonding	Figure
1	Plane along a line	H//H/H//H//H	
2	Plane along a skew line	\overline{PRPPR}	
		\overline{PRPRR}	

3.2. Combination of Subspaces

The idea of creating new subspaces by combining lower order subspaces is to intersect one of the joints and connect the links of those joints to each other and remove the joint as shown schematically in Figure 3.2. These combinations of mechanisms create new mechanisms in different subspaces and these mechanisms give a topological basis for the creation of overconstrained mechanisms.

The formula for calculating the subspace number for the integration of two subspaces can be given as

$$\lambda_{\text{combined}} = \lambda_1 + \lambda_2 - 1. \quad (3.2)$$

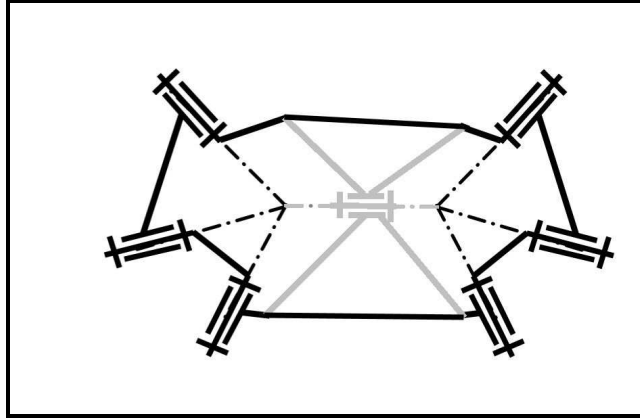


Figure 3.2. Combination of two spherical four bar mechanism.

In the case of combination of three subspaces the formula for calculating new subspace number will be

$$\lambda_{\text{combined}} = \lambda_1 + \lambda_2 + \lambda_3 - 2 . \quad (3.3)$$

If we write a general equation from Equation (3.2) and Equation (3.3) as shown in Equation (3.4).

$$\sum_{i=1}^n \lambda_i = \lambda_{\text{combined}} + n - 1 , \quad (3.4)$$

where n is the number of subspaces to be combined.

3.2.1. Combined Overconstrained Mechanisms in Subspace $\lambda=3$

Using Equation (3.4) only one condition for mechanisms in $\lambda=3$ subspace is possible where there is two subspaces λ_1 and λ_2 and they both are equal to two. As shown in Table 3.5 there is only two groups of motion in $\lambda=2$ is possible and in $\lambda=3$ only the combination of this two group can be accomplished as new mechanisms. The integration of this two subspaces with $\lambda=2$ gives us four types of mechanisms with 2 different motion groups (Table 3.8).

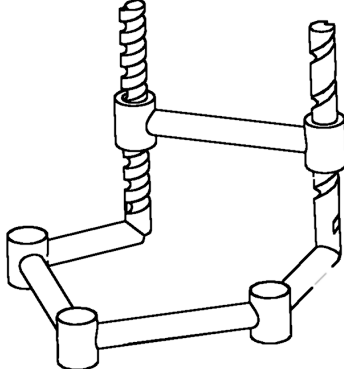
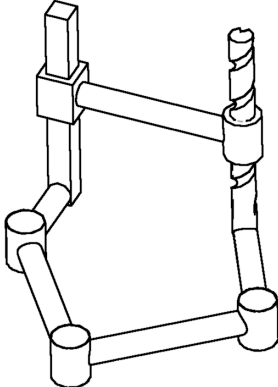
Table 3.8. Combined overconstrained mechanisms in $\lambda=3$.

#	Number of subspaces to combine	Motions of combined subspaces	Bonding	Figure
1	2, 2	Plane around cylinder	$H=HPP$	
2			$H=HPR$	
3	2, 2	Cylinder on plane	$H=\dot{H}PP$	
4			$H=\dot{R}PP$	

3.2.2. Combined Overconstrained Mechanisms in Subspace $\lambda=4$

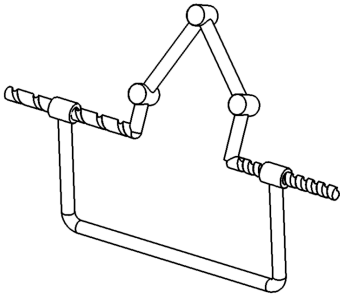
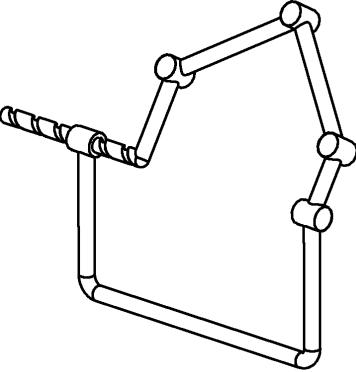
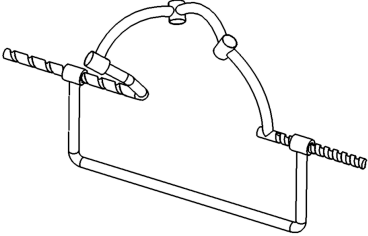
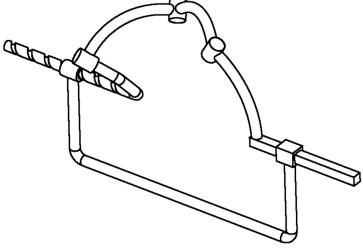
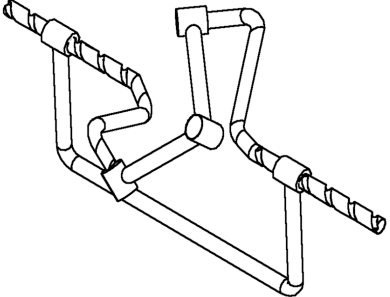
If Equation (3.4) is solved for $\lambda_{\text{combined}}=4$ then the combination of the mechanisms in $\lambda=4$ must be $\lambda_1=3$ with $\lambda_2=2$ or the combination of three $\lambda=2$ subspaces. To construct the conditions (Table 3.5 (1-8)) for the first case $\lambda=3$ mechanisms from Table 3.6 are added to mechanisms listed in Table 3.1 and Table 3.2. For the second case where three $\lambda=2$ mechanisms are integrated together (Table 3.9), $\lambda=2$ mechanisms from Table 3.9(2) are combined with the pre-combined linkages listed in Table 3.8. Four types of mechanisms are listed in Table 3.9 (9-12).

Table 3.9. Combined overconstrained mechanisms in $\lambda=4$.

#	Combined Subspaces	Motions of combined subspaces	Bonding	Figure
1	2, 3	Cylinder and plane	$\overline{\text{H}}\overline{\text{H}}\overline{\text{R}}\overline{\text{R}}\overline{\text{R}}\overline{\text{R}}$	
2	2, 3		$\overline{\text{H}}\overline{\text{P}}\overline{\text{R}}\overline{\text{R}}\overline{\text{R}}\overline{\text{R}}$	

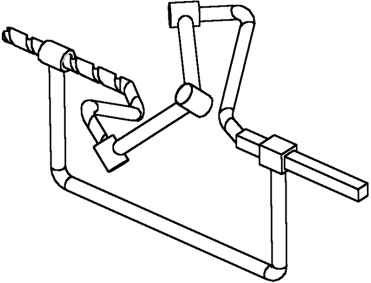
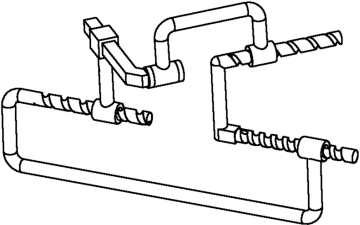
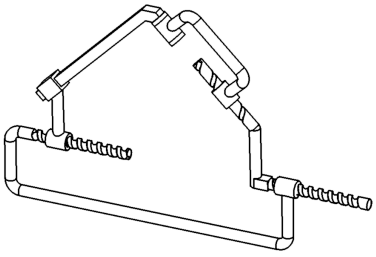
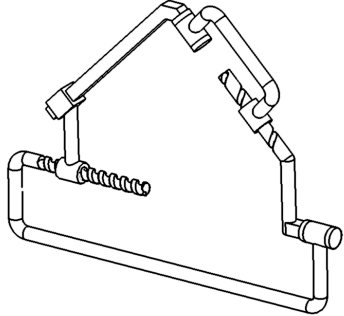
(cont. on next page)

Table 3.9. (cont.)

3	2, 3	Plane around cylinder	$H=H \perp \bar{R}\bar{R}\bar{R}$	
4	2, 3		$H=P \perp \bar{R}\bar{R}\bar{R}$	
5	2, 3	Cylinder and sphere	$H=\bar{H}\bar{R}\bar{R}\bar{R}$	
6	2, 3		$\bar{H}\bar{P}\bar{R}\bar{R}\bar{R}$	
7	2, 3	Torus and Cylinder	$H=H\bar{R}\bar{R}\bar{R}$	

(cont. on next page)

Table 3.9. (cont.)

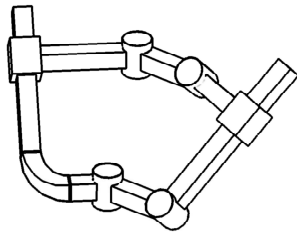
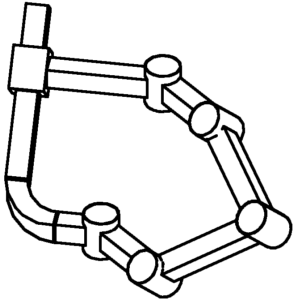
8	2, 3	Torus and Cylinder	$\bar{H}(\overline{PRRR})_T$	
9	2, 2, 2	Plane with Double Cylinder	$H=HH=R \cdot P$	
10	2, 2, 2		$\dot{H}=\dot{H}\dot{H}=R \cdot P$	
11	2, 2, 2		$\dot{H}=\dot{R}\dot{H}=R \cdot P$	

3.2.3. Combined Overconstrained Mechanisms in Subspace $\lambda=5$

For the enumeration of combined mechanisms in $\lambda=5$ using Equation (3.4) we get three kinds of combinations. First is the connection of two $\lambda=3$ mechanisms as listed in Table 3.10 (1-21). Another type of combination is integration of $\lambda=4$ mechanisms with a $\lambda=2$ mechanism is listed in Table 3.10 (22-24) and from the combination of a $\lambda=3$ and two $\lambda=2$ mechanisms resulted in six mechanisms with three groups of motion as shown in Table 3.10 (25-31)

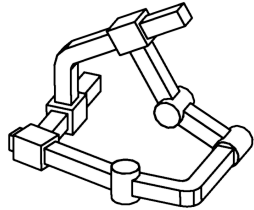
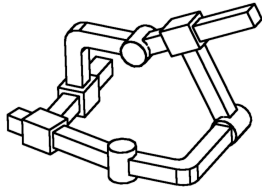
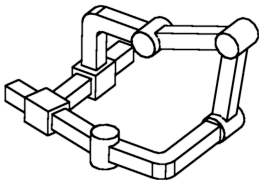
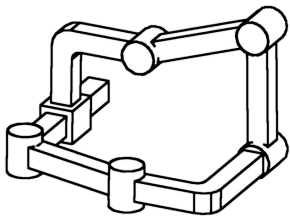
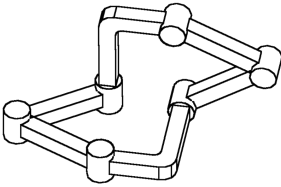
Overconstrained mechanisms are moving in lower subspaces such as spherical, planar, hyperbolical, toroidal and combinations of these. In this section these spaces and intersections are investigated.

Table 3.10. Combined overconstrained mechanisms in $\lambda=5$.

#	Number of subspaces to combine	Motions of combined subspaces	Bonding	Figure
1	2	Hyperboloid and Plane	$(RPR)_H (RPR)_E$	
2	2		$(RPR)_H (RRR)_E$	

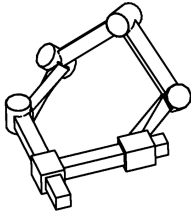
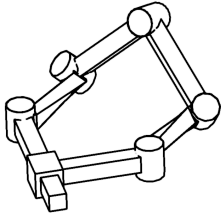
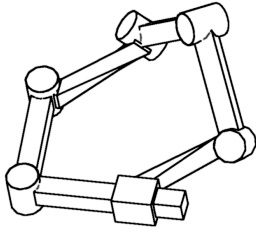
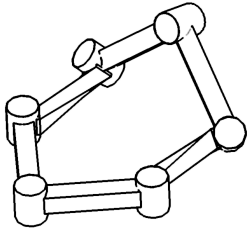
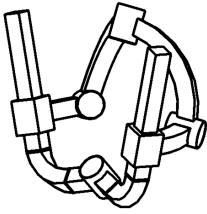
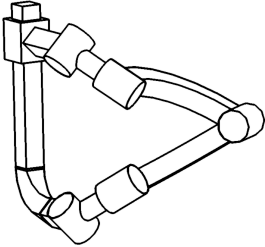
(cont. on next page)

Table 3.10. (cont)

3	2	Plane and Plane	$(PPR)_E (RRP)_E$	
4	2		$PRRPRP$ $(PPR)_E (PRP)_E$	
5	2		$(RRR)_E (RPP)_E$	
6	2	Plane and Plane	$(RRR)_E (RRP)_E$	
7	2		$(RRR)_E (RRR)_E$	

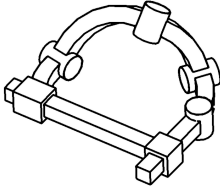
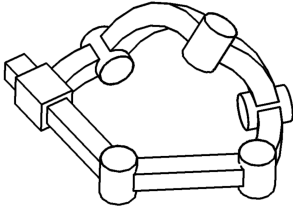
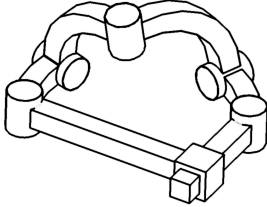
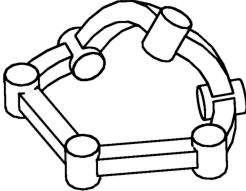
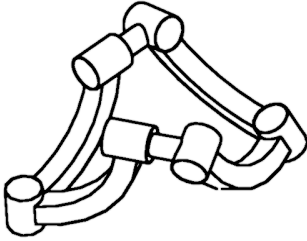
(cont. on next page)

Table 3.10. (cont)

8	2	Plane and Torus	$(RPP)_E(RRR)_T$	
9	$(RPR)_E(RRR)_T$			
10	$(RRP)_E(RRR)_T$			
11	2	Plane and Torus	$(RRR)_E(RRR)_T$	
12	2	Spherical and Hyperboloid	$(PRP)_H(RRR)_S$	
13	2		$(RPR)_H(RRR)_S$	

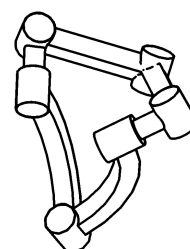
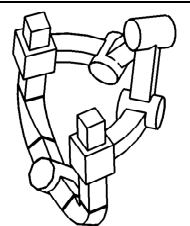
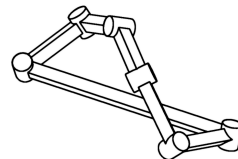
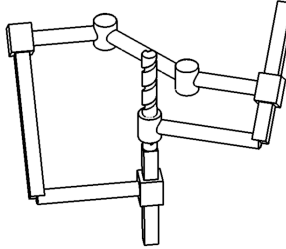
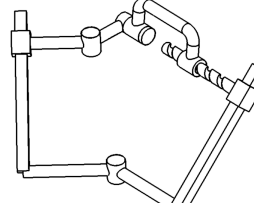
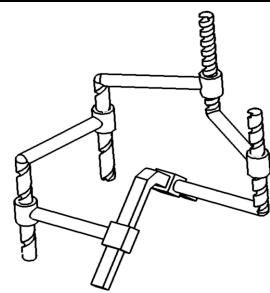
(cont. on next page)

Table 3.10. (cont)

14	2	Spherical and Planar	$(PPR)_E(RRR)_S$	
15	2		$(PPR)_E(RRR)_S$	
16	2		$(RPR)_E(RRR)_S$	
17	2		$(RRR)_E(RRR)_S$	
18	2	Double Spherical	$(RRR)_S(RRR)_S$	

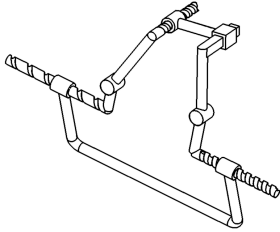
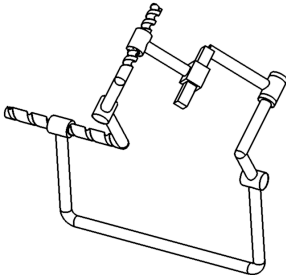
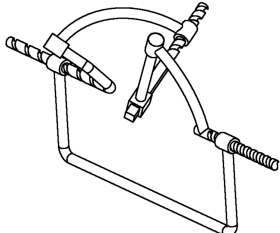
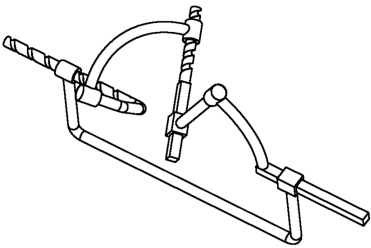
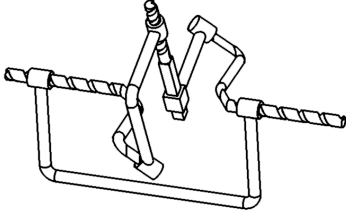
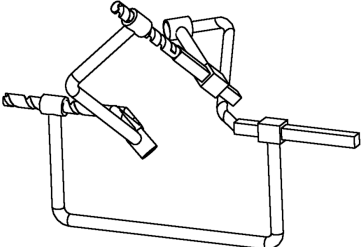
(cont. on next page)

Table 3.10. (cont)

19	2	Spherical and Toroidal	$(RRR)_S(RRR)_T$	
20	2	Toroidal and hyperboloid	$(PRP)_H(RRR)_T$	
21	2	Toroidal and Toroidal	$(RRR)_T(RRR)_T$	
22	2	Hyperboloid cylindrical and planar	$P\bar{R}\bar{R}P\bar{P}\bar{H}$	
23	2		$(PRP)_H\bar{R}\bar{R}=H$	
24	2	Double Planar and cylindrical	$\bar{H}\bar{H}\bar{H}\bar{H}\bar{P}\bar{P}$	

(cont. on next page)

Table 3.10. (cont)

25	3	Planar and double cylindrical	$H=H \perp \overline{RPHR}$	
26	3		$H=R \perp \overline{RPHR}$	
27	3	Spherical and double cylindrical	$H=HR\dot{P}=\dot{H}R$	
28	3		$H//P\dot{R}\dot{P}=\dot{H}R$	
29	3	Toroidal and double cylindrical	$H=H(RP=HR)_T$	
30	3		$H//P(RP=HR)_T$	

3.3. Mathematical Models of Overconstrained Subspaces

Describing the geometry of the subspaces mathematically is a challenging task. In this section mathematical models of some intersecting geometries are described which will lead to the mathematical modeling of subspaces.

3.3.1. Intersection of Two Non-Parallel Planes with Sphere

The main equation of intersection of the two non parallel planes P1 and P2 with sphere (Figure 3.3.a) can be described as

$$\begin{aligned} l_1x + m_1y + n_1z &= d_4 \\ l_2x + m_2y + n_2z &= f_4 \\ (x - x_A)^2 + (y - y_A)^2 + (z - z_A)^2 &= a^2 \end{aligned} \quad (3.5)$$

where: $d_4 = l_1x_D + m_1y_D + n_1z_D$, $f_4 = l_2x_B + m_2y_B + n_2z_B$, $D \in P1$, $B \in P2$, and

$\mathbf{e}_1 = [l_1 \ m_1 \ n_1]^T$, $\mathbf{e}_2 = [l_2 \ m_2 \ n_2]^T$ are unit vectors of normals respect to planes P1 and P2

Let point A(x_A , y_A , z_A) will not belong to planes P1 and P2, and the radius of sphere equal a. The point C(x_C , y_C , z_C) is the point of intersection of the planes P1 and P2 with sphere. The problem is to define the coordinates of point C in frame coordinate system XYZ. Let us introduce moving coordinate system (U_1 , U_2 , U_3) with the origin A, then coordinates of point C can be described as:

$$U_{1C} = x_C - x_A, \quad U_{2C} = y_C - y_A, \quad U_{3C} = z_C - z_A \quad (3.6)$$

Substituting Equation (3.6) in Equation (3.5) yields

$$\begin{aligned} a) \quad l_1U_{1C} + m_1U_{2C} + n_1U_{3C} &= d \\ b) \quad l_2U_{1C} + m_2U_{2C} + n_2U_{3C} &= f \\ c) \quad (U_{1C})^2 + (U_{2C})^2 + (U_{3C})^2 &= a^2 \end{aligned} \quad (3.7)$$

where: $d = d_4 - l_1x_A - m_1y_A - n_1z_A$, $f = f_4 - l_2x_A - m_2y_A - n_2z_A$.

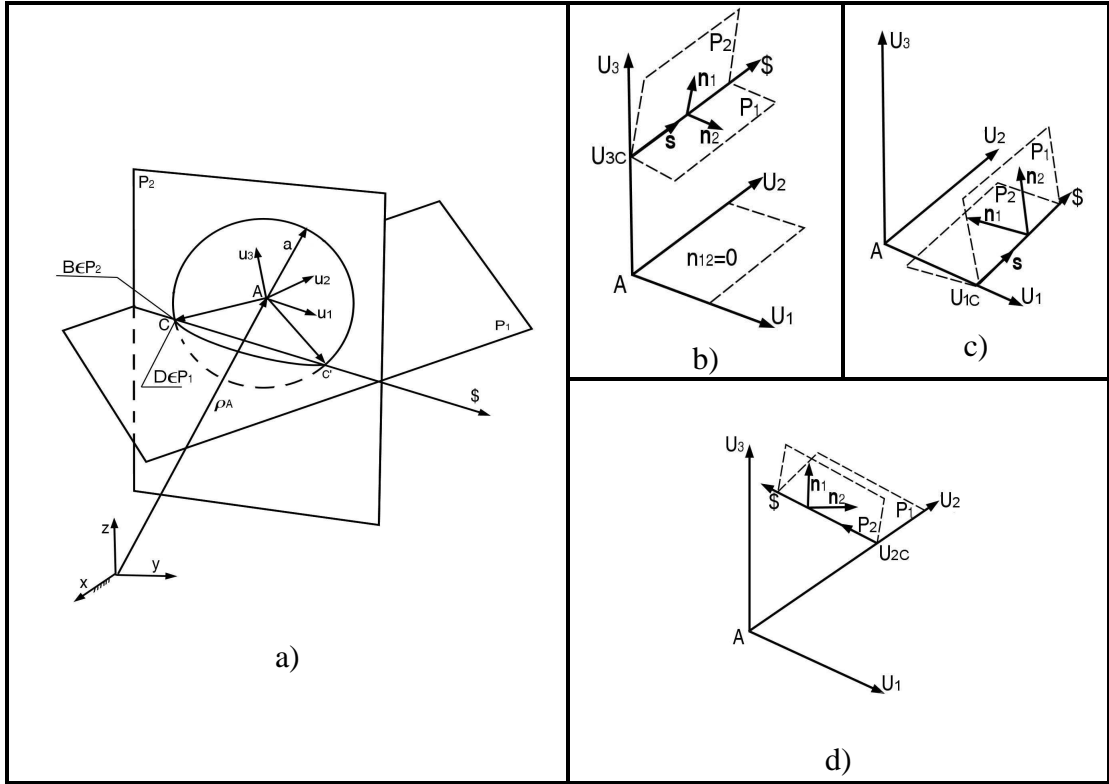


Figure 3.3. Intersection of two non-parallel planes with sphere.

Eliminating U_{1C} , U_{2C} and U_{3C} in turn from linear Equations (3.7) we will get three linear Equations of line as the intersection of two planes as

$$\begin{aligned}
 a) \quad & n_{12}U_{2C} - m_{12}U_{3C} - P = 0 \\
 b) \quad & l_{12}U_{3C} - n_{12}U_{1C} - Q = 0 \quad , \\
 c) \quad & m_{12}U_{1C} - l_{12}U_{2C} - R = 0
 \end{aligned} \tag{3.8}$$

where: $(l_{12}, m_{12}, n_{12}, P, Q, R)$ are Plücker coordinates of line (axes of screw),

$$l_{12} = \begin{vmatrix} m_1 & n_1 \\ m_2 & n_2 \end{vmatrix}, m_{12} = \begin{vmatrix} n_1 & l_1 \\ n_2 & l_2 \end{vmatrix}, n_{12} = \begin{vmatrix} l_1 & m_1 \\ l_2 & m_2 \end{vmatrix}, P = \begin{vmatrix} f & l_2 \\ d & l_1 \end{vmatrix}, Q = \begin{vmatrix} f & m_2 \\ d & m_1 \end{vmatrix}, R = \begin{vmatrix} f & n_2 \\ d & n_1 \end{vmatrix}. \tag{3.9}$$

In Equations (3.9) l_{12}, m_{12}, n_{12} are the projections of normal vectors $\mathbf{s}_1 \times \mathbf{s}_2 = \mathbf{S}_1$ onto axes of system coordinates. Non parallelism of two planes is described by condition $l_{12} \neq m_{12} \neq n_{12} \neq 0$.

Solution of system of Equations (3.7) are achieved by substituting expressions

$$\begin{aligned} U_{1C} &= n_{12}^{-1}(l_{12}U_{3C} - Q) \\ U_{2C} &= n_{12}^{-1}(m_{12}U_{3C} + P) \end{aligned} \quad (3.10)$$

From Equation (3.8) in Equation (3.7c) that gives quadratic equation with respect to unknown parameter U_{3C} as

$$(l_{12}^2 + m_{12}^2 + n_{12}^2)U_{3C} + 2(m_{12}P - l_{12}Q)U_{3C} + (P^2 + Q^2 - a^2n_{12}^2) = 0. \quad (3.11)$$

A solution of Equation (3.11) describes two real values U_{3C} and corresponding two values for U_{1C} and U_{2C} from Equations (3.10).

If discriminant of Equation (3.11) is less than zero, it means that the line of intersection of planes P1 and P2 will not intersect with the sphere. If discriminant is equal to zero the line of intersection of planes P1 and P2 is tangent to the surface of sphere. According to these definitions the following three cases can be described:

If $n_{12} = 0$ (Figure 5.1b), then from Equations (3.8) follow that line lie on the plane $U_{3C} = -Pm_{12}^{-1} = Ql_{12}^{-1}$ that is parallel to plane (U_1, U_2) . Substituting $U_{3C} = -Pm_{12}^{-1}$ and expression $U_{1C} = (l_{12}U_{2C} + R)m_{12}^{-1}$ from Equation (3.8c) to third Equation (3.7c) we can get quadratic equation with respect to U_{2C} as

$$(l_{12}^2 + m_{12}^2)U_{2C}^2 + 2l_{12}RU_{2C} + (P^2 + R^2 - a^2m_{12}^2) = 0. \quad (3.12)$$

Solution of Equation (3.12) describe two real values for U_{2C} , and corresponding U_{1C} can be found from Equation (3.8c) and U_{3C} from Equation (3.8a)

If $l_{12} = 0$ (Figure 5.1c), then the line lie on plane $U_{1C} = -Qn_{12}^{-1} = Rm_{12}^{-1}$ that is parallel to plane (U_2, U_3) . Using expression $U_{1C} = -Qn_{12}^{-1}$ and $U_{2C} = (m_{12}U_{3C} + P)n_{12}^{-1}$ then Equation (3.7c) yields

$$(m_{12}^2 + n_{12}^2)U_{3C} + 2m_{12}PU_{3C} + (Q^2 + P^2 - a^2n_{12}^2) = 0. \quad (3.13)$$

Solution of Equation (3.13) gives two real values for U_{3C} .

If $m_{12}=0$ (Figure 5.1d), we will get the line on the plane $U_{2C} = -Rl_{12}^{-1} = Pn_{12}^{-1}$ that is parallel to plane (U_3, U_1) . Then using expression $U_{2C} = -Rl_{12}^{-1}$ and $U_{3C} = (n_{12}U_{1C} + Q)l_{12}^{-1}$ the last equation of system Equation (3.7c) is solved respect to U_{1C} as,

$$(l_{12}^2 + n_{12}^2)U_{1C}^2 + 2n_{12}QU_{1C} + (R^2 + Q^2 - a^2l_{12}^2) = 0 \quad (3.14)$$

After solution of one of quadratic Equations (3.12-3.14) and using Equations (3.8) we can get values U_{1C} , U_{2C} , U_{3C} , and respect to Equation (3.6) are define parameters x_C , y_C , z_C . For choice one of solution of system Equations (3.7) characterizing the condition of assembly it is needed to bring in parameter $K(0,1)$ the value of that is get involved with first or second solution of system.

For having only one solution for the choice the mixed multiplication of three vectors \overline{CB} , \overline{CA} , \mathbf{e}_1 are taken in to account. If $(\overline{CB} \times \overline{CA}) \cdot \mathbf{e}_1 > 0$ we will have x_C , y_C , z_C when $K=0$, if $(\overline{CB} \times \overline{CA}) \cdot \mathbf{e}_1 < 0$ we will have x_C , y_C , z_C when $K=1$. The mixed multiplication of vectors yields:

$$L_1(N_2U_{2C} - M_2U_{3C}) + M_1(N_2U_{1C} - L_2U_{3C}) + N_1(M_2U_{1C} - L_2U_{2C}) < 0$$

3.3.2. Intersection of Two Spheres with a Plane

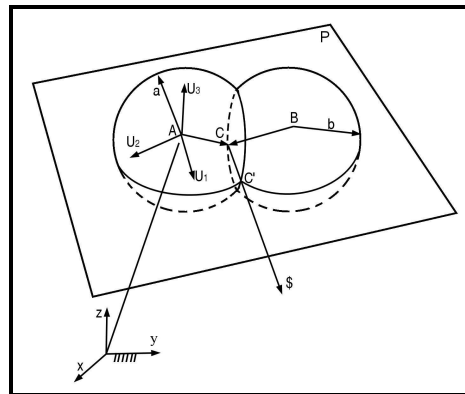


Figure 3.4. Intersection of two spheres and a plane.

Intersection of a plane with two spheres (Figure 3.4) can be introduced as

$$\begin{aligned}
 a) \quad & l_1 U_{1C} + m_1 U_{2C} + n_1 U_{3C} = d \\
 b) \quad & (x_C - x_B)^2 + (y_C - y_B)^2 + (z_C - z_B)^2 = b^2 . \\
 c) \quad & U_{1C}^2 + U_{2C}^2 + U_{3C}^2 = a^2
 \end{aligned} \tag{3.15}$$

Adding to the left part of Equations (3.15b) by expressions $\pm x_A, \pm y_A, \pm z_A$, and after some transformations we get equation of plane as intersection of two spheres, Equations (3.15) convert in the form

$$\begin{aligned}
 a) \quad & l_1 U_{1C} + m_1 U_{2C} + n_1 U_{3C} = d \\
 b) \quad & f_1 U_{1C} + f_2 U_{2C} + f_3 U_{3C} = f , \\
 c) \quad & U_{1C}^2 + U_{2C}^2 + U_{3C}^2 = a^2
 \end{aligned} \tag{3.16}$$

where, $f_1 = x_A - x_B$, $f_2 = y_A - y_B$, $f_3 = z_A - z_B$, $f = (b^2 - a^2 - f_1^2 - f_2^2 - f_3^2)/2$.

Determinations of the point of intersection of planes are calculated by using solutions of Equations (3.16).

3.3.3. Intersection of Three Spheres

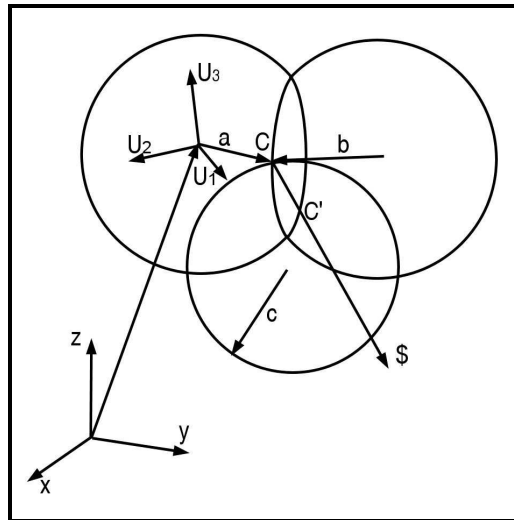


Figure 3.5. Intersection of three spheres.

The basic equations of intersection of three spheres (Figure 3.5) are given by

$$\begin{aligned}
 a) \quad & (x_C - x_D)^2 + (y_C - y_D)^2 + (z_C - z_D)^2 = c^2 \\
 b) \quad & (x_C - x_B)^2 + (y_C - y_B)^2 + (z_C - z_B)^2 = b^2 \\
 c) \quad & (x_C - x_A)^2 + (y_C - y_A)^2 + (z_C - z_A)^2 = a^2
 \end{aligned} \tag{3.17}$$

where a,b,c are radii of three intersecting spheres with coordinates of centers in points $A(x_A, y_A, z_A)$, $B(x_B, y_B, z_B)$, $C(x_C, y_C, z_C)$.

Therefore, it is required expressions of coefficients of three linear line Equations (3.8) and corresponding values of coordinates of point $C(x_C, y_C, z_C)$. Adding in the left side of Equations (3.17 a,b) by expressions $\pm x_A, \pm y_A, \pm z_A$, and after some transformations we will get the system similar (3.16) with following coefficients

$$\begin{aligned}
 d_1 U_{1C} + d_2 U_{2C} + d_3 U_{3C} &= d \\
 f_1 U_{1C} + f_2 U_{2C} + f_3 U_{3C} &= f, \\
 U_{1C}^2 + U_{2C}^2 + U_{3C}^2 &= a^2
 \end{aligned} \tag{3.18}$$

$$\begin{aligned}
 \text{where; } d_1 = x_A - x_D, d_2 = y_A - y_D, d_3 = z_A - z_D, d &= (c^2 - a^2 - d_1^2 - d_2^2 - d_3^2) / 2, \\
 f_1 = x_A - x_B, f_2 = y_A - y_B, f_3 = z_A - z_B, f &= (b^2 - a^2 - f_1^2 - f_2^2 - f_3^2) / 2.
 \end{aligned}$$

Solution of given mathematical model also come by solving quadratic Equation (3.11), where coefficients of these Equations correspond to Equations (3.18). So we can find U_{3C} , then U_{1C} and U_{2C} from Equations (3.8) and then respect to Equations (3.6) are defined coordinates (x_C, y_C, z_C) and (x_C', y_C', z_C') .

3.3.4. Intersection of Plane and Sphere

Intersection of plane and sphere is the circle as introduced in (Figure 3.6). The solution of Equations that describe connection of plane with sphere can be described as

$$\begin{aligned}
 a) \quad & l_2 U_{1C} + m_2 U_{2C} + n_2 U_{3C} = f \\
 b) \quad & U_{1C}^2 + U_{2C}^2 + U_{3C}^2 = a^2
 \end{aligned} \tag{3.19}$$

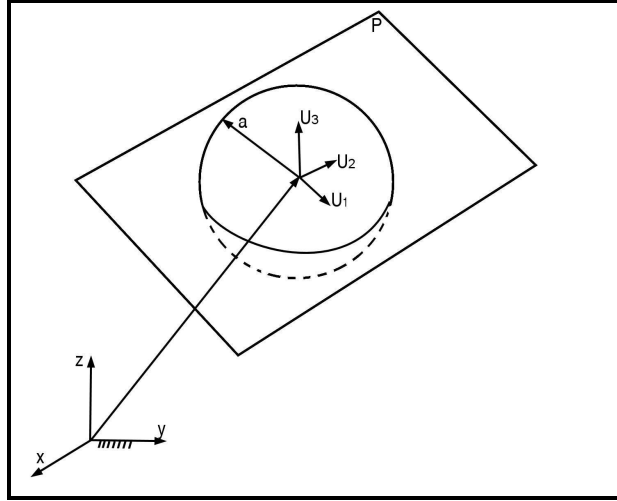


Figure 3.6. Intersection of plane and sphere.

Assume that value U_{1C} is given, then solution of Equations (3.19) respect to parameter U_{3C} yields

$$U_{3C} = (1 - l_2^2)^{-1} \left\{ (f - U_{1C} l_2) n_2 \pm m_2 \left[(1 - l_2^2)(a^2 - f^2) - (U_{1C} - l_2 f)^2 \right]^{0.5} \right\}. \quad (3.20)$$

Hence, using Equation (3.20) it has within changing of parameter U_{1C} , it means corresponding location of points as intersection plane with sphere.

CHAPTER 4

STRUCTURAL SYNTHESIS OF OVERCONSTRAINED MANIPULATORS

As a definition a multi loop manipulator can be specified as a closed loop mechanism with an end-effector that is connected to the base by at least two independent loops and its actuators should be distributed to each leg. These manipulators have some advantages when compared with serial manipulators such as higher precision, robustness, stiffness and load carrying capacity. It is also obvious that multi loop manipulators should consist of multi mobility loops. In addition, multi loop manipulators can be referred as the manipulators that have more than two legs and consist of either one platform or many platforms that are connected by hinges or branches. During the structural synthesis of overconstrained multi loop manipulators, both legs and the loops of the manipulator should be considered and the general mobility formula for multi loop manipulators with variable general constraint should also be developed.

4.1. Degree of Screw and Mathematical Models of Kinematic Pairs

In order to form a kinematic pair, exactly two rigid bodies must be contacted to each other by a surface, a line or a point. Kinematic pairs respect to their contact geometries can be divided as Type I (surface, $T_1=1$), Type II (line $T_2=2$), Type III (point, $T_3=3$). Due to the fact that the unconstrained space has six independent motions $3R$ $3P$ and kinematic pairs need constraint $C(1\div 5)$ in order to be defined properly degree of freedom $f=6-C$.

In order to define the mathematical models of the kinematic pairs by using transformation unit screw concept we will have additional input and as a result output unit screws. Thus, if the maximum DoF of kinematic pair $f_{\max}=5$, it means that the number of variables are changed from one to five. If each variable corresponds to

variable of unit screws and adding input and output unit screws we can describe maximum number of unit screws of kinematic pair as $\$_{\max}=7$.

Taking from seven, a number of constraint “C” and number of unit screw with variable pitch “S” that belong to translation motion, and adding the number of contact type “T” we obtain the following new structural formula of the degree of screw (Do\$) for kinematic pair as

$$\$ = 7 - C - S + T. \quad (4.1)$$

It is important to note that any screw that carries two independent motions as rotation around the screw axis and translation along the screw axis is called to have variable pitch. The most common kinematic pairs in all types and degree of screws are shown in Table 4.1 with their kinematic representations by using Equation (4.1).

In order to define the mathematical models of the kinematic pairs by using transformation unit screw concept, the last output screw should be defined in terms of variable “ $\tilde{}$ ” constant “ $\bar{}$ ” or dependent variable $a_{ik} = \mu \alpha_{ik}$. As seen in Table 4.1, the screw structures resemble each other but the parameter structures of all the joints are different. Assuming that the first two screws $\$_i$ and $\$_j$ are known, the final output screw can be computed by using Equation (2.17). Let’s look at the mathematical models of the first four joints in Table 4.1. The mathematical models of the revolute, prismatic, helical and cylindrical joints are introduced as $\$_k (l_k, m_k, n_k, P_k, Q_k, R_k)$ in Equation (2.17). It is clear that the mathematical models are the same for all of the four joints in terms of formulation structure, however the behavior of the parameters a_{ik} and α_{ik} are different for each joint. For instance, both of the parameters a_{ik} and α_{ik} are independent variables in cylindrical joint $C(\tilde{a}_{ik}, \tilde{\alpha}_{ik})$ while they are dependent on each other in the case of helical joint $H(\tilde{a}_{ik} = \mu \alpha_{ik})$. In the revolute joint $R(\bar{a}_{ik}, \tilde{\alpha}_{ik})$ or in the prismatic joint $P(\tilde{a}_{ik}, \bar{\alpha}_{ik})$ one of the parameters is constant and other is variable. After the sequential operations are carried out in Equation (2.17) mathematical models of the screw structure of spherical with finger joint $S_f(\tilde{\alpha}_{ik}, \tilde{\alpha}_{jk+1}, a_{ik} = a_{jk+1} = 0)$, spherical joint $S(a_{ik} = a_{jk+1} = a_{kk+2} = 0, \tilde{\alpha}_{ik}, \tilde{\alpha}_{jk+1}, \tilde{\alpha}_{kk+2})$, spherical in slot joint $S_S(\tilde{a}_{ik}, a_{jk+1} = a_{kk+2} = a_{k+1k+3} = 0, \tilde{\alpha}_{ik}, \tilde{\alpha}_{jk+1}, \tilde{\alpha}_{kk+2}, \tilde{\alpha}_{k+1k+3})$, spherical in torus joint

$S_t(\bar{a}_{jk+1}, a_{ik} = a_{kk+2} = a_{k+1k+3} = 0, \tilde{\alpha}_{ik}, \bar{\alpha}_{jk+1}, \tilde{\alpha}_{kk+2}, \tilde{\alpha}_{k+1k+3})$, spherical on plane joint $S_p(\tilde{a}_{ik}, \tilde{a}_{jk+1}, a_{k+1k+3} = a_{k+2k+4} = 0, \bar{\alpha}_{ik}, \bar{\alpha}_{jk+1}, \tilde{\alpha}_{kk+2}, \tilde{\alpha}_{k+1k+3}, \tilde{\alpha}_{k+2k+4})$ will be computed respectively.

Table 4.1. Kinematic representations of kinematic pairs.

#	Kinematic Pair	T	C	f	S	\$	Kinematic diagram
1	Revolute R	1	5	1	0	3	
2	Prismatic P	1	5	1	0	3	
3	Helical H	1	5	1	0	3	

(cont. on next page)

Table 4.1. (cont.)

4	Cylinder C	1	4	2	1	3	
5	Spherical with finger Sf	1	4	2	0	4	
6	Spherical S	1	3	3	0	5	

(cont. on next page)

Table 4.1. (cont.)

7	Spherical in slot Ss	2	2	4	1	6	
8	Spherical in torus St	2	2	4	1	6	
9	Spherical on plane Sp	3	1	5	2	7	

It is clear to note that the simple planar surface can be represented by two screws. The intersection of two planar surfaces will result in a line that can be presented by three screws and the intersection of three planar surfaces that will result in a point can be represented by four screws. In the light of these, the number of screws to define a kinematic pair is equal to the number of screws (Equation 4.1) needed to represent the orientation of its associated contact geometry.

4.2. Novel Mobility Equation of Mechanisms

Having learned the idea behind the degree of screw (Do\$) of kinematic pairs by the help of recurrent screws, the subject can be extended beyond by applying screw theory to mobility equation for the mechanisms and robot manipulators. Definition of mobility is that in any position of a mechanical system it defines the difference between the number of independent screw and number of independent differential constraint equations.

The mobility equation applies to mechanisms without exception is,

$$M = \sum_{i=1}^j \tilde{\$}_i - \sum_{K=1}^L \lambda_K, \quad (4.2)$$

where M is mobility of mechanism, $\tilde{\$}$ is number of independent unit screws, λ_K is number of independent loop-closure equations.

The Equation (4.2) can be applied to all kinematic chains and mechanisms with mixed number of space λ_K (2,3,4,5,6). If the number of λ is identical in each independent loop then Equation (4.2) becomes

$$M = \sum_{i=1}^j \tilde{\$}_i - \lambda L. \quad (4.3)$$

In this case the degree of independent screw of kinematic pair is the number of independent screw needed to describe the relative positions of pairing elements. Pairing element occurs by assembly of surfaces, lines or points of a solid body through which it may contact with another solid body. Each solid body can be described by screws \$, so the independent degree of screw ($\tilde{\$}$) of kinematic pair, Equation (4.1) can be introduced also in the following form as

$$\tilde{\$} = \$ + S - (T + 1), \quad (4.4)$$

where S is number of unit screws with variable pitch.

Combining Equations (4.4) and (4.2), we have the mobility equations with mixed or constant number of independent loop-closure equations in each independent loop in the general form as

$$M = \sum_{i=1}^j \tilde{\$}_i - \sum_{K=1}^L \lambda_K + q - j_p, \quad (4.5)$$

$$M = \sum_{i=1}^j \tilde{\$}_i - \lambda L + q - j_p, \quad (4.6)$$

where q is the number of excessive links and j_p is the number of passive joints.

The Equations (4.5) and (4.6) shows that the mobility number is associated with the motion of the kinematic pair and with the constraint of an independent loop. The conclusions of the equations (4.2-4.6) can be summarized in the following forms.

- The number of space within which the mechanism operates, λ is equal to the number of independent, scalar, differential loop-closure equations.
- The total number of independent unit screws of loop is determined by the rank of the coefficient matrix of the loop-closure equations.
- A mobility equation applicable for mixed or constant constraint reduces to Equations (4.5) or (4.6).

4.3. Simple Overconstrained Structural Groups

It is known that overconstrained manipulators can be obtained by taking appropriate overconstrained simple structural group and adding the required number of actuators. The geometry of actuator joints must be satisfied by the geometry of simple overconstrained structural group. Simple structural group is the smallest kinematic chain with zero mobility.

Let $\sum \tilde{\$}_h$, $\sum \tilde{\$}_b$ and $\sum \tilde{\$}_l$ denote the total number of independent screws of hinges, branches and legs of the manipulator respectively. A platform in subspace with general constraint one usually has j_p independent joints, that $2 \leq j_p \leq 5$. By definition, the number of independent screws follows as

$$\sum_{i=1}^j \tilde{\$} = \sum_{h=1}^{j_h} \tilde{\$}_h + \sum_{b=1}^{j_b} \tilde{\$}_b + \sum_{l=1}^{j_l} \tilde{\$}_l \quad (4.7)$$

Taking mobility $M=0$ and a number of variable pitch $S=0$ in Equation (4.3), we can reach following equation for simple structural group described in Equation (4.8).

$$\sum_{i=1}^j \tilde{\$} = \lambda L \quad (4.8)$$

The number of independent loops in a closed simple structure is obtained from Equation (4.8) as

$$L = \frac{1}{\lambda} \sum_{i=1}^j \tilde{\$}. \quad (4.9)$$

At the same time the number of independent loop in simple structural group will be

$$L = j_p - n_p - n_b - n_h, \quad (4.10)$$

where j_p is the total number of joints on the platforms, n_p is the number of platforms, n_b is the number of branches between platforms and n_h is the number of hinges between platforms.

4.4. Simple Overconstrained Structural Groups with General Constraint One

For overconstrained kinematic chain with one platform where number of joints on platform are $2 \leq j_p \leq 5$ and subspace number $\lambda = 5$, the simple structural group can be obtained by using Equations (4.10) and (4.5) respectively: $L = (1, 2, 3, 4)$, $\sum \tilde{\$} = \lambda L = (5, 10, 15, 20)$ and $j_l = j_p^{-1} \sum \tilde{\$} (2-3, 3-3-4, 2-2-4, 4-4-4-3, 4-4-4-4-4)$, where j_l

is the number of joints in the legs. Distribution of constraints in the legs for the simple structural groups with general constraint one are shown in Table 4.2 and by using these values possible structural groups with constraint conditions (see Table 3.2) are tabulated in Table 4.3.

Table 4.2. Distribution of conditions to joints of simple structural groups in $\lambda=5$

Number of legs	2	3	4	5
Number of joints attached to first condition	3	6	9	12
Number of joints attached to second condition	2	4	6	8

If we will have two or more platforms with $j_p \geq 6$ and $\lambda = 5$ connected each other by branches then the total number of legs of overconstrained simple structural group is described as,

$$n_l = j_p - 2n_b - 2n_h. \quad (4.11)$$

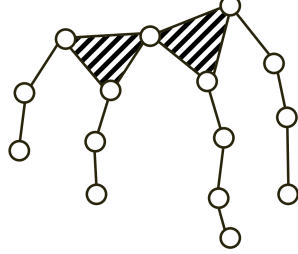
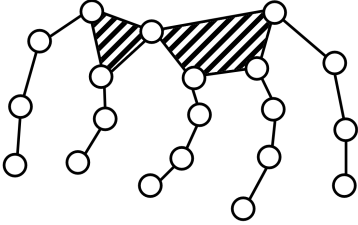
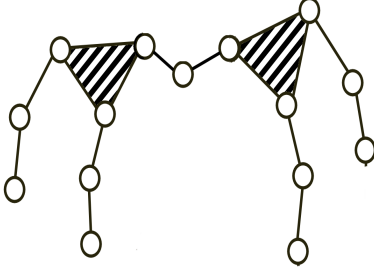
Example 4.4.1: Let's take, two platforms $n_p = 2$ with joints $j_p = (3+3)$ connected by hinge $n_h = 1$, so the number of legs is $n_l = j_p - 2n_h = 6 - 2 \cdot 1 = 4$. The number of independent loops is $L = j_p - n_p - n_b - n_h = 6 - 2 - 0 - 1 = 3$. Thus, the total number of independent screws will be calculated as $\sum \tilde{\$} = \lambda L = 5 \cdot 3 = 15$ or $\sum \tilde{\$} = \sum \tilde{\$}_l + \sum \tilde{\$}_h = 14 + 1 = 15$ and number of joints in each leg is calculated as $j_l = n_l^{-1} \sum \tilde{\$}_l = 4^{-1} \cdot 14 = (3, 3, 4, 4)$. Connections of constrained joints are shown in Table 4.4-1

Example 4.4.2: Two platforms $n_p = 2$ with joints $j_p = (3+4)$ connected by branch $n_h = 1$, so the number of legs is $n_l = j_p - 2n_h = 7 - 2 \cdot 1 = 5$ and the number of independent loops is $L = j_p - n_p - n_b - n_h = 7 - 2 - 0 - 1 = 4$. Thus, the total number of independent screws will be $\sum \tilde{\$} = \lambda L = 5 \cdot 4 = 20$ or $\sum \tilde{\$} = \sum \tilde{\$}_l + \sum \tilde{\$}_h = 19 + 1 = 20$ and number of joints in each legs is $j_l = n_l^{-1} \sum \tilde{\$}_l = 5^{-1} \cdot 19 = (3, 4, 4, 4, 4)$. Connections of constrained joints are shown in Table 4.4-2

Table 4.3. Simple structural groups with general constraint one.

L	S	j _p	Figure	j _t	Connection of joints by two conditions						
					1	2	3	4	5	6	
1	5	2		2	-2-2	-1-2	-1-1				
				3	-1-1-1	-1-1-2	-1-2-2				
2	10	3		3	-2-2-2	-1-2-2	-1-2-2	-1-1-2	-1-1-2		
				3	-1-1-1	-1-1-2	-1-1-1	-1-1-2	-1-1-1		
				4	-1-1-1-2	-1-1-1-2	-1-1-2-2	-1-1-2-2	-1-2-2-2		
				2	-2-2	-1-2	-1-1	-1-1			
				4	-1-1-1-2	-1-1-2-2	-1-2-2-2	-1-1-2-2			
				4	-1-1-1-2	-1-1-1-2	-1-1-1-2	-1-1-2-2			
3	15	4		3	-2-2-2	-1-2-2	-1-1-2	-1-1-2	-1-1-1	-1-1-1	
				4	-1-1-1-2	-1-1-2-2	-1-2-2-2	-1-1-2-2	-1-1-2-2	-1-2-2-2	
				4	-1-1-1-2	-1-1-1-2	-1-1-1-2	-1-1-2-2	-1-1-2-2	-1-1-2-2	
				4	-1-1-1-2	-1-1-1-2	-1-1-1-2	-1-1-1-2	-1-1-2-2	-1-1-1-2	
4	20	5		4	-1-2-2-2	-1-1-2-2					
				4	-1-1-2-2	-1-1-2-2					
				4	-1-1-1-2	-1-1-2-2					
				4	-1-1-1-2	-1-1-1-2					
				4	-1-1-1-2	-1-1-1-2					

Table 4.4. Simple structural groups with multiple platforms.

#	L	\$	j_p	Figure	j_l	Connection of joints by two conditions		
1	3	15	3+3		1	3	-1-1-2	
						3	-1-1-2	
					4	-1-1-2-2		
					4	-1-1-2-2		
2	4	20	3+4		1	4	-1-2-2	
						3	-1-1-1-2	
					4	-1-1-2-2		
					4	-1-1-2-2		
3	3	15	3+3		3	3	-1-1-2	
						3	1-	-1-2-2
						3	1-	-1-2-2
						3	1-	-1-1-2

Example 4.4.3: Two platforms $n_p = 2$ with joints $j_p = (3+3)$ connected by branch $n_b = 1$, with 3 joints, so the number of legs is $n_l = j_p - 2n_b = 6 - 2 \cdot 1 = 4$ and the number of independent loops is $L = j_p - n_p - n_b - n_h = 6 - 2 - 1 - 0 = 3$. Thus, after calculating total number of loops the total number of independent screws can be calculated as $\sum \tilde{\$} = \lambda L = 5 \cdot 3 = 15$ or $\sum \tilde{\$} = \sum \tilde{\$}_l + \sum \tilde{\$}_b = 12 + 3 = 15$ and the number of joints in each legs will be calculated as $j_l = n_l^{-1} \sum \tilde{\$}_l = 4^{-1} \cdot 12 = (3, 3, 3, 3)$. Connections of constrained joints are shown in Table 4.4-3.

Table 4.5. Number of simple structural groups of $\lambda=5$.

Simple Structural Groups of $\lambda=5$			2 Loops / 3Legs		3 Loops / 4Legs	4Loops / 5Legs	Number of Simple Structural Groups
	Geometry of Subspace	Symetry	3-3-4	2-4-4	4-4-4-3	4-4-4-4-4	
1	P-P	x 1	5	4	6	2	17
2	H-P	x 2	10	8	12	4	34
3	P-S	x 2	10	8	12	4	34
4	Et-P	x 2	10	8	12	4	34
5	Ec-P	x 2	10	8	12	4	34
6	H-S	x 2	10	8	12	4	34
7	H-Et	x 2	10	8	12	4	34
8	S-S	x 1	5	4	6	2	17
9	Et-S	x 2	10	8	12	4	34
10	Et-Et	x 1	5	4	6	2	17
Total			85	68	102	34	289

Example 4.4.4: As an example, single platform with three legs is selected. From Table 4.3 leg configuration is selected as 3-3-4 with condition number 4, where each leg has conditions as 1-1-2, 1-1-2, 1-1-2-2. As the overconstraint condition spherical-spherical geometry is selected. Resulted simple structural group is shown in Figure 4.1.

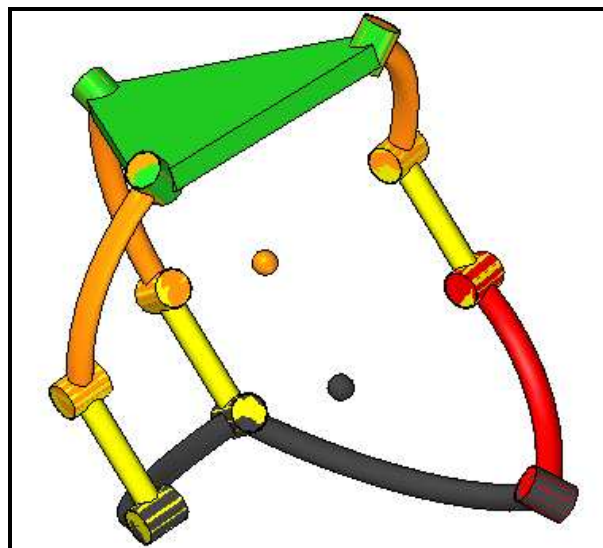


Figure 4.1. Simple structural group with one platform and three legs in $\lambda=5$.

Example 4.4.5: A two platform manipulator with four legs is selected. The shape of the simple structural group is shown in Table 4.4-1. Structural geometry is selected as spherical-spherical and conditions of these joints are described as 1 for the connection of the platforms and then 1-1-2, 1-1-2, 1-1-2-2, and 1-1-2-2 for the legs. Simple structural group with two platforms is shown in Figure 4.2.

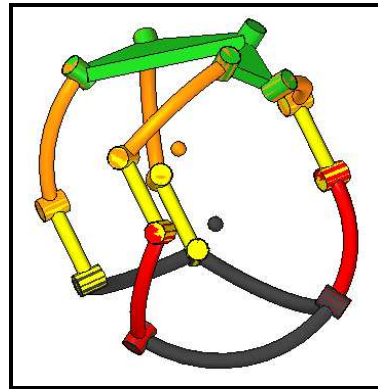


Figure 4.2. Simple structural group with two platform and four legs in $\lambda=5$.


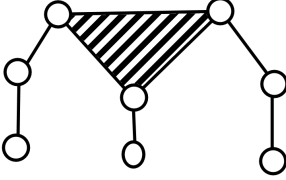
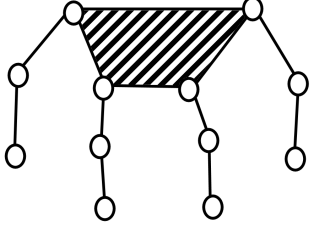
4.5. Simple Overconstrained Structural Groups with General Constraint Two

For overconstrained kinematic chain with one platform $2 \leq j_p \leq 4$ and $\lambda = 4$, the simple structural group can be obtained by using Equations (4.10) and (4.8) respectively: $L = (1, 2, 3)$, $\sum \tilde{\$} = \lambda L = (4, 8, 12)$ and $j_l = j_p^{-1} \sum \tilde{\$} (2-2, 2-3-3, 3-3-3-3)$. The distribution of conditions (see Table 3.3) to the legs of simple structural groups with general constraint two are described in Table 4.6 and Table 4.7 and possible structural groups are shown in Table 4.8.

Table 4.6. Distribution of conditions to joints of simple structural groups in $\lambda=4$

Number of legs	2	3	4
Number of joints attached to first condition	3	5	7
Number of joints attached to second condition	1	3	5

Table 4.7. Simple structural groups with general constraint two.

L	$\$$	j_p	Figure	j_l	Connection of joints by two conditions
1	4	2		2	-1-2
				2	-1-1
2	8	3		2	-1-2
				3	-1-1-2
				3	-1-1-2
3	12	4		3	-1-1-2
				3	-1-1-2
				3	-1-1-2
				3	-1-2-2

If we will have two or more platforms with $j_p \geq 6$ and $\lambda = 4$ connected each other by branches, then, the total number of legs of overconstrained simple structural group is defined as

$$n_l = j_p - 2n_b - 2n_h \quad (4.12)$$

Example 4.5.1: Two platforms $n_p = 2$ with joints $j_p = (3+3)$ connected by branch $n_h = 1$, so the number of legs will be $n_l = j_p - 2n_h = 6 - 2 \cdot 1 = 4$. Number of independent loops will be $L = j_p - n_p - n_b - n_h = 6 - 2 - 0 - 1 = 3$. Thus, the total number of independent screws will be $\sum \tilde{\$} = \lambda L = 4 \cdot 3 = 12$ or $\sum \tilde{\$} = \sum \tilde{\$}_l + \sum \tilde{\$}_b = 11 + 1 = 12$ and the number of joints in each leg will be $j_l = n_l^{-1} \sum \tilde{\$}_l = 4^{-1} \cdot 11 = (2, 3, 3, 3)$. Connections of constrained joints are shown in Figure 4.3.

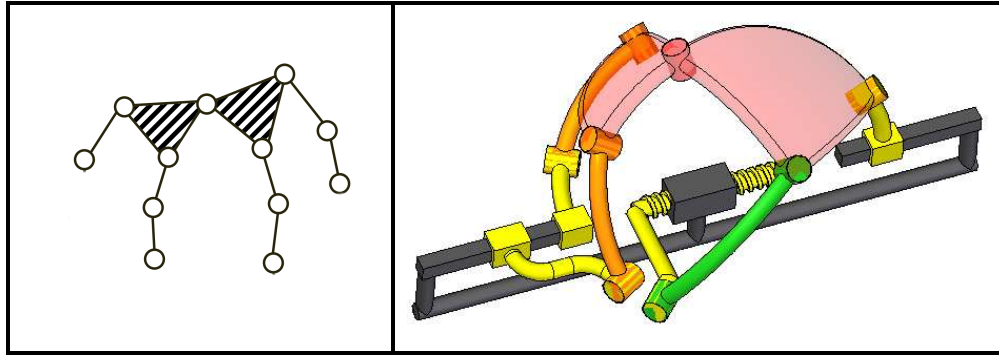


Figure 4.3. Two platform structural group with general constraint two.

Table 4.8. Number of simple structural groups of $\lambda=4$.

Simple Structural Groups of $\lambda=4$		1 Loop / 2Legs	2 Loops / 3Legs	3 Loops / 4Legs	Number of Structural Groups
	Geometry of Subspace	2-2	2-3-3	3-3-3-3	
1	Plane-Skew Line	2	1	1	4
2	Plane-Perpendicular Line	2	1	1	4
3	Plane-Parallel Line	2	1	1	4
4	Sphere-Intersecting Line	2	1	1	4
Total		8	4	4	16

Example 4.5.2: A simple structural group is used with a single platform with three legs which is described in Table 4.8 with overconstraint condition Spherical Surface - Line geometry. Resulted simple structural group is shown in Figure 4.4.

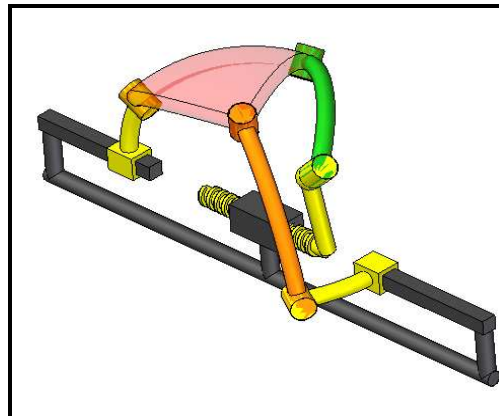


Figure 4.4. Simple structural group with one platform and three legs in $\lambda=4$.

4.6. Structural Design of Overconstrained Parallel Manipulators

To design a manipulator in a subspace, first, a motion type must be selected. Then, with respect to this motion, a suitable geometry will be decided. A structural group with decided number of platforms and number of legs must be generated as described in previous sections. Then, construction of overconstrained manipulator is just a matter of adding mobile joints to the system with suitable conditions. The constraint conditions of the loops of multi loop manipulator should be consistent. Mobility of the manipulator that will be equal to the number of input joints added to the structural group

Algorithm for the structural synthesis can be summarized as

- 1- Decision for the objective motion (m) of platform and DoF of the Manipulator.
- 2- Selection of suitable subspace geometry for the motion (λ , Chapter 3).
- 3- Determination of needed number of platforms (n_p).
- 4- Determination of number of joints on platforms (j_p).
- 5- Determination of number of legs (n_l), branches (n_b), and hinges (n_h) in the system.
- 6- Calculation of number of loops (L) (Equation 4.10).
- 7- Calculation of total number of joints to describe a simple structural group Equation (4.6).
- 8- Selection of condition combination for the joints to adapt to subspace geometry.
- 9- Addition of input joints with consistent conditions with the structural group.

Example 4.6.1: DoF of the manipulator is selected to be 3, and the subspace number should be $\lambda \geq 3$ and decided to be $\lambda=5$. There will be only one platform ($n_p=1$) with three joints ($j_p=3$). There are no branches or hinges in the system because there is only one platform, thus the number of legs will be three ($n_l=3$). The number of loops will be calculated as $L= j_p-n_p=2$. Total number of joints of the simple structural group will be $\sum \tilde{\$} = \lambda L=5 \cdot 2=10$ and distribution of joints on legs can be calculated as $j_l = j_p^{-1} \sum \tilde{\$} = (3-3-4, 2-2-4)$. From this two combination, (3-3-4) will be used for this manipulator. Structural group is constructed by selecting appropriate conditions for the joints as shown in Figure 4.5.a. Three inputs (Figure 4.5.b) will be added to the simple structural group and manipulator shown in Figure 4.5.c is constructed.

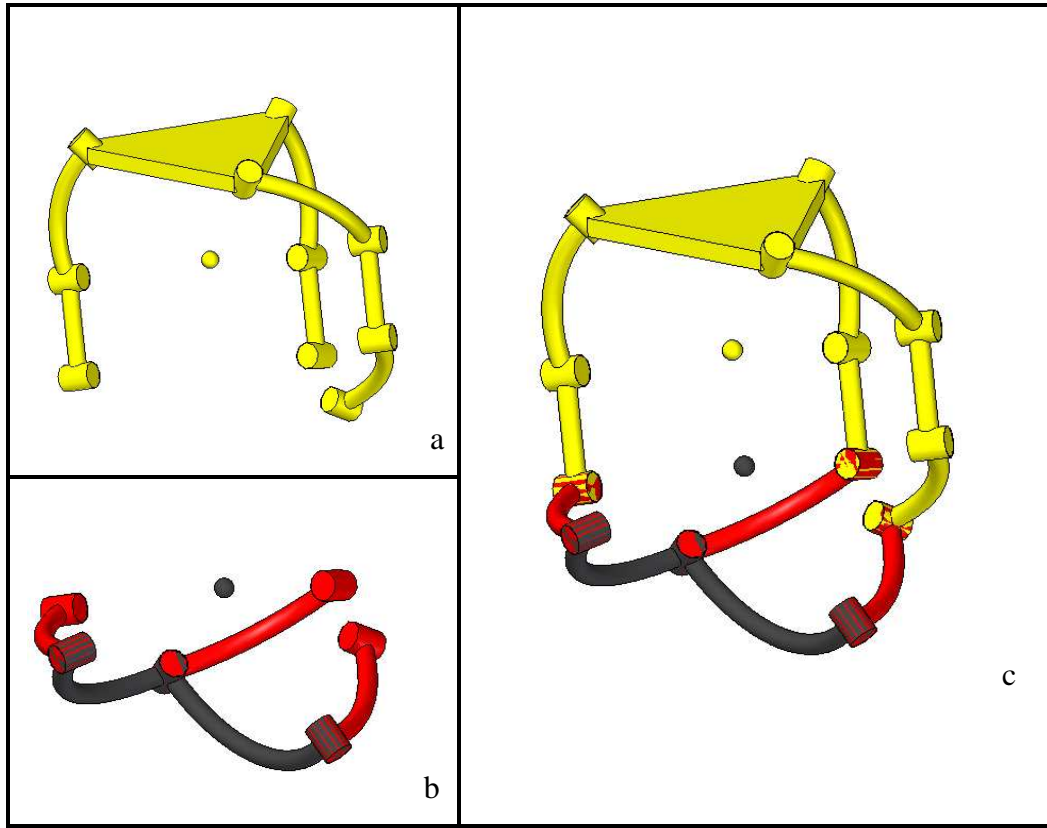


Figure 4.5. Three DoF manipulator with one platform in $\lambda=5$.

Example 4.6.2: DoF of the manipulator is selected to be 4, and the subspace number should be $\lambda \geq 4$ and decided to be $\lambda=5$. It is decided to have two platforms ($n_p=2$) and both platforms will have three joints each ($j_p=3+3=6$).

There will be no branches but one hinge will connect two platforms. The number of legs will be from Equation (4.12) ($n_l=6-2 \cdot 1=4$). Number of loops will be calculated as $L=j_p-n_p-n_h=2$. Total number of joints of the simple structural group will be $\sum \tilde{\$} = \lambda L = 5 \cdot 3 = 15$ and distribution of joints on legs will be $j_l = j_p^{-1} \sum \tilde{\$} = (3-3-4-4)$. Structural group can be constructed by selecting appropriate conditions for the joints as shown in Figure 4.6.a. Four inputs (Figure 4.6.b) will be added to the simple structural group with consistent conditions and manipulator shown in Figure 4.6.c will be constructed.

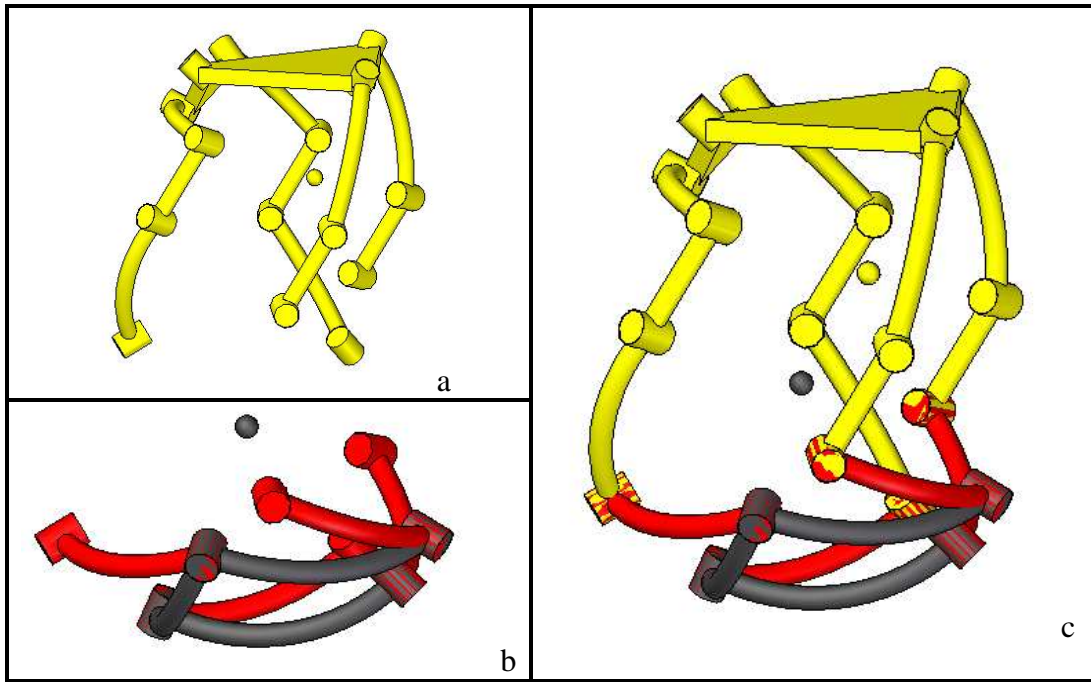


Figure 4.6. Four DoF manipulator with two platforms in $\lambda=5$.

Example 4.6.3: DoF of the manipulator is selected to be 3, and the subspace number should be $\lambda \geq 3$ and decided to be $\lambda=4$. There will be only one platform ($n_p=1$) with three joints ($j_p=3$). There are no branches or hinges in the system, number of legs will be three ($n_l=3$). The number of loops will be calculated as $L= j_p- n_p=2$. Total number of joints of the simple structural group will be $\sum \tilde{\$} = \lambda L=4 \cdot 2=8$ and distribution of joints on legs will be $j_l = j_p^{-1} \sum \tilde{\$} = (2-3-3)$. Structural group is constructed and three inputs are added to create manipulator shown in Figure 4.7.

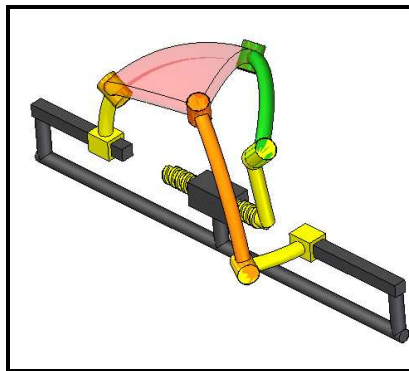


Figure 4.7. Three DoF manipulator with one platform in $\lambda=4$.

Example 4.6.3: 4 DoF manipulator is selected and the subspace number should be $\lambda \geq 3$ and decided to be $\lambda=4$. There will be two platforms ($n_p=2$) with four joints ($j_p=4$). There will be one hinge in the system, number of legs will be four ($n_l=6-2=4$). Number of loops will be calculated as $L= j_p-n_h=3$. Total number of joints of the simple structural group will be $\sum \tilde{\$} = \lambda L=4 \cdot 3=12$ and distribution of joints on legs can be calculated as $j_l = j_p^{-1} \sum \tilde{\$} = (2-3-3-3)+1$. Structural group is constructed and three inputs are added to create manipulator shown in Figure 4.8.

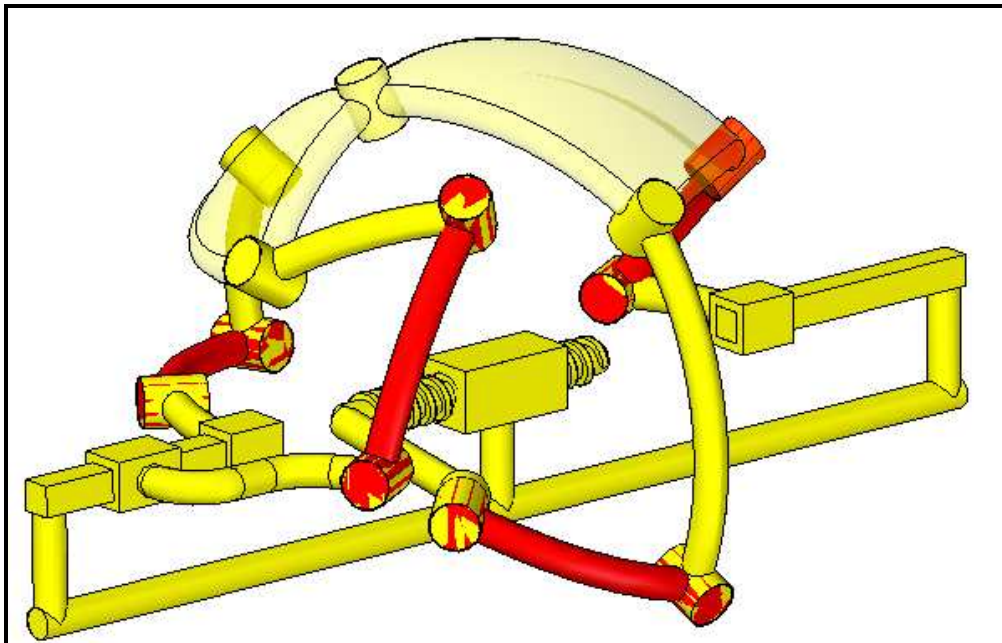


Figure 4.8. Four DoF manipulator with two platforms in $\lambda=4$

CHAPTER 5

KINEMATIC SYNTHESIS OF PARALEL MECHANISMS

In this chapter, an investigation on the function generation synthesis of overconstrained mechanisms will be presented with a novel method. Function generation synthesis method will be applied to a double spherical six bar mechanism and a planar-spherical six bar mechanism. Furthermore, a motion generation synthesis of a parallel mechanism is presented by another method.

5.1. Kinematic Synthesis of Overconstrained Mechanisms

In this section, function generation synthesis of overconstrained mechanisms will be investigated. For the synthesis, two mechanisms are used. The first one is a double spherical six bar mechanism and the second is a planar-spherical six bar mechanism. The synthesis of these kinds of mechanisms is difficult, but the mechanisms can be separated into two sections by using an imaginary joint and solved recurrently.

Two different methods as interpolation approximation and least squares approximation will be used during synthesis procedure. Theory of screws is used to derive the objective function of the planar and spherical parts of overconstrained mechanisms.

It is assumed that there are two four bar mechanisms where output of the first one is the input for the second four bar. Function generation synthesis procedure starts with a desired function as $y = f(x)$. The range of x is given as $x_0 \leq x \leq x_m$ and respectively $y_0 \leq y \leq y_m$ where $y_0 = f(x_0)$ and $y_m = f(x_m)$.

Initially, the function $y = f(x)$ is scaled for the input (ϕ) and output (ψ) of the mechanism where the range of input is $\phi_0 \leq \phi \leq \phi_m$ and range of output is $\psi_0 \leq \psi \leq \psi_m$. The scale equation will be

$$\phi = a_1 x + a_2 \quad , \quad \psi = b_1 y + b_2 \quad (5.1)$$

and the desired function for output angle will be

$$\psi = b_1 f\left(\frac{\phi - a_2}{a_1}\right) + b_2. \quad (5.2)$$

After defining the input output relations, a function is found by making synthesis of the first four bar linkage as

$$\tilde{\psi} = \psi(\phi, \mathbf{c}), \quad (5.3)$$

where $\bar{\mathbf{c}}$ is the designed construction parameters of the first four bar linkage.

After defining the output $\tilde{\psi}$ as the input of the second four bar linkage and desired output is set as $\psi = \psi(\phi)$ another synthesis operation will be done for the second four bar linkage. A function with respect to ϕ , \mathbf{c} and \mathbf{d} will be found as

$$\hat{\psi} = \psi(\phi, \mathbf{c}, \mathbf{d}), \quad (5.4)$$

where \mathbf{c} and \mathbf{d} are vector of construction parameters for the first and second four bar linkages respectively. The error in the synthesis can be calculated by the difference between designed and desired outputs as shown in Equation (5.5).

$$e = \psi - \psi(\phi, \mathbf{c}, \mathbf{d}) \quad (5.5)$$

5.1.1. Function Generation Synthesis with a Double Spherical Mechanism

Double spherical linkage is a one constrained mechanism which belongs to subspace $\lambda = 5$. It has six revolute joints whose axes are intersecting three by three in two different points as shown in Figure 5.1.

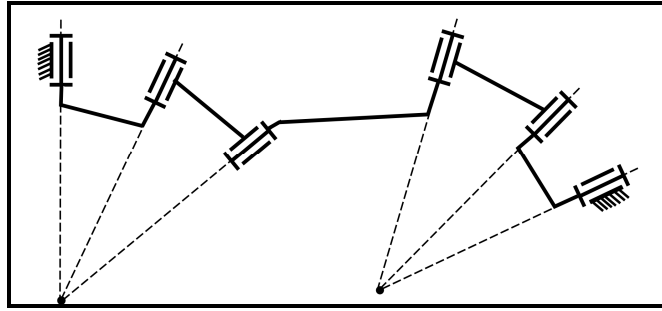


Figure 5.1. Double spherical six bar linkage.

The function generation synthesis of the double spherical linkage mechanism is described as two spherical four bar linkages. As shown in Figure 5.2 an imaginary revolute joint is attached between two parts of the mechanism that gives ability to solve the equations for the mechanism separately.

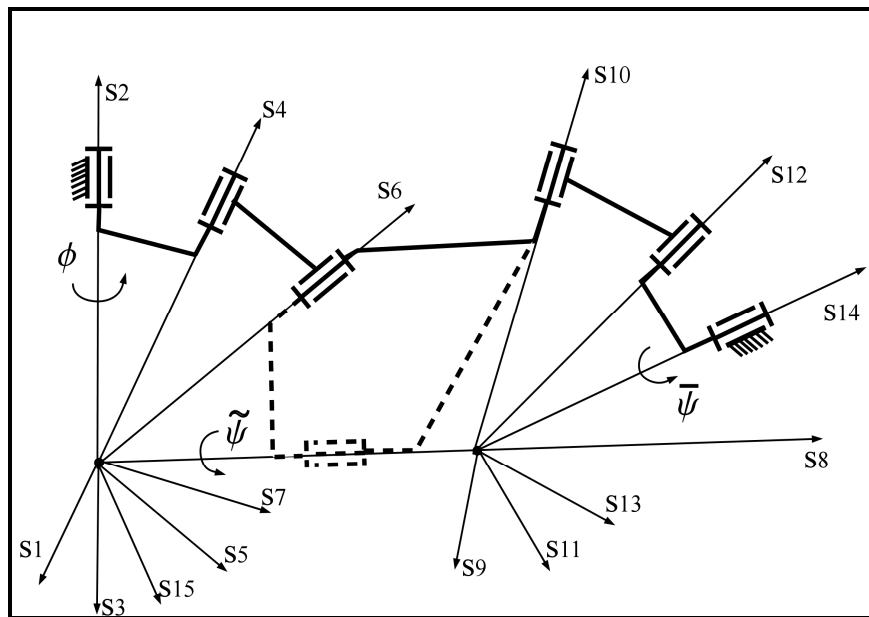


Figure 5.2. Double spherical mechanism as two spherical four bar linkages with unit vector axes.

The sequence of finding unit vectors is important to finding the objective functions of four bar linkages. Since $\mathbf{s}_1 = (1,0,0)$ and $\mathbf{s}_2 = (0,0,1)$, vector \mathbf{s}_3 will be calculated using \mathbf{s}_1 , \mathbf{s}_2 and $\alpha_{1,3}$ then \mathbf{s}_4 will be calculated using \mathbf{s}_2 , \mathbf{s}_3 , and $\alpha_{2,4}$. Vector \mathbf{s}_8 will be calculated using $\mathbf{s}_2, \mathbf{s}_1$ and $\alpha_{2,8}$ then \mathbf{s}_{15} will be calculated using \mathbf{s}_1 , \mathbf{s}_8 and $\alpha_{1,15}$.

Next, \mathbf{s}_6 will be calculated using \mathbf{s}_8 , \mathbf{s}_{15} and $\alpha_{8,6}$ for the first four link of the mechanism. Further, for the second part of the mechanism \mathbf{s}_{14} will be calculated using \mathbf{s}_8 , \mathbf{s}_1 and $\alpha_{8,14}$ then \mathbf{s}_{13} will be calculated using $\mathbf{s}_1, \mathbf{s}_{14}$, and $\alpha_{1,13}$. Vector \mathbf{s}_{12} will be calculated using \mathbf{s}_{14} , \mathbf{s}_{13} and $\alpha_{14,12}$ then \mathbf{s}_9 will be calculated using \mathbf{s}_1 , \mathbf{s}_8 and $\alpha_{1,9}$. Finally \mathbf{s}_{10} will be calculated using \mathbf{s}_8 , \mathbf{s}_9 and $\alpha_{8,10}$.

The objective function of the first four-bar will be

$$\mathbf{s}_6 \cdot \mathbf{s}_4 = C\alpha_{4,6}. \quad (5.6)$$

Substituting values of \mathbf{s}_4 and \mathbf{s}_6 and arranging will result in Equation (5.7).

$$\begin{aligned} & -C\alpha_{4,6} + C\alpha_{2,4}C\alpha_{2,8}C\alpha_{8,6} + C\alpha_{1,3}C\alpha_{8,6}S\alpha_{2,4}S\alpha_{2,8} \\ & + C\alpha_{1,3}C\alpha_{1,15}C\alpha_{2,8}S\alpha_{2,4}S\alpha_{8,6} - C\alpha_{1,15}C\alpha_{2,4}S\alpha_{2,8}S\alpha_{8,6}, \\ & + S\alpha_{1,3}S\alpha_{1,15}S\alpha_{2,4}S\alpha_{8,6} = 0 \end{aligned} \quad (5.7)$$

where the input ϕ is $\alpha_{1,3}$ and output ψ is $\alpha_{1,15}$.

The function can be written in the polynomial form if divided by $-S\alpha_{2,4}S\alpha_{8,6}$ as

$$P_0f_0(\phi) + P_1f_1(\phi) + P_2f_2(\phi) + P_3f_3(\phi) - F(\phi) = 0, \quad (5.8)$$

where $P_0 = (C\alpha_{4,6} - C\alpha_{2,4}C\alpha_{2,8}C\alpha_{8,6})S^{-1}\alpha_{2,4}S^{-1}\alpha_{8,6}$, $P_1 = -S^{-1}\alpha_{8,6}C\alpha_{8,6}S\alpha_{2,8}$, $P_2 = -C\alpha_{2,8}$, $P_3 = S^{-1}\alpha_{2,4}C\alpha_{2,4}S\alpha_{2,8}$, $f_0(\phi) = 1$, $f_1(\phi) = C\phi$, $f_2(\phi) = C\phi C\psi$, $f_3(\phi) = C\psi$, $F(\phi) = S\phi S\psi$.

For describing the objective function of second spherical four bar linkage, Equation (5.9) will be used.

$$\mathbf{s}_{12} \cdot \mathbf{s}_{10} = C\alpha_{10,12}, \quad (5.9)$$

where the input $\tilde{\psi}$ is $\alpha_{1,9}$ and output ψ is $\alpha_{1,13}$. The function can be written in the polynomial form if divided by $-S\alpha_{8,10}S\alpha_{14,12}$ to get

$$R_0 g_0(\tilde{\psi}) + R_1 g_1(\tilde{\psi}) + R_2 g_2(\tilde{\psi}) + R_3 g_3(\tilde{\psi}) - G(\tilde{\psi}) = 0, \quad (5.10)$$

where $R_0 = (C\alpha_{10,12} - C\alpha_{8,10} C\alpha_{8,14} C\alpha_{14,12}) S^{-1} \alpha_{8,10} S^{-1} \alpha_{14,12}$, $R_1 = -S^{-1} \alpha_{14,12} C\alpha_{14,12} S\alpha_{8,14}$,
 $R_2 = -C\alpha_{8,14}$, $R_3 = S^{-1} \alpha_{8,10} C\alpha_{8,10} S\alpha_{8,14}$, $g_0(\tilde{\psi}) = 1$, $g_1(\tilde{\psi}) = C\tilde{\psi}$, $g_2(\tilde{\psi}) = C\tilde{\psi} C\psi$,
 $g_3(\tilde{\psi}) = C\psi$, $G(\tilde{\psi}) = S\tilde{\psi} S\psi$.

Linear approximation will be used. For exact solution, we need 4 points of the function, thus $n=4$ and precision points are distributed with exact synthesis equally in the range of x as shown in Equation (5.11).

$$x_j = x_0 + j(x_{n+1} - x_0)/(n+1), \quad j = 1, n \quad (5.11)$$

Values of y is described for a given function as

$$y_j = f(x_j), \quad j = 0, n+1. \quad (5.12)$$

The distance between precision points will be calculated by using Equation (5.13)

$$\delta = (x_{n+1} - x_0)/(n+1). \quad (5.13)$$

The scaled equations of input and output variables are given in Equation (5.1) the constant parameters will be calculated using Equations (5.14).

$$\begin{aligned} a_1 &= -((-\phi_0 + \phi_2)/(x_0 - x_{n+1})), & a_2 &= -((x_{n+1}\phi_0 - x_1\phi_{n+1})/(x_0 - x_{n+1})) \\ b_1 &= -((-\psi_0 + \psi_{n+1})/(y_0 - y_{n+1})), & b_2 &= -((y_{n+1}\psi_0 - y_1\psi_{n+1})/(y_0 - y_{n+1})) \end{aligned} \quad (5.14)$$

General form of equations derived from the objective function is shown in equation (5.15).

$$0 = \sum_{k=0}^{n-1} P_k f_k(\phi_i) - F(\phi_i), \quad i = 1, n \quad (5.15)$$

The number of precision points is 4 thus 4 linear equations with 4 unknowns are acquired from Equation (5.15) which can be written in the matrix vector form as

$$\begin{bmatrix} f_0(\phi_1) & f_1(\phi_1) & f_2(\phi_1) & f_3(\phi_1) \\ f_0(\phi_2) & f_1(\phi_2) & f_2(\phi_2) & f_3(\phi_2) \\ f_0(\phi_3) & f_1(\phi_3) & f_2(\phi_3) & f_3(\phi_3) \\ f_0(\phi_4) & f_1(\phi_4) & f_2(\phi_4) & f_3(\phi_4) \end{bmatrix} \cdot \begin{bmatrix} P_0 \\ P_1 \\ P_2 \\ P_3 \end{bmatrix} = \begin{bmatrix} F(\phi_1) \\ F(\phi_2) \\ F(\phi_3) \\ F(\phi_4) \end{bmatrix}. \quad (5.16)$$

By multiplying both sides of Equation (5.16) with inverse of matrix $[f_{k,i}]$ results as

$$\mathbf{P} = [f_{k,i}]^{-1} \cdot \mathbf{F} \quad (5.17)$$

Values of P_i ($i=1,n$) could be found by using Equation (5.17) and which construction values of first spherical four bar can be found as shown in Equations (5.18).

$$\begin{aligned} \alpha_{2,8} &= \text{ArcCos}(-P_2), \\ \alpha_{2,4} &= \text{ArcCot}(\text{Csc}(\alpha_{2,8}) P_3), \\ \alpha_{8,6} &= -\text{ArcCot}(\text{Csc}(\alpha_{2,8}) P_1), \\ \alpha_{4,6} &= \text{ArcCos}(\text{Sin}(\alpha_{2,4}) \text{Sin}(\alpha_{8,6}) (\text{Cos}(\alpha_{2,8}) \text{Cot}(\alpha_{2,4}) \text{Cot}(\alpha_{8,6}) + P_0)). \end{aligned} \quad (5.18)$$

Solving objective function with the found parameters with respect to ϕ will give us the output as a function of input

$$\tilde{\psi} = \psi(\phi, \mathbf{c}), \quad (5.19)$$

where $\mathbf{c} = [\alpha_{2,8} \ \alpha_{2,4} \ \alpha_{8,6} \ \alpha_{4,6}]^T$.

Moreover, the error can be calculated by the difference of desired function and defined function by the first four bar linkage as shown in Equation (5.20).

$$e_1 = |\psi - \tilde{\psi}| = \left| \left(b_1 f\left(\frac{\phi - a_2}{a_1}\right) + b_2 \right) - \psi(\phi, \mathbf{c}) \right| \quad (5.20)$$

To find the mechanism that will generate minimum error an algorithm must be applied and a relation between precision points and error must be established. Precision points are selected as equally spaced in the beginning. Then the combination of each point between $\pm 0.5\delta$ range with 0.15δ step is applied to the procedure of synthesis. After each selection of precision points P_i values are controlled if they are real numbers, value of P_2 is checked if it is in the range $-1 < P_2 < 1$. If all these values are satisfied then the results of the synthesis procedure is added to a list with construction parameters and related error. Finally best approximation is selected with the criteria both minimum error and constructability.

General form of equations derived from the objective function of the second spherical four bar is shown in Equation (5.21).

$$0 = \sum_{k=0}^{n-1} R_k g_k(\tilde{\psi}_i) - G(\tilde{\psi}_i), \quad i = 1, n \quad (5.21)$$

Number of precision points is again 4 thus 4 linear equations with 4 unknowns are also acquired from Equation (5.21) which can be written in the matrix vector form,

$$\begin{bmatrix} g_0(\tilde{\psi}_1) & g_1(\tilde{\psi}_1) & g_2(\tilde{\psi}_1) & g_3(\tilde{\psi}_1) \\ g_0(\tilde{\psi}_2) & g_1(\tilde{\psi}_2) & g_2(\tilde{\psi}_2) & g_3(\tilde{\psi}_2) \\ g_0(\tilde{\psi}_3) & g_1(\tilde{\psi}_3) & g_2(\tilde{\psi}_3) & g_3(\tilde{\psi}_3) \\ g_0(\tilde{\psi}_4) & g_1(\tilde{\psi}_4) & g_2(\tilde{\psi}_4) & g_3(\tilde{\psi}_4) \end{bmatrix} \begin{bmatrix} R_0 \\ R_1 \\ R_2 \\ R_3 \end{bmatrix} = \begin{bmatrix} G(\tilde{\psi}_1) \\ G(\tilde{\psi}_2) \\ G(\tilde{\psi}_3) \\ G(\tilde{\psi}_4) \end{bmatrix}. \quad (5.22)$$

By multiplying both sides of Equation (5.22) with inverse of matrix $[g_{k,i}]$ results as,

$$\mathbf{R} = [g_{k,i}]^{-1} \cdot \mathbf{G}. \quad (5.23)$$

The values of R_i ($i=1,n$) could be found by using Equation (5.23) and which construction values of second spherical four bar can be found as shown in Equations (5.24).

$$\begin{aligned}
\alpha_{8,14} &= \text{ArcCos}(-R_2) \\
\alpha_{14,12} &= \text{ArcCot}(-R_1 / \text{Sin}(\alpha_{8,14})) \\
\alpha_{8,10} &= -\text{ArcCot}(R_3 / \text{Sin}(\alpha_{8,14})) \\
\alpha_{10,12} &= \text{ArcCos}(\text{Sin}(\alpha_{8,10})\text{Sin}(\alpha_{14,12})(\text{Cos}(\alpha_{8,14})\text{Cot}(\alpha_{8,10})\text{Cot}(\alpha_{14,12}) + R_0))
\end{aligned} \tag{5.24}$$

Solving objective function with the found parameters with respect to ϕ will give us the output as a function of input as,

$$\hat{\psi} = \psi(\phi, \mathbf{c}, \mathbf{d}), \tag{5.25}$$

where $\mathbf{d} = \{\alpha_{8,14}, \alpha_{14,12}, \alpha_{8,10}, \alpha_{10,12}\}$.

Error of the six bar mechanism can be calculated by the difference of desired function and defined function by both four bar linkage as shown in Equation (5.20).

$$e_2 = |\psi - \hat{\psi}| = \left| \left(b_1 f\left(\frac{\phi - a_2}{a_1}\right) + b_2 \right) - \psi(\phi, \mathbf{c}, \mathbf{d}) \right| \tag{5.26}$$

The same procedure to find the mechanism best suits the function with constructability is applied also to the second spherical four bar linkage. Here R_1 value is checked if it is in the range $-1 < R_1 < 1$.

Example 5.1: In the case of a numerical example function to be synthesized is selected to be $y = x^2$. Selected range of x , input angle and output angle of the desired six bar mechanism is shown in Table 5.1.

Table 5.1. Design ranges of input output parameters.

#	Range	Minimum	Maximum
1	x	1	2
2	y	1	4
3	ϕ	0.4π	π
4	ψ	0.1π	0.6π

Table 5.2. Precision points used in the synthesis.

#	Precision points	1	2	3	4
x_i	First mechanism	1.2	1.4	1.6	1.8
Δx_i	Shift for first mechanism	0	0	0	0
$\tilde{\psi}_i$	Second mechanism	1.63	2.01	2.38	2.76
$\Delta \tilde{\psi}_i$	Shift for second mechanism	-0.09	-0.09	0.05	0.13

Precision points are calculated as shown in Table 5.2. For this precision points parameters of the six bar mechanism will be; $\bar{c} = \{\alpha_{2,8} = 1.12, \alpha_{2,4} = 0.91, \alpha_{8,6} = 1.11, \alpha_{4,6} = 1.54\}$, $\bar{d} = \{\alpha_{8,1} = -0.177, \alpha_{14,12} = 0.099, \alpha_{8,10} = -0.175, \alpha_{10,12} = 0.096\}$.

In Figure 5.3 designed mechanism is shown with two intersection points.

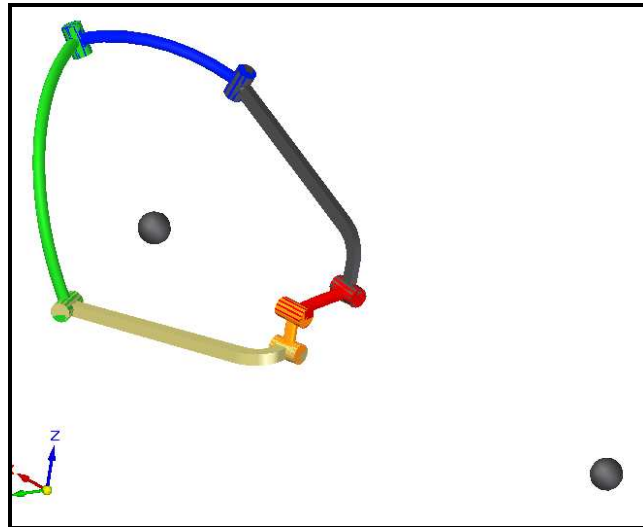


Figure 5.3. Designed double spherical six bar mechanism.

In Figure 5.4.a scaled desired function and designed function is shown for the first spherical linkage. In Figure 5.4.b error is shown and total error of first mechanism is calculated as 0.0899.

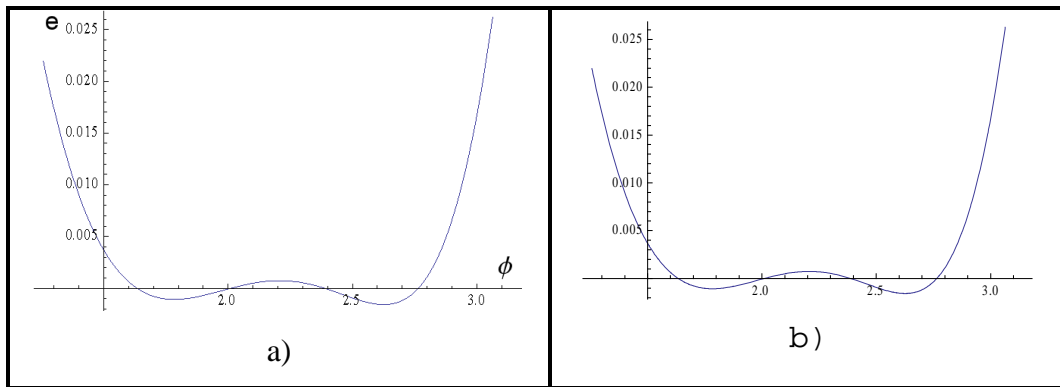


Figure 5.4. a) Designed and desired functions of first spherical linkage, b) Error of first spherical linkage.

In Figure 5.5.a, scaled desired function and designed function is shown for the second spherical linkage. In Figure 5.5.b, error of the second mechanism is shown and calculated as 0.033 and total error generated by six bar linkage is 0.113.

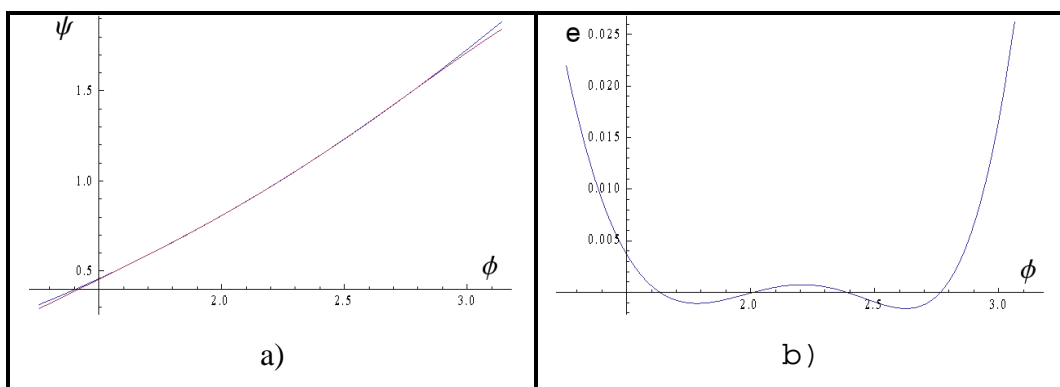


Figure 5.5. a) Designed and desired functions of 6R linkage, b) Error of 6R linkage.

5.1.2. Function Generation Synthesis with Planar Spherical Mechanism

Planar-spherical six bar is a one DoF mechanism working in subspace $\lambda = 5$. It has six revolute joints where axes of the first three are parallel and axes of other three recurrent revolute are intersecting as shown in Figure 5.6.

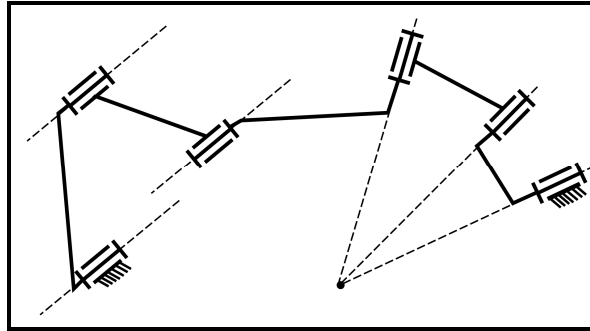


Figure 5.6. Planar-spherical six bar linkage.

The input output function synthesis of the planar-spherical linkage mechanism can be described as two four bar linkages where first is a planar four bar and second is a spherical four bar as shown in Figure 5.7.

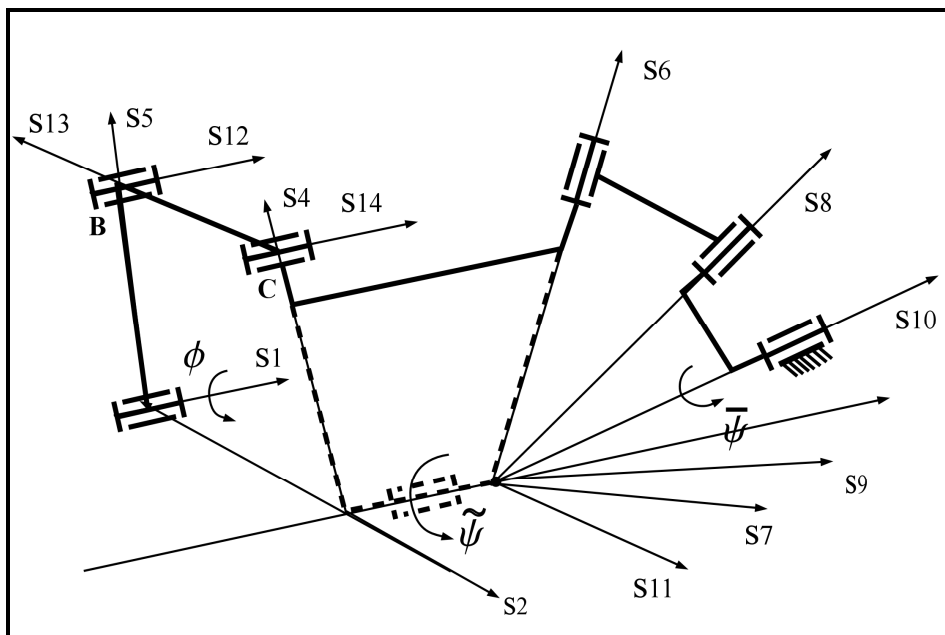


Figure 5.7. Planar-spherical mechanism shown as a planar and a spherical four bar linkages with screw axes.

The sequence of defining screws for planar-spherical linkage is as follows. $\mathbf{s}_1 = (1,0,0)$ and $\mathbf{s}_2 = (0,0,1)$ is given in x and z coordinates, \mathbf{s}_3 is parallel to \mathbf{s}_1 thus it is equal to \mathbf{s}_1 . Hence, \mathbf{s}_4 will be calculated using \mathbf{s}_2 , \mathbf{s}_3 , and $\alpha_{2,4}$. The vector \mathbf{s}_5 will be calculated using \mathbf{s}_2 , \mathbf{s}_1 and $\alpha_{2,5}$ for defining the objective function of planar four-bar

linkage part. Further, for the second part (spherical four-bar) of the mechanism \mathbf{s}_{10} will be calculated using $\mathbf{s}_3, \mathbf{s}_2$ and $\alpha_{3,10}$, then \mathbf{s}_9 will be calculated using $\mathbf{s}_2, \mathbf{s}_{10}$, and $\alpha_{2,9}$. The vector \mathbf{s}_8 will be calculated using $\mathbf{s}_{10}, \mathbf{s}_9$ and $\alpha_{10,8}$, then \mathbf{s}_{11} will be calculated using $\mathbf{s}_2, \mathbf{s}_3$ and $\alpha_{2,11}$. Finally, \mathbf{s}_6 will be calculated using $\mathbf{s}_3, \mathbf{s}_{11}$ and $\alpha_{3,6}$.

The objective function of the planar four-bar will be calculated from Equation (5.27).

$$|\mathbf{B} - \mathbf{C}| = a_{12,14} \quad (5.27)$$

\mathbf{B} and \mathbf{C} vector can be found from $\mathbf{B} = a_{1,12}\mathbf{s}_5$, $\mathbf{C} = a_{1,3}\mathbf{s}_2 + a_{3,14}\mathbf{s}_4$, Equation (5.27) can be written in open form as, $(x_B - x_C)^2 + (y_B - y_C)^2 = a_{12,14}^2$.

Substituting values of vector \mathbf{B} and \mathbf{C} in to Equation (5.27) gives us the objective function of the planar four bar linkage as,

$$-a_{12,14}^2 + a_{3,14}^2 + a_{1,12}^2 + a_{1,3}^2 - 2 a_{1,12} a_{1,3} C\alpha_{2,5} - 2 a_{3,14} a_{1,12} C(\alpha_{2,5} - \alpha_{2,4}) + 2 a_{3,14} a_{1,3} C\alpha_{2,4} = 0 \quad (5.28)$$

where the input ϕ is $\alpha_{2,5}$ and output ψ is $\alpha_{2,4}$. The function can be written in the polynomial form if divided by $2 a_{3,14} a_{1,12}$ as,

$$P_0 f_0(\phi) + P_1 f_1(\phi) + P_2 f_2(\phi) - F(\phi) = 0, \quad (5.29)$$

$$\text{where, } P_0 = \frac{-a_{12,14}^2 + a_{3,14}^2 + a_{1,12}^2 + a_{1,3}^2}{2 a_{3,14} a_{1,12}}, \quad P_1 = -\frac{a_{1,3}}{a_{3,14}}, \quad P_2 = \frac{a_{1,3}}{a_{1,12}}, \quad f_0(\phi) = 1, \quad f_1(\phi) = C\phi,$$

$$f_2(\phi) = C\psi, \quad F(\phi) = C(\phi - \psi).$$

The objective function of second spherical four bar linkage will be calculated from,

$$\mathbf{s}_{10} \cdot \mathbf{s}_8 = C\alpha_{10,8}, \quad (5.30)$$

where the input $\tilde{\psi}$ is $\alpha_{2,11}$ and output ψ is $\alpha_{2,9}$.

The function can be arranged and written in the polynomial form as

$$R_0 g_0(\tilde{\psi}) + R_1 g_1(\tilde{\psi}) + R_2 g_2(\tilde{\psi}) + R_3 g_3(\tilde{\psi}) - G(\tilde{\psi}) = 0, \quad (5.31)$$

where; $R_0 = (C\alpha_{6,8} - C\alpha_{3,6}C\alpha_{3,10}C\alpha_{10,8})S^{-1}\alpha_{3,6}S^{-1}\alpha_{10,8}$, $R_1 = -S^{-1}\alpha_{10,8}C\alpha_{10,8}S\alpha_{3,10}$,
 $R_2 = -C\alpha_{3,10}$, $R_3 = S^{-1}\alpha_{3,6}C\alpha_{3,6}S\alpha_{3,10}$, $g_0(\tilde{\psi})=1$, $g_1(\tilde{\psi})=C\tilde{\psi}$, $g_2(\tilde{\psi})=C\tilde{\psi}C\psi$,
 $g_3(\tilde{\psi})=C\psi$, $G(\tilde{\psi})=S\tilde{\psi}S\psi$.

Linear approximation will be used for the planar four bar part of the system. For exact solution, we need 3 positions of the function, thus n=3 and precision points are distributed with exact synthesis equally in the range of x. Equations (5.11-5.15) can be used also for this procedure for n=3. The number of precision points is three, thus three linear equations with three unknowns are acquired from Equation (5.29) for this case, which can be written in the matrix vector form,

$$\begin{bmatrix} f_0(\phi_1) & f_1(\phi_1) & f_2(\phi_1) \\ f_0(\phi_2) & f_1(\phi_2) & f_2(\phi_2) \\ f_0(\phi_3) & f_1(\phi_3) & f_2(\phi_3) \end{bmatrix} \begin{bmatrix} P_0 \\ P_1 \\ P_2 \end{bmatrix} = \begin{bmatrix} F(\phi_1) \\ F(\phi_2) \\ F(\phi_3) \end{bmatrix} \quad (5.32)$$

By multiplying both sides of Equation (5.32) with inverse of matrix $[f_{k,i}]$ results in Equation (5.33)

$$\mathbf{P} = [f_{k,i}]^{-1} \mathbf{F}. \quad (5.33)$$

Values of P_i (i=1,2,3) could be found by using Equation (5.33) and construction values of first planar four bar can be found as shown in Equation (5.34)

$$a_{1,3} = 1, a_{12,14} = \sqrt{a_{3,14}^2 + a_{1,12}^2 + a_{1,3}^2 - 2 a_{3,14} a_{1,12} P_0}, a_{3,14} = -\frac{a_{1,3}}{P_1}, a_{1,12} = \frac{a_{1,3}}{P_2} \quad (5.34)$$

where $a_{1,3}$ must be given as design parameter then other link length values can be found respectively.

Solving objective function with the found parameters with respect to ϕ will give us the output as a function of input as described in Equation (5.19), where $\mathbf{c} = \{a_{3,14}, a_{1,12}, a_{12,14}\}$. Then error ($e_1 = |\psi - \tilde{\psi}|$) can be calculated by the difference of desired function and defined function by planar four bar linkage as shown in Equation (5.20).

To find the mechanism that will generate minimum error an algorithm must be applied and a relation between precision points and error must be established. Precision points are selected as equally spaced in the beginning. Then the combination of each point between a range with 0.15δ step is applied to the procedure of synthesis. The ranges are $\{-0.95\delta, +0.4\delta\}$, $\{-0.6\delta, +0.6\delta\}$, $\{-0.4\delta, +0.95\delta\}$ for three precision points respectively.

After each selection of precision points, P_i ($i=1, 2, 3$) values are controlled if they are real numbers, value of P_1 is checked to be negative. If all these values are satisfied then the results of the synthesis procedure is added to a list with construction parameters and related error. Finally the best approximation is selected with the criteria both minimum error and constructability.

In the synthesis of spherical part of the mechanism number of precision points (m) wanted to be more than the number of construction parameters (n). This problem can be solved by using least square approximation method and best fitting function can be found with respect to the given design point set. The least square approximation method suggests that, when the sum of squared errors (η) is a minimum function it will be the best fitting function.

$$\eta = \sum e^2 = \sum_{i=1}^m (F(\tilde{\psi}_i, \mathbf{d}) - F(\tilde{\psi}_i))^2 \quad (5.35)$$

The minimum error is reached when the partial derivatives of Equation (5.35) with respect to construction parameters are zero.

$$\frac{\partial \eta}{\partial P_i} = 0, \quad i = 0, 1, \dots, n-1 \quad (5.36)$$

For the synthesis of spherical four bar linkage Equation (5.36) can be written in the form,

$$\eta = \sum_{i=1}^m \left(\sum_{k=0}^3 R_k g_k(\tilde{\psi}_i) - G(\tilde{\psi}_i) \right)^2 . \quad (5.37)$$

For m precision points and n = 4 parameters Equation (5.37) can be written in matrix form,

$$\sum [g_{k,i}] \cdot \mathbf{R} = [[g_{k,i}]^T \cdot \mathbf{G}_{k,i}], \quad (5.38)$$

where $G = \{[\sum_{i=1}^m g_R(\tilde{\psi}_i)G(\tilde{\psi}_i)]\}_0^3$ and $\mathbf{R} = \{R_k\}_0^3$ can be found by solving Equation (5.38) as described in Equation (5.39).

$$\mathbf{R} = [\sum_{i=1}^m g_{k,i}(\tilde{\psi}_i)] \cdot \mathbf{G} . \quad (5.39)$$

Construction values of spherical four-bar can be found from Equations (5.40).

$$\begin{aligned} \alpha_{3,10} &= \text{ArcCos}(-R_2) \\ \alpha_{10,8} &= \text{ArcCot}(-R_1 / \text{Sin}(\alpha_{3,10})) \\ \alpha_{3,6} &= -\text{ArcCot}(R_3 / \text{Sin}(\alpha_{3,10})) \\ \alpha_{6,8} &= \text{ArcCos}(\text{Sin}(\alpha_{3,6})\text{Sin}(\alpha_{10,8})(\text{Cos}(\alpha_{3,10})\text{Cot}(\alpha_{3,6})\text{Cot}(\alpha_{10,8}) + R_0)) \end{aligned} \quad (5.40)$$

Solving objective function with the found parameters with respect to ϕ will give us the output as a function of input as shown in Equation (5.25), where $\mathbf{d} = \{\alpha_{3,10}, \alpha_{10,8}, \alpha_{3,6}, \alpha_{6,8}\}$.

Error of the six bar mechanism can be calculated by the difference of desired function and defined function by both four bar linkage as shown in Equation (5.20). For finding the mechanism best suiting to the function with constructability with minimum error a random function is added to the each precision point where the range is $-1\delta < \Delta < 1\delta$ and R_2 value is checked to be in the range $-1 < R_2 < 1$ where all R_i ($i=1, 2, 3, 4$) values are real numbers.

Example 5.2; As a numerical example function to be synthesized is selected to be $y = x^2$. Selected range of x , input angle and output angle of the desired six bar mechanism is shown in Table 5.3

Table 5.3. Ranges of parameters.

#	Range	Minimum	Maximum
1	x	1	10
2	ϕ	0.1π	0.5π
3	ψ	0.05π	0.7π

Precision points are calculated as shown in Table 5.4 and Table 5.5. For this precision points parameters of the six bar mechanism will be $\mathbf{c} = \{ a_{1,3} = 1, a_{3,14} = 1.637, a_{1,12} = 1.052, a_{12,14} = 0.812 \}$, $\mathbf{d} = \{ \alpha_{3,10} = 0.858, \alpha_{10,8} = 0.1789, \alpha_{3,6} = 0.945, \alpha_{6,8} = 0.104 \}$. In Figure 5.8 the designed mechanism is shown.

Table 5.4. Precision points for the first linkage.

#	Precision points	1	2	3
x_i	Initial	3.25	5.5	7.75
Δx_i	Shift	0.225	1.035	1.8
x_i	Final	3.475	6.535	9.55

Table 5.5. Precision points of the second linkage.

Precision points	1	2	3	4	5	6	7	8	9	10
Initial	0.428	0.542	0.656	0.771	0.885	0.999	1.113	1.228	1.342	1.456
Shift	0.085	0.042	0.076	0.058	0.051	0.102	0.015	0.095	0.036	0.059
final	0.343	0.584	0.732	0.712	0.937	1.101	1.129	1.132	1.379	1.516

In Figure 5.9.a, scaled desired function and designed function are shown for the planar linkage. In Figure 5.9.b, error of planar linkage is shown and error of first mechanism is calculated as 0.675.

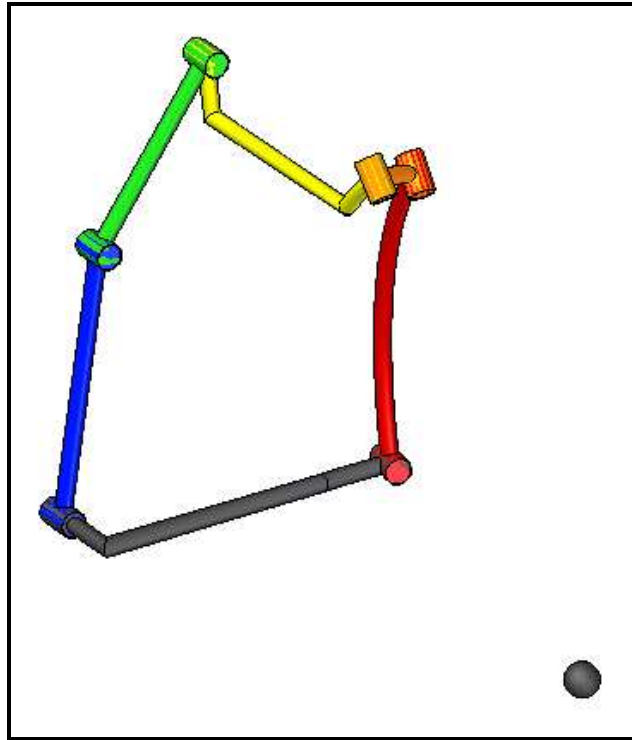


Figure 5.8. Designed planar-spherical six bar mechanism.

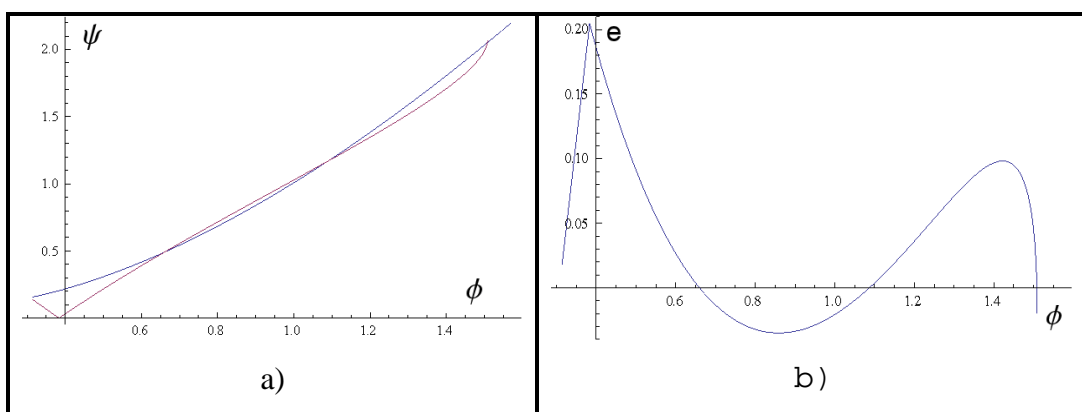


Figure 5.9. a) Designed and desired function of planar linkage, b) Error of planar linkage.

In Figure 5.10.a, scaled desired function and designed function is shown for the second spherical linkage. In Figure 5.10.b, error of second mechanism is shown and calculated as 0.213 and total error generated by six bar linkage is 0.888.

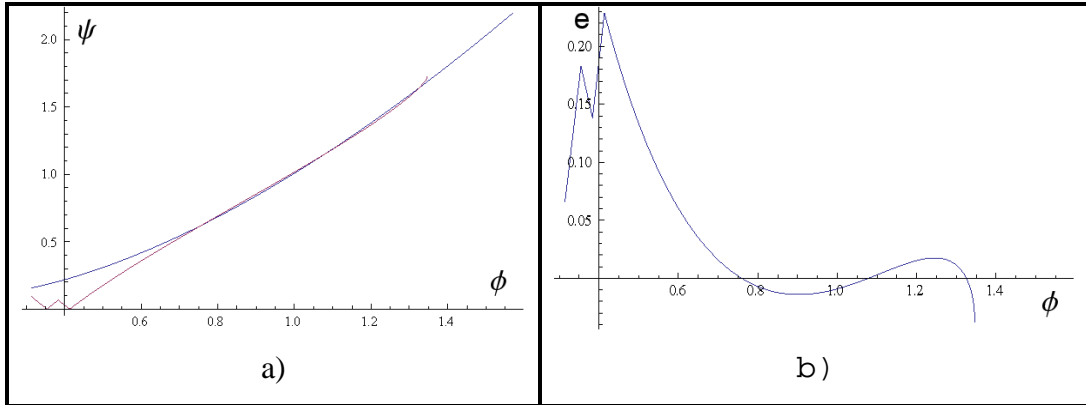


Figure 5.10. a) Designed and desired output functions of spherical linkage, b) Error of spherical linkage.

5.1.3 Motion Generation Synthesis of Planar Spherical Mechanism

In this section, motion generation of a planar-spherical mechanism is done for three positions of the end effector. The screw axes of the mechanism are shown in Figure 5.11. Mechanism is fixed to the ground from two parallel revolute joints and an end effector will be placed on the axis of the joint s_{15} . Three positions of the end effector are given as three positions for point C and three orientations of vector s_{15} .

The synthesis procedure starts with the synthesis of first leg of the planar part of the mechanism which can be defined with four parameters, two link parameters $a_{2,10}, a_{10,8}$ and two joint parameters $\alpha_{1,9}, \alpha_{9,11}$. The objective function for the first leg of the planar part will be derived from Equation (5.41).

$$a_{2,10}\mathbf{s}_9 + a_{10,8}\mathbf{s}_{11} = \mathbf{p}_C \quad (5.41)$$

If the values of vectors s_9 and s_{11} are substituted in to Equation (5.41) Equations (5.42) will be reached.

Solving the polynomial equation (5.43) for three points of ρ_C will give us parameters $\alpha_{1,9}$, $a_{2,10}$ and $a_{10,8}$. Then, a value is set for the angle $\alpha_{1,9} + \alpha_{9,11}$ is set as ϕ_1 and it will be calculated for three positions from Equation (5.44).

$$\phi_1(\rho_{CX}, \rho_{CY}) = ATan\left[\frac{(\rho_{CY} - a_{2,10}S\alpha_{1,9})/a_{10,8}}{(\rho_{CX} - a_{2,10}C\alpha_{1,9})/a_{10,8}}\right] \quad (5.44)$$

The second step is the synthesis of first leg of spherical part of the mechanism. Given parameters are $\mathbf{s} = \{s_x, s_y, s_z\}$ and input angle $\alpha_{1,11}$ which is known as ϕ_1 from Equation (5.44). Design parameters are $\alpha_{8,13}$, $\alpha_{13,15}$ and $\alpha_{11,12}$. Objective function will be found from Equation (5.45)

$$\mathbf{s} = \mathbf{s}_{15} \quad (5.45)$$

Substituting values of \mathbf{s} and \mathbf{s}_{15} into Equation (5.45) results in

$$\begin{aligned} s_x &= C_{13,15}S_{1,12}S_{8,13} + S_{13,15}(C_{8,13}C_{12,14}S_{1,12} + C_{1,12}S_{12,14}) \\ s_y &= S_{1,12}S_{12,14}S_{13,15} - C_{1,12}(C_{13,15}S_{8,13} + C_{8,13}C_{12,14}S_{13,15}) \\ s_z &= C_{8,13}C_{13,15} - C_{12,14}S_{8,13}S_{13,15} \end{aligned} \quad (5.46)$$

Eliminating $S_{12,14}$ and $C_{12,14}$ from Equations (5.46) results in

$$s_z C_{8,13} + (-s_y C_{1,12} + s_x S_{1,12})S_{8,13} - C_{13,15} = 0. \quad (5.47)$$

$\alpha_{1,12}$ can be written as $\alpha_{1,11} + \alpha_{11,12}$ and substituted into Equation (5.47) and objective function will be

$$R_0 g_0 + R_1 g_1 + R_2 g_2 = G, \quad (5.48)$$

where, $R_0 = -C_{13,15}Csc_{11,12}Csc_{8,13}$, $R_1 = Cot_{8,13}Csc_{11,12}$, $R_2 = -Cot_{11,12}$, $g_0 = 1$, $g_1 = s_x$, $g_2 = s_y C_{1,11} + s_x S_{1,11}$, $G = s_x C_{1,11} + s_y S_{1,11}$.

Solving Equation (5.48) for three positions give us three design parameters

$\alpha_{11,12}$, $\alpha_{8,13}$ and $\alpha_{13,15}$.

In the third step of synthesis, a kinematic analysis for the second leg of spherical part will be done. Constant design parameters $\alpha_{8,17}$, $\alpha_{17,15}$ and $\alpha_{7,16}$ will be given. Equation (5.49) can be written in the left part of the equation are the given orientation of the end effector and on the right part is \mathbf{s}_{15} which is calculated from the second leg by using parameters $\alpha_{8,17}$, $\alpha_{17,15}$, $\alpha_{7,16}$, $\alpha_{16,18}$ and $\alpha_{1,7}$.

$$\mathbf{s} = \mathbf{s}_{15}^* \quad (5.49)$$

From Equation (5.49) $\alpha_{16,18}$ have been eliminated and Equation (5.50) have been found.

$$s_Z C_{8,17} + (-s_Y C_{(1,7+7,16)} + s_X S_{(1,7+7,16)}) S_{8,17} - C_{17,15} = 0 \quad (5.50)$$

Equation (5.50) has been solved to find values of $\alpha_{1,7}$ for three positions of the end effector. Values of $\alpha_{1,7}$ will be used in next step as input variable.

On the last step of synthesis a close loop equation have been written for the second leg of planar part as shown in Equation (5.51)ç.

$$a_{2,4} \mathbf{s}_3 + a_{4,6} \mathbf{s}_5 + a_{6,8} \mathbf{s}_7 = \mathbf{p}_C \quad (5.51)$$

Expanding Equation (5.51) results as

$$\begin{aligned} a_{2,4} C_{1,3} + a_{4,6} C_{1,5} + a_{6,8} C_{1,7} &= \rho_{CX} \\ a_{2,4} S_{1,3} + a_{4,6} S_{1,5} + a_{6,8} S_{1,7} &= \rho_{CY} \end{aligned} \quad (5.51)$$

where $\alpha_{1,5} = \alpha_{1,3} + \alpha_{3,5}$, $\alpha_{1,7} = \alpha_{1,3} + \alpha_{3,5} + \alpha_{5,7}$. Eliminating $\alpha_{1,5}$ from Equations (5.51) will give the objective function as shown in polynomial form in Equation (5.52).

$$T_0 h_0 + T_1 h_1 + T_2 h_2 + T_3 h_3 = H, \quad (5.52)$$

where, $T_0 = 0.5(-a_{4,6}^2 + a_{2,4}^2 + a_{6,8}^2)$, $T_1 = -a_{6,8}$, $T_2 = -a_{2,4}$, $T_3 = a_{6,8}a_{2,4}$, $h_0 = 1$,
 $h_1 = \rho_{CX}C_{1,7} + \rho_{CY}S_{1,7}$, $h_2 = \rho_{CX}C_{1,3} + \rho_{CY}S_{1,3}$, $h_3 = C_{(1,7-1,3)}$, $H = -0.5(\rho_{CX}^2 + \rho_{CY}^2)$.

After giving a value for $\alpha_{1,3}$ and Equation (5.52) have been solved for three position of point C and profound three values of $\alpha_{1,7}$. Design parameters $a_{2,4}, a_{4,6}, a_{6,8}$ have been found by this process. A designed manipulator for three positions is shown in Figure 5.12.

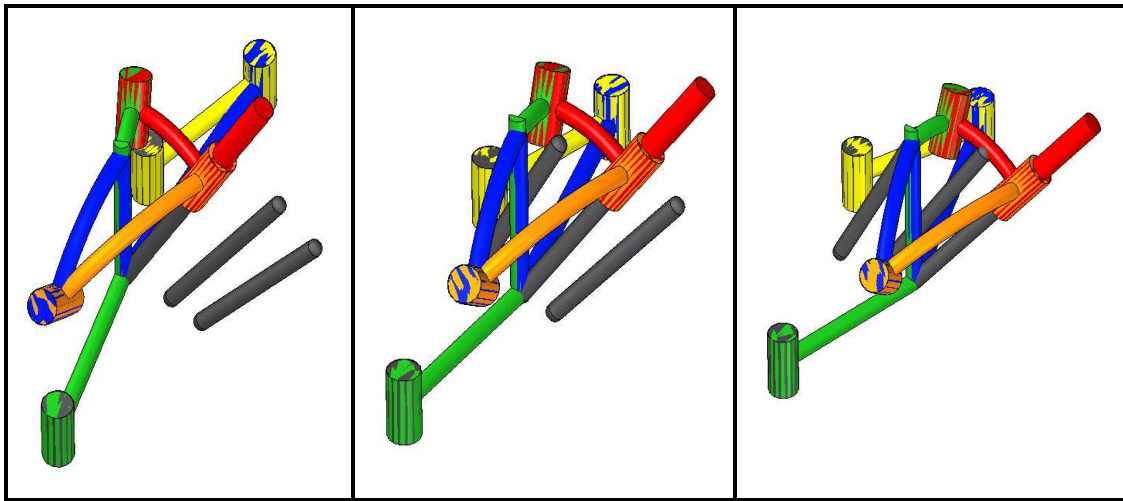


Figure 5.12. Three desired positions for the designed planar-spherical manipulator.

5.2 Kinematic Synthesis of Multi Loop Platform Mechanisms

In this section, a novel procedure for synthesis of multi loop platform mechanisms will be described with an example. Multi loop mechanism selected as example is one DoF with three legs and leg joint configurations are RS-RS-CS. In Figure 5.13, mechanism is shown with all constant (constructive) and variable parameters. Pre-designed conditions of the mechanism are that all fixed kinematic pivots, two revolute and one cylindrical has parallel axes.

Main target for synthesis is generation of a platform with three legs where center point on the platform C pass through three given points in space with coordinates $\rho_1(x_1, y_1, z_1)$, $\rho_2(x_2, y_2, z_2)$, $\rho_3(x_3, y_3, z_3)$.

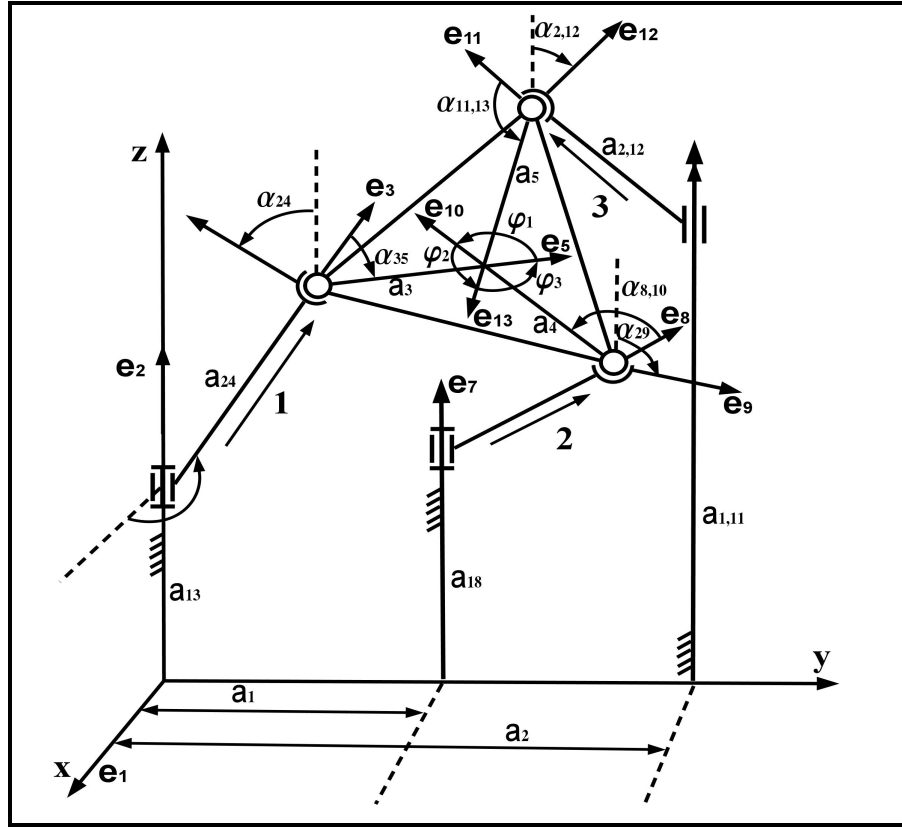


Figure 5.13. Parameters of RS-RS-CS parallel mechanism.

Synthesis problem is divided into three steps. On the first step, synthesis of kinematic chain which is denoted in Figure 5.13 as leg 1 will be described. Then, inverse task analysis will be done for this leg. On the second step leg 2 in Figure 5.13 will be solved with respect to objective functions $\mathbf{e}_{10} \cdot \mathbf{e}_5 = \cos \varphi_1$, and the synthesis parameters are a_{18}, a_{29}, a_4 . For the third step of synthesis procedure leg 3 in Figure 5.13 the objective functions $\mathbf{e}_{13} \cdot \mathbf{e}_5 = \cos \varphi_3$ and $\mathbf{e}_{13} \cdot \mathbf{e}_{10} = \cos \varphi_2$, with synthesis parameters $a_2, a_{2,12}, a_5$ will be solved. For the platform a_3, a_4, a_5 lengths are distances from edges of the triangle center C of platform and angles $\varphi_1, \varphi_2, \varphi_3$ define form of the triangle platform. To center C not to be outside of the triangle the angles $\varphi_1, \varphi_2, \varphi_3$ will not be set as synthesis parameters and they will be given as $\varphi_1 = \varphi_2 = \varphi_3 = 120^\circ$.

For the first step let solve the inverse kinematic chains of leg 1. Close loop equations from the frame to point C in the vector form can be written as,

$$\mathbf{p}_C = a_{13}\mathbf{e}_2 + a_{24}\mathbf{e}_3 + a_3\mathbf{e}_5. \quad (5.53)$$

By using recurrent screw equations values of $\mathbf{e}_2, \mathbf{e}_3, \mathbf{e}_5$ are found and substituted in Equation (5.53) and get

$$x_C = -S_{13}(a_3 C_{24} S_{35}) + C_{13}(a_{24} + a_3 C_{35}), \quad (5.54)$$

$$y_C = S_{13}(a_{24} + a_3 C_{35}) + C_{13}(a_3 C_{24} S_{35}), \quad (5.55)$$

$$z_C = a_{13} + a_3 S_{24} S_{35}. \quad (5.56)$$

Solutions of Equation (5.54) and (5.55) with respect to S_{13} and C_{13} will yield

$$S_{13} = [y_C(a_{24} + a_3 C_{35}) - x_C(a_3 C_{24} S_{35})](x_C^2 + y_C^2)^{-1}, \quad (5.57)$$

$$C_{13} = [x_C(a_{24} + a_3 C_{35}) + y_C(a_3 C_{24} S_{35})](x_C^2 + y_C^2)^{-1}. \quad (5.58)$$

If Equations (5.54-5.56) will be squared and added it will result in

$$x_C^2 + y_C^2 + (z_C - a_{13})^2 = a_{24}^2 + a_3^2 + 2a_{24}a_3 C_{35} \quad (5.59)$$

From Equation (5.59) value of C_{35} is found as

$$C_{35} = [x_C^2 + y_C^2 + (z_C - a_{13})^2 - a_{24}^2 - a_3^2](2a_{24}a_3)^{-1} \quad (5.60)$$

From known trigonometric equation $S_{35}^2 + C_{35}^2 = 1$ we can find S_{35}

$$S_{35} = \pm(1 - C_{35}^2)^{0.5}. \quad (5.61)$$

From Equation (5.56) S_{24} can be found as,

$$S_{24} = (z_C - a_{13})(a_3 S_{35})^{-1}. \quad (5.62)$$

With respect to trigonometric equation $S_{24}^2 + C_{24}^2 = 1$ we have

$$C_{24} = \pm(1 - S_{24}^2)^{0.5}. \quad (5.63)$$

Respect to values $S_{13}, C_{13}, S_{24}, C_{24}, S_{35}, C_{35}$ we can find the values of unknown angles $\alpha_{13}, \alpha_{24}, \alpha_{35}$. As a result, we get four solutions of inverse task for given values of construction parameters on leg 1. These solutions provide determination of three derived value of vector $\mathbf{e}_5\{L_5, M_5, N_5\}$ for given point $\mathbf{p}_C\{x_C, y_C, z_C\}$.

Magnitude of the value of \mathbf{e}_5 are defined by using recurrent equations and described as

$$L_5 = -S_{13}C_{24}S_{35} + C_{13}C_{35}, \quad (5.64)$$

$$M_5 = C_{13}C_{24}S_{35} + S_{13}C_{35}, \quad (5.65)$$

$$N_5 = S_{24}S_{35}. \quad (5.66)$$

Furthermore, in the second step kinematic chain of leg 2 will be investigated. Loop closure equations for the leg 2 in the vector form can be written as,

$$\mathbf{p}_C = a_1\mathbf{e}_6 + a_{18}\mathbf{e}_2 + a_{29}\mathbf{e}_8 + a_4\mathbf{e}_{10}. \quad (5.67)$$

Equation (5.67) can be written in the scalar form by substituting values of vectors as,

$$x_C = -S_{18}(a_4C_{29}S_{810}) + C_{18}(a_{29} + a_4C_{810}), \quad (5.68)$$

$$y_C = a_1 + S_{18}(a_{29} + a_4C_{810}) + C_{18}(a_4C_{29}S_{810}), \quad (5.69)$$

$$z_C = a_{18} + a_4S_{29}S_{810}. \quad (5.70)$$

Rearranging Equations (5.68-5.70) for simplicity gives us

$$a_4C_{29}S_{810} = (y_C - a_1)C_{18} - x_C S_{18}, \quad (5.71)$$

$$a_{29} + a_4C_{810} = (y_C - a_1)S_{18} + x_C C_{18}, \quad (5.72)$$

$$z_C = a_{18} + a_4S_{29}S_{810}. \quad (5.73)$$

From Equation (5.72) value of C_{810} can be written as

$$C_{810} = [(y_C - a_1)S_{18} + x_C C_{18} - a_{29}]a_4^{-1}. \quad (5.74)$$

From trigonometric relations value of S_{810} can be found as

$$S_{810} = \pm(1 - C_{810}^2)^{0.5}. \quad (5.75)$$

By using Equations (5.74) and (5.75) α_{810} can be determined. From Equations (5.71) and (5.73) C_{29} and S_{29} are derived as

$$C_{29} = [(y_C - a_1)C_{18} - x_C S_{18}](a_4 S_{810})^{-1}, \quad (5.76)$$

$$S_{29} = (z_C - a_{18})(a_4 S_{810})^{-1}. \quad (5.77)$$

By using Equations (5.76) and (5.77) α_{29} can be found. For finding variable angles α_{810} and α_{29} squares of Equations (5.71-5.73) are summed and get

$$S_{18}(y_C - a_1) + C_{18}x_C = \frac{1}{2a_{29}}[x_C^2 + (y_C - a_1)^2 + (z_C - a_{18})^2 + a_{29}^2 - a_4^2]. \quad (5.78)$$

Moreover, describing additional conditions of rigidity of triangle in point C Equation (5.79) is presented.

$$\mathbf{e}_5 \cdot \mathbf{e}_{10} = \text{Cos } \varphi_1 = -\frac{1}{2}. \quad (5.79)$$

Rearranging Equation (5.79) in another form results in

$$a_4^{-1}(\mathbf{p}_C - \mathbf{p}) \cdot \mathbf{e}_5 = \text{Cos } \varphi_1 = -\frac{1}{2}. \quad (5.80)$$

Describing Equation (5.80) in the coordinate form gives us Equation (5.81).

$$S_{18}M_5 + C_{18}L_5 = a_{29}^{-1}(L_5x_C + M_5y_C + N_5z_C + a_4 \cdot \frac{1}{2} - a_{18}N_5 - a_1M_5). \quad (5.81)$$

Solutions of Equations (5.78) and (5.81) respect to S_{18} and C_{18} yields

$$S_{18} = (0.5R_2L_5 - x_C(R_1 - a_{18}N_5 - a_1M_5)) / (a_{29}[L_5(y_C - a_1) - M_5x_C]), \quad (5.82)$$

$$C_{18} = ((y_C - a_1)(R_1 - a_{18}N_5 - a_1M_5) - 0.5R_2M_5) / (a_{29}[L_5(y_C - a_1) - M_5x_C]), \quad (5.83)$$

where $R_1 = L_5x_C + M_5y_C + N_5z_C + 0.5a_4$, $R_2 = x_C^2 + (y_C - a_1)^2 + (z_C - a_{18})^2 + a_{29}^2 - a_4^2$.

From Equations (5.82) and (5.83) angle α_{18} can be found. By using trigonometric identity $S_{18}^2 + C_{18}^2 = 1$ and Equations (5.82) and (5.83) objective functions for synthesis of parameters a_{18}, a_{29}, a_4 can be defined as

$$\begin{aligned} &0.25R_2^2(L_5^2 + M_5^2) + (R_1 - a_{18}N_5 - a_1M_5)^2[x_C^2 + (y_C - a_1)^2] \\ &- R_2(R_1 - a_{18}N_5 - a_1M_5)[L_5x_C + M_5(y_C - a_1)] = a_{29}^2[L_5(y_C - a_1) - M_5x_C]^2. \end{aligned} \quad (5.84)$$

After setting an arbitrary design parameter for a_1 , using a numerical method system of three nonlinear equations for given three parameters can be solved to determine a_{18}, a_{29}, a_4 . Output coordinates of unit vector $\mathbf{e}_{10}\{L_{10}, M_{10}, N_{10}\}$ are calculated using recurrent equations to get

$$L_{10} = -S_{18}C_{29}S_{810} + C_{18}C_{810}, \quad (5.85)$$

$$M_{10} = C_{18}C_{29}S_{810} + S_{18}C_{810}, \quad (5.86)$$

$$N_{10} = S_{29}S_{810}. \quad (5.87)$$

For the third step of the task kinematic chains of leg 3 is described and loop closure equations are found as

$$a_5C_{2,12}S_{11,13} = (y_C - a_2)C_{1,11} - x_C S_{1,11} \quad (5.88)$$

$$a_{2,12} + a_5C_{11,13} = (y_C - a_2)S_{1,11} + x_C C_{1,11}, \quad (5.89)$$

$$a_5S_{2,12}S_{11,13} = z_C - a_{1,11}, \quad (5.90)$$

From Equation (5.89) value of $C_{11,13}$ can be found as

$$C_{11,13} = [(y_C - a_2)S_{1,11} + x_C C_{1,11} - a_{2,12}]a_5^{-1} \quad (5.91)$$

Value of $S_{11,13}$ can be found using Equation (5.91) and trigonometric identity.

$$S_{11,13} = \pm(1 - C_{11,13}^2)^{0.5} \quad (5.92)$$

From (5.76) and (5.78) values of $C_{2,12}$ and $S_{2,12}$ can be defined as

$$C_{2,12} = [(y_C - a_2)C_{1,11} - x_C S_{1,11}](a_5 S_{11,13})^{-1} \quad (5.93)$$

$$S_{2,12} = (z_C - a_{1,11})(a_5 S_{11,13})^{-1} \quad (5.94)$$

By using the values of $S_{11,13}$, $C_{11,13}$, $C_{2,12}$ and $S_{2,12}$ angles $\alpha_{11,13}$ and $\alpha_{2,12}$ can be determined. For eliminating angles $\alpha_{11,13}$, $\alpha_{2,12}$ Equations (5.88) to (5.90) are squared and then summed as

$$S_{1,11}(y_C - a_2) + C_{1,11}x_C = \frac{1}{2a_{2,12}} [(z_C - a_{1,11})^2 + (y_C - a_2)^2 + x_C^2 + a_{2,12} - a_5^2]. \quad (5.95)$$

Then two conditions from the rigidity of triangle platform are described in Equations (5.96, 5.97) as

$$\mathbf{e}_{13} \cdot \mathbf{e}_5 = \text{Cos } \varphi_3 = -0.5, \quad (5.96)$$

$$\mathbf{e}_{13} \cdot \mathbf{e}_{10} = \text{Cos } \varphi_2 = -0.5 \quad (5.97)$$

or

$$[(\mathbf{p}_C - \mathbf{p}) \cdot \mathbf{e}_5]a_5^{-1} = -0.5, \quad (5.98)$$

$$[(\mathbf{p}_C - \mathbf{p}) \cdot \mathbf{e}_{10}]a_5^{-1} = -0.5. \quad (5.99)$$

Equations (5.98, 5.99) can be described in coordinate form as follows

$$a_{2,12}C_{1,11}L_5 + (a_2 + a_{2,12}S_{1,11})M_5 + a_{1,11}N_5 = \boldsymbol{\rho}_C \cdot \mathbf{e}_5 + \frac{a_5}{2}, \quad (5.100)$$

$$a_{2,12}C_{1,11}L_{10} + (a_2 + a_{2,12}S_{1,11})M_{10} + a_{1,11}N_{10} = \boldsymbol{\rho}_C \cdot \mathbf{e}_{10} + \frac{a_5}{2}. \quad (5.101)$$

If Equation (5.100) multiplied by N_{10} and Equation (5.101) multiplied by N_5 and subtracted from other, Equation (5.102) will be found.

$$\begin{aligned} & a_{2,12}C_{1,11}(L_5N_{10} - L_{10}N_5) + (a_2 + a_{2,12}S_{1,11})(M_5N_{10} - M_{10}N_5) \\ & = (\boldsymbol{\rho}_C \cdot \mathbf{e}_5)N_{10} - (\boldsymbol{\rho}_C \cdot \mathbf{e}_{10})N_5 + \frac{a_5}{2}(N_{10} - N_5). \end{aligned} \quad (5.102)$$

Equations (5.100, 5.102) can be described in the following form as

$$S_{1,11}M_5 + C_{1,11}L_5 = \frac{1}{a_{2,12}}(\boldsymbol{\rho}_C \cdot \mathbf{e}_5 + \frac{a_5}{2} - a_2M_5 - a_{1,11}N_5), \quad (5.103)$$

$$\begin{aligned} & S_{1,11}(M_5N_{10} - M_{10}N_5) + C_{1,11}(L_5N_{10} - L_{10}N_5) \\ & = \frac{1}{a_{2,12}}[\boldsymbol{\rho}_C \cdot \mathbf{e}_5N_{10} - \boldsymbol{\rho}_C \cdot \mathbf{e}_{10}N_5 + \frac{a_5}{2}(N_{10} - N_5) - a_2(M_5N_{10} - M_{10}N_5)]. \end{aligned} \quad (5.104)$$

Solution of Equations (5.103) and (5.104) with respect to $S_{1,11}$ and $C_{1,11}$ define two expressions as

$$S_{1,11} = \frac{R_3 + \frac{a_5}{2}(L_5 - L_{10}) - a_{1,11}R_4}{a_{2,12}R_5} - \frac{a_2}{a_{2,12}}, \quad (5.105)$$

$$C_{1,11} = \frac{R_6 - \frac{a_5}{2}(M_5 - M_{10}) + a_{1,11}R_1}{a_{2,12}R_5}, \quad (5.106)$$

where $R_3 = \boldsymbol{\rho}_C \cdot \mathbf{e}_{10}L_5 - \boldsymbol{\rho}_C \cdot \mathbf{e}_5L_{10}$, $R_4 = L_5N_{10} - L_{10}N_5$, $R_5 = L_5M_{10} - L_{10}M_5$,
 $R_6 = -\boldsymbol{\rho}_C \cdot \mathbf{e}_{10}M_5 + \boldsymbol{\rho}_C \cdot \mathbf{e}_5M_{10}$, $R_7 = M_5N_{10} - M_{10}N_5$.

From the values of $S_{1,11}$ and $C_{1,11}$, value of $\alpha_{1,11}$ can be found. Using trigonometric identity $S_{1,11}^2 + C_{1,11}^2 = 1$ we get equations with respect to $a_{1,11}$ as

$$a_{1,11}^2(R_4^2 + R_7^2) + 2a_{1,11}(R_7R_9 - R_4R_8 + a_2R_5R_4) + R_8^2 + R_9^2 - 2a_2R_8R_5 + R_5^2(a_2^2 - a_{2,12}^2) = 0, \quad (5.107)$$

where $R_8 = R_3 + \frac{a_5}{2}(L_5 - L_{10})$, $R_9 = R_6 - \frac{a_5}{2}(M_5 - M_{10})$.

If we use the values $S_{1,11}$ and $C_{1,11}$ from Equations (5.105) and (5.106) in (5.95) we get other expressions for determination of $a_{1,11}$.

$$a_{1,11} = R_{11} / R_{12} \quad (5.108)$$

where

$$R_{11} = [2a_2R_8R_5 - R_8^2 - R_9^2 - R_5^2(a_2^2 - a_{2,12}^2)] \frac{R_5}{2} - [x_C R_9 - \frac{R_5 R_{10}}{2} + (y_C - a_2)(R_8 - R_5 a_2)](R_4^2 + R_7^2)$$

$$R_{12} = (R_7 R_9 - R_4 R_8 + a_2 R_5 R_4) R_5 - [(y_C - a_2) R_4 - R_5 z_C - x_C R_7](R_4^2 + R_7^2)$$

Equation (5.108) is objective function for synthesis parameters $a_2, a_{2,12}, a_5$, a numerical method is used to find $\mathbf{p}_C(x_C, y_C, z_C)$ and three non linear equations are solved with respect to three construction parameters.

Thus, the synthesis parameters in this mechanism are $a_{18}, a_{29}, a_4, a_2, a_{2,12}, a_5$ and will be given arbitrarily in the design process. Other construction parameters are $a_{13}, a_{24}, a_3, a_1, \varphi_1, \varphi_2, \varphi_3$. The designed mechanism gives to the center C generates given three point in space \mathbf{p}_C . The variable parameters are determined from expressions given above. Numerical example for solving this task respect to 6 parameters is given in Table 5.6. Here x_i, y_i, z_i are given parameters of the task, but $a_{18}, a_{29}, a_4, a_2, a_{2,12}, a_5$ are parameters found from synthesis. Designed Parallel mechanism is shown in Figure 5.14.

Table 5.6. Parameters of the synthesis and construction.

Given points of center C				Arbitrary parameters	
	x_i	y_i	z_i	$a_{1,3}$	1.0
1	0.44558	2.793871	1.1025453	$a_{2,4}$	2.0
2	-0.0262626	3.293184	1.257827	a_3	1.73205
3	0.0730888	3.140754	2.184055	a_1	4.0
Synthesized parameters					
$a_{1,8}$	$a_{2,9}$	a_4	a_2	$a_{2,12}$	a_5
2.0	1.0	1.73205	4.5	2.0	1.73205

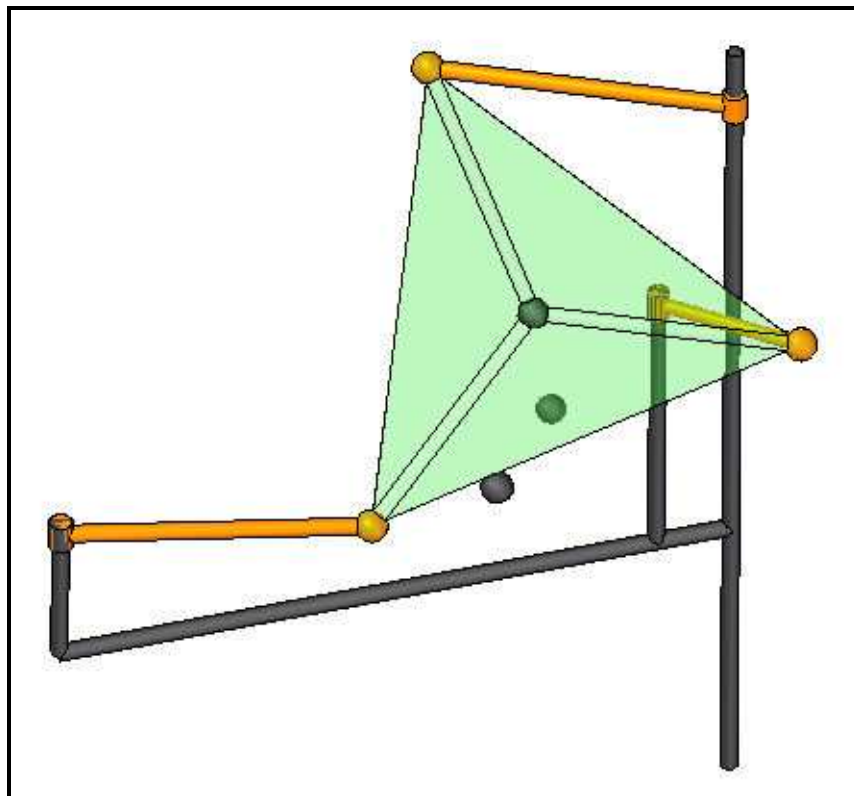


Figure 5.14. Designed parallel mechanism with three objective points.

CHAPTER 6

AN EXPERIMENTAL CHARACTERIZATION OF EARTHQUAKE EFFECTS ON MECHANISM OPERATION BY USING A PARALLEL MANIPULATOR

In the last decade parallel manipulators have been proposed for new application areas because of their better characteristics such as higher stiffness, velocity and acceleration motion, and payload capacity, with respect to those of serial manipulators. In this thesis these properties of parallel manipulators have been used to investigate experimentally the effects of earthquakes on the operation of mechanical systems by the help of CaPaMan (Cassino Parallel Manipulator), which is a 3 DoF robot designed in 1997, (Ceccarelli 1997). CaPaMan being a less degree of freedom manipulator and having similar properties with overconstrained manipulators is the motivation to use it.

For investigating the earthquake characteristics and earthquake resistant constructions, earthquake simulators are commonly used for experimental tests in the field of Civil Engineering. For dynamic testing of structures subjected to earthquake accelerations and for experimenting effects on structures small scale uni-axial servo-hydraulic seismic simulators have become popular as shown by Conte and Trombetti (2000) and Kuehn et al. (1998). A number of new large scale seismic simulator facilities have recently been, presented as in the works of Crewe and Severn (2001), Ogawa et al. (2001) and Shortreed et al. (2001). Furthermore some exceptional simulators are also made for outdoor even with 6 DoF motion in the studies of Bruneau et al. (2002). It is important to have earthquake simulators that can reproduce earthquakes with main real characteristics. Generally, most of the earthquake simulators are shaking tables, which are actuated by hydraulic actuators fixed on the base. High payload capacity, high motion speeds, and high accelerations are the main characteristics of the shaking tables but they refer to seismic translational motions only.

A new earthquake simulator is a suitable application of CaPaMan which can simulate not only translational motion but also 3D waving motions of earthquakes. Performances and suitable formulation for the operation of CaPaMan as earthquake simulator have been presented by theoretical investigations and experimental

validations in the works of Ceccarelli et al. (1999, 2002), Ottaviano and Ceccarelli (2006) and Carvalho and Ceccarelli (2002). In fact, the operation of CaPaMan can be easily adjusted to obtain any kind of earthquake in terms of magnitude, frequency and duration by giving suitable input motion.

A novel field of interest can be recognized in investigating the effects of earthquake motion on the operation of machinery. Although vibrations and their isolations are well known as affecting the machinery operation, the specific characteristics of earthquake actions on machinery are not yet fully explored. In previous works of Selvi and Ceccarelli (2010), the effects of earthquakes on mechanism operation are shown with experiments on a slider-crank mechanism and a robotic hand.

In this chapter of the thesis the effects of earthquake on the operation of mechanical systems have been investigated by an analysis and reproduction of an earthquake motion. This chapter illustrates a specific activity that has been focused in determining experimentally the effects of earthquake motion on mechanism operation by looking at the changes in the motion (acceleration) or force outputs of the mechanisms. Experimental tests have been carried out by using a slider-crank linkage with dc and servo motors, robot leg linkage, a small car model, and LARM Hand as test-bed mechanisms with acceleration or force sensors.

6.1. Earthquake Motion Characteristics

A sudden and sometimes catastrophic movement of a part of the surface of the Earth is called an earthquake which results from the dynamic release of elastic strain energy that radiates seismic waves. Large earthquakes can cause serious destruction and massive loss of life through a variety of types of damage such as fault rupture, vibratory ground motion, inundation, various kinds of permanent ground failure, and fire or a release of hazardous materials, but even buildings/constructions collapses and vehicles/machinery operations crashes. Ground motion is the dominant and most widespread cause of damages as interpreted in the study of Chen and Scawthorn (2003).

In general an earthquake has three phases such as an initial phase, which corresponds to the beginning of the seismic motion, an intermediate phase where the maximum acceleration peaks and displacements occur and a final phase representing the end of the earthquake. Main characteristics of an earthquake are frequency, amplitude

and acceleration magnitude, since the resonance of a system is determined by frequency value, duration of the stress action due to a seismic motion, amplitude and acceleration magnitude of an earthquake.

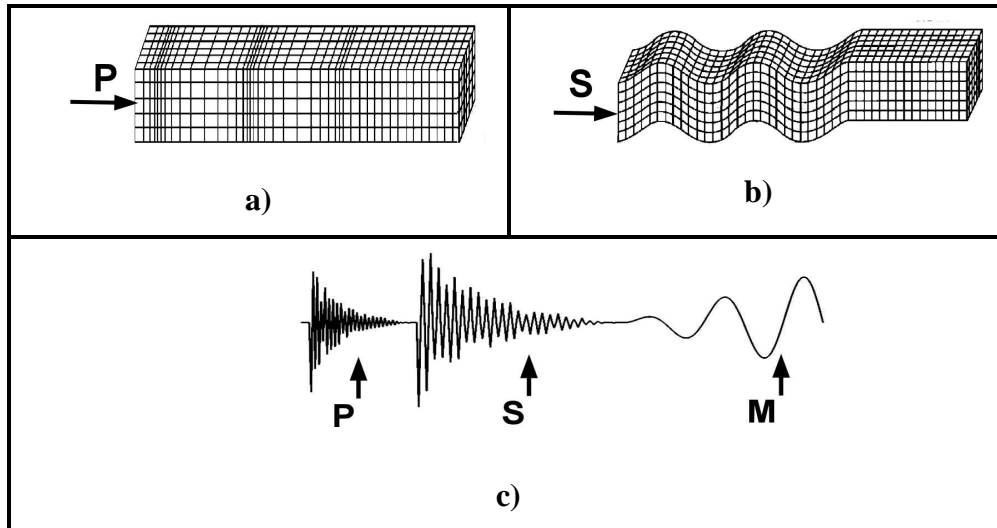


Figure 6.1. Basic characteristics of seismic waves; a) Compression and expansion waves, b) Transversal waves, c) Types of seismograms (Source: Carvalho and Ceccarelli 2002).

The period of a seismic cycle and characteristic length for each seismic wave must be identified to define the seismic motion. As shown in Figure 6.1, main types of seismic waves can be considered as the compression expansion waves P, transversal waves S, and superficial waves M. They can be classified by referring to the spread speed and terrain movements. S waves are transversal waves and the usual period of the S waves is between 0.5 and 1 second. The P waves spread through a spring-like-motion with a typical period between 0.1 and 0.2 second. Both P and S waves occur close to the epicenter. Unlike P and S waves, M waves occur on the surface of the terrain at a considerable distance from the epicenter of the earthquake and usually they have a period from 20 second to 1 minute. In Figure 6.1.c main differences among the seismic waves are represented in terms of acceleration magnitude and characteristic period of oscillating motion, which is responsible of a periodical excitation of structures that can be damaged when resonance situation occurs.

Usually, critical resonant motion is analyzed in terms of translational seismic components, but even angular motion can strongly contribute to the resonant excitation. Thus, unlike most of the simulators where the 3D motion of the terrain due to

earthquake waves has not been taken into account in this study 3D motion capability of CaPaMan parallel manipulator have been used to simulate earthquake motion with its full motion effects.

6.2. Operation of Mechanisms

As mentioned in the IFToMM terminology (2003) a machine is “*a mechanical system that performs a specific task, such as the forming of material, and the transference and transformation of motion and force.*” and mechanism is defined as a “*constrained system of bodies designed to convert motions of, and forces on, one or several bodies into motions of, and forces on, the remaining bodies*”. Mechanisms, which can be considered the core parts for machines are combination of gears, cams, linkages, springs etc.

Operation of mechanisms can be characterized by input, task and output. Task and output of mechanisms can differ with respect to desired results. These desired results are task goals for mechanisms, which can be classified as function generation, point guidance and body guidance. Considerations for designing mechanisms for those and other tasks are related to characteristics of operation such as general operation performance, repeatability of operation frequency, efficiency, reliability, precision and accuracy. Also vibrations that can occur during the operation can be considered and some isolation can be applied to machine basements.

Machinery operations are usually aimed to perform motions and actions with the task performance that are related to the machinery aim and also interaction with users and environments. The machinery aim can be in general understanding as described by mechanical properties whose performance indices can be expressed in term of motion characteristics and action transmission with efficiency features both from kinematical and energy view points. Machinery interactions can be understood as related to the effects toward the surrounding environment and mainly as from the viewpoint of human-machine interactions. Those last features will include issues on comfort and safety that can make strong constraints to machinery operations with limited range of feasible operations. Thus, machinery operations can be described and characterized by performance indices which can be formulated for general but specific aspects that permit both design procedures towards optimal solutions and experimental

control/monitoring of successful operation. Special attention is today addressed to safety as interaction with human users, even when using a machine under critical, risky situations which can be characterized by impact, high accelerations or changed operation outputs. Also efficiency in force transmission and energy consumption is of great importance in modern machinery.

Unfortunately in general the effects of earthquakes are neglected during machine design. The difficulty to determine the effects of the earthquakes is due to different types of totally random waves caused by them, as mentioned in Section 6.2.

An illustrative example for machinery operation can be given as referring to the running of a train. Input for trains is the action of actuators for wheel motion. Task for the train is the body guidance of the train and the output is a stable motion with the features comfort, safety, efficiency and reliability. A general operation performance of the train is related to vibrations which effect also comfort. Characteristics of train motions are strongly affected by actions on machinery operations. Comfort in train task is felt by human users mainly in terms of acceleration of the train cars. But this task efficiency is a result from the transmission of motions and forces from the mechanism for the wheel actuation and car guidance in relative motion during the run. Those characteristics are demanded in more robust outputs in faster trains. Any disturbance can produce not only uncomfortable operation, but even risks of disasters in train run, as it can be the case of an earthquake.

For a mechanism it is necessary to have a fixed reference for defining the motion. Usually ground is taken as the reference for machines and manipulators. When an earthquake occur these fixed link starts to move and even the frame applies force acting on the machines or manipulators. The effect of these unexpected random forces and motions on machines must be investigated to see the unexpected changes of the outputs. This knowledge can give useful feedback for the design and operation of machines that can work without affected by earthquakes.

6.2.1. An Example with a Slider Crank Mechanism

The slider-crank mechanism in Figure 6.2.a is often used to convert rotary motion into alternating linear motion or vice versa. A slider-crank kinematic chain consists of four bodies that are linked with three revolute joints and one prismatic joint.

Four different mechanisms or inversions of this kinematic chain are possible depending on which body is grounded, namely the crank, connecting link, sliding link or slot link. One of the inversions of slider crank mechanism is used in internal combustion engines (automobiles, trucks and small engines), with application of perhaps a billion engines makes the slider crank mechanism one of the most used mechanisms in the world.

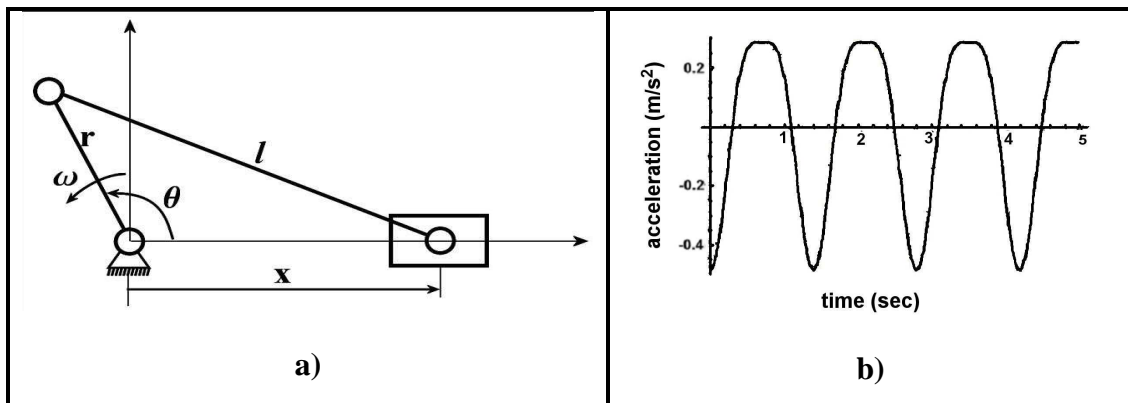


Figure 6.2. A test-bed slider-crank mechanism; a) Kinematic parameters, b) Slider accelerations with stationary frame (43 rpm).

In Figure 6.2.a kinematic parameters of the slider crank are shown, acceleration equation as output of the slider can be calculated from the acceleration equation of the slider with respect to input rotation as,

$$\ddot{x} = -r\alpha \left(\sin\theta + \frac{r \sin 2\theta}{2l} \right) - r\omega^2 \left(\cos\theta + \frac{r \cos 2\theta}{l} \right) \quad (6.1)$$

A numerical computation is shown in Figure 6.2.b which shows a nearly harmonic motion.

6.2.2. An Example with a Leg Mechanism

Another example for mechanism operation is an eight-bar linkage mechanism as shown in Figure 6.3.a. Top part of the linkage mechanism with links abcdmf is a Chebyshev four bar mechanism to produce near-linear motion and second part with

links z_2, z_3, z_4, z_5 is a pantograph mechanism to invert and scale the motion. This mechanism is designed to use for walking robots with one DoF as shown in Figure 6.3.b. Rickshaw robot is designed as a biped walking robot with low-cost design and easy operation in terms of compactness, and light weight.

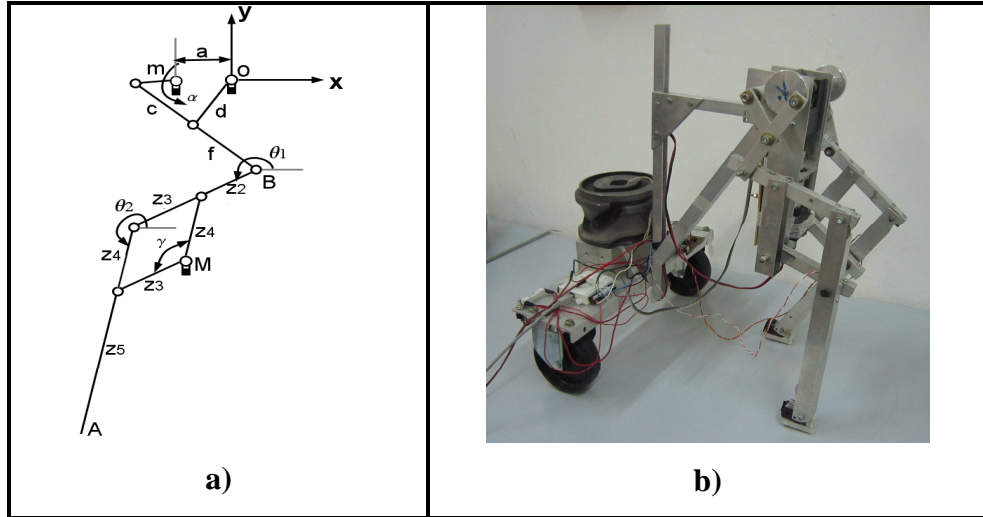


Figure 6.3. Leg mechanism; a) Kinematic parameters, b) Rickshaw robot (Source: Ottaviano et al. 2010).

Position of the point A can be calculated by using Equation (6.2) as

$$\begin{aligned} x_A &= M_x + z_3 \cos \theta_1 + z_5 \cos \theta_2 \\ y_A &= M_y + z_3 \sin \theta_1 + z_5 \sin \theta_2 \end{aligned} \quad (6.2)$$

where, $\theta_1 = \theta_B - \alpha_1 + \pi$, $\theta_2 = \pi + \theta_1 - \gamma$, $\gamma = \cos^{-1} \left((-P_B^2 + z_2^2 + z_4^2) / 2P_B z_2 \right)$,
 $\theta_B = \tan^{-1} (y_{BO} / x_{BO})$, $\alpha_1 = \cos^{-1} \left((P_B^2 + z_2^2 - z_4^2) / 2z_2 z_4 \right)$, $P_B = \sqrt{x_{BO}^2 + y_{BO}^2}$,
 $x_{BO} = x_B - M_x$, $y_{BO} = y_B - M_y$.

The position of B can be formulated by closure equations of Chebyshev four bar linkage. Acceleration of point A of the leg mechanism has been calculated two times derivation of Equation (6.2) with respect to time and the result is shown in Figure 6.4.a with input speed of 150 rpm and Figure 6.4.b with input speed of 257 rpm.

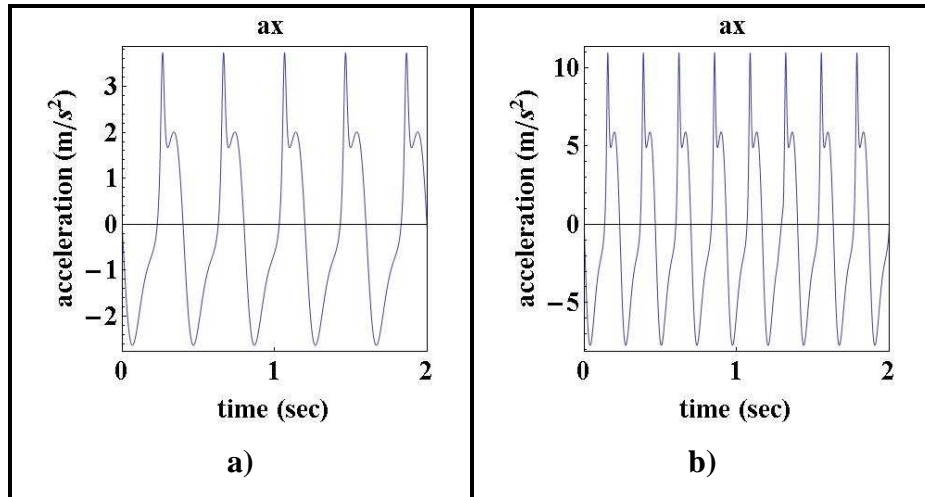


Figure 6.4. Acceleration of point A along x direction with stationary frame; a) 150 rpm, b) 257 rpm.

6.3. An Experimental Evaluation

The CaPaMan prototype is shown in Figure 6.5. Laboratory test-bed prototype for earthquake simulator consists of CaPaMan prototype with sensors, a controller for its operation and an acquisition board connected to the computer in order to acquire the components of the linear accelerations occurring along the axes of the reference system belonging to the mobile platform, (Ceccarelli et al. 1999).

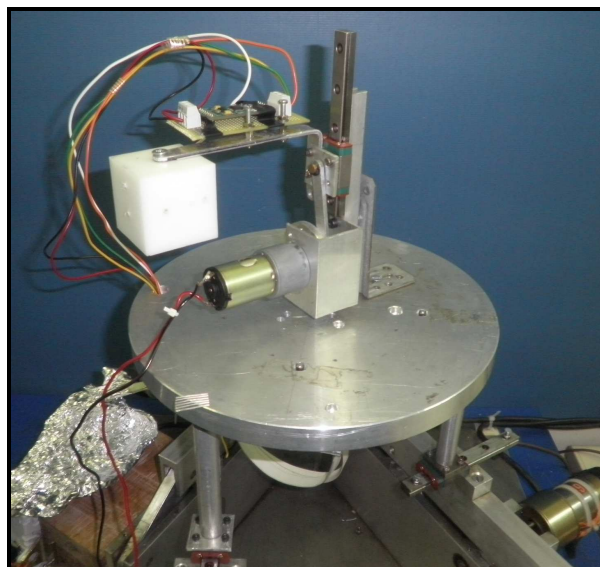


Figure 6.5. An experimental setup at LARM with the slider-crank mechanism.

The minimum numbers of accelerometers need to directly calculate the angular velocity for a 3D motion of a rigid body is twelve. In this section four of three axis accelerometers are placed in the corners to keep symmetry and using the mathematical calculations in the study of Schopp (2009), this configuration of 4 sensors is used to keep the replacement errors of sensor minimum.

Four three axis accelerometers are planned to be placed under the platform of the CaPaMan with dimensions as shown in Figures 6.6.a and 6.6.b, and placed accelerometers shown in Figures 6.6.c and 6.6.d. The control system scheme layout for CaPaMan manipulator is shown in Figure 6.7. Data for simulating the earthquake is send to the servo motor controller (Scorbot-ER V) by using the ACL programming language. The motors move the mobile platform and by the help of accelerometers the acceleration information of the mobile platform through the NI-DAQ 6210 is processed and visualized with the LabView software.

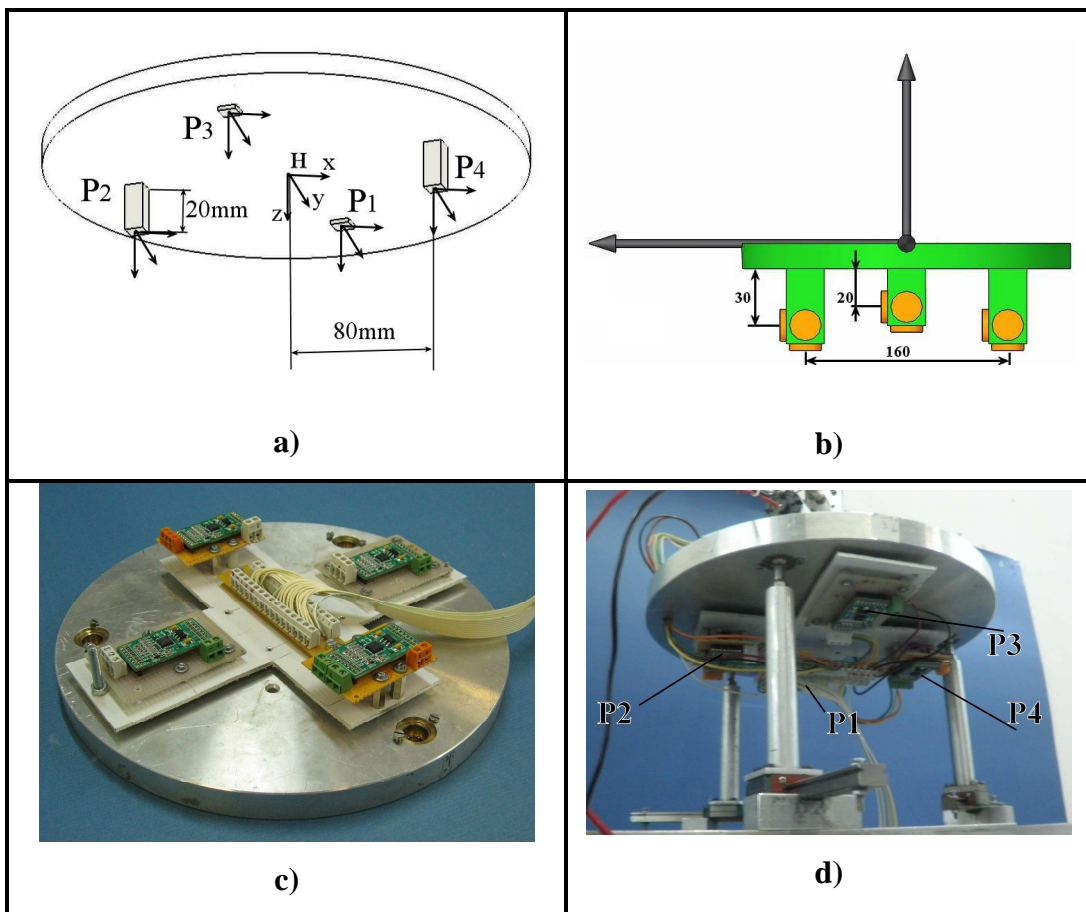


Figure 6.6. CaPaMan platform with accelerometer sensors; a) Scheme, b) Sensor locations, c) Sensor installation, d) Test lay-out.

A suitable Virtual Instrument has been developed in LabView environment to manage the signals coming from the sensors. Then, the measured acceleration data from the accelerometers have been used to estimate the accelerations of the point H at the centre of the movable plate and the plate angular velocity.

For characterization of earthquake effects on mechanism two types of earthquakes are simulated. Characteristic phases of the simulated earthquakes (Carvalho and Ceccarelli (2002)) are given in Table 6.1 and a reference earthquake simulation Figure 6.8 is given for defining parameters for earthquake characteristics

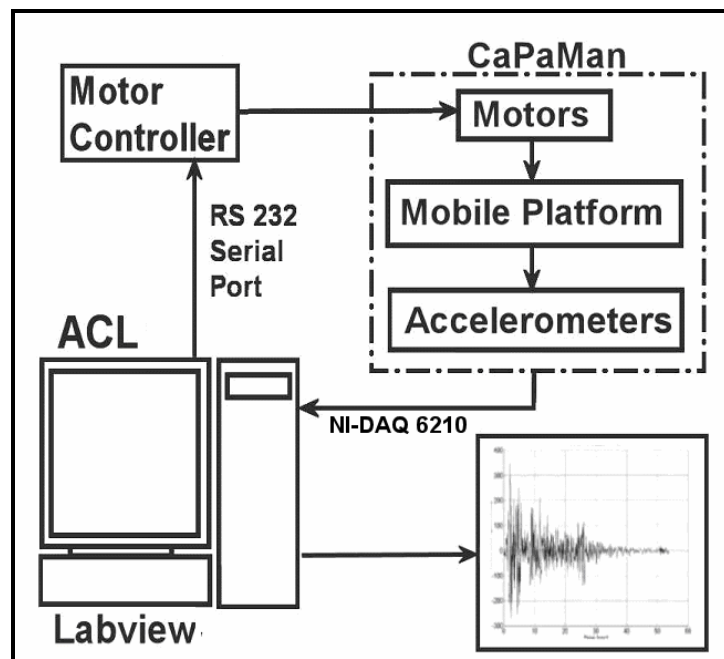


Figure 6.7. Control system layout for CaPaMan as an earthquake simulator.

Table 6.1. The characteristics of simulated earthquakes.

	Total Time (sec)	ΔT_{\max} (sec)	ΔT_{\min} (sec)	Number of oscillations	Maximum Frequency (Hz)
Earthquake Type 1	45	2.0	0.8	30	1.2
Earthquake Type2	50	2.0	1.5	30	0.8

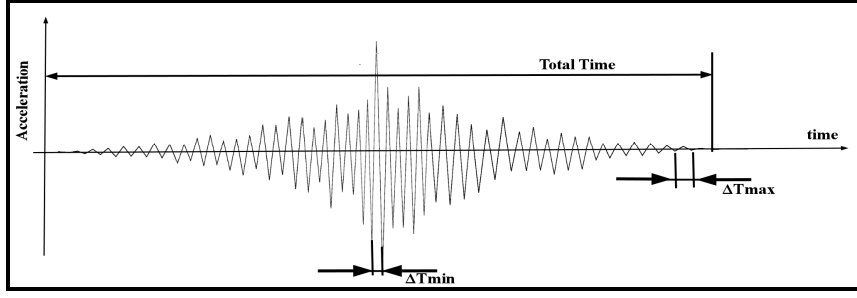


Figure 6.8. Typical characteristics of simulate earthquake.

Accelerometer data of the simulated earthquake type 1 is shown in Figure 6.9. To calculate the linear angular accelerations and angular velocities around center point H first the relation of an accelerometer on a rigid body must be expressed. Let the acceleration of a point P fixed on a rigid body with a position \mathbf{r} expressed by Equation (6.3) (Field and Ziwet 1916, Schopp 2009).

$$\mathbf{a}_p = \mathbf{a}_B + \boldsymbol{\alpha}_B \times \mathbf{r} + \boldsymbol{\omega}_B \times (\boldsymbol{\omega}_B \times \mathbf{r}) \quad (6.3)$$

where acceleration \mathbf{a}_B , the angular velocity $\boldsymbol{\omega}_B$ and the angular acceleration $\boldsymbol{\alpha}_B$ are described for the relative movement of the rigid body O_B with respect to the fixed frame O_F . The terms of the equation $\boldsymbol{\alpha}_B \times \mathbf{r}$ can be described as tangential acceleration and $\boldsymbol{\omega}_B \times (\boldsymbol{\omega}_B \times \mathbf{r})$ as centripetal acceleration. In order to calculate the acceleration as measured by a sensor that is attached at position \mathbf{r} within a body the sensitivity axis \mathbf{s} and the sensors' metrological signal offset \mathbf{a}_0 must be added in above equation to give

$$\mathbf{a}_s = \mathbf{s}^T (\mathbf{a}_B + \boldsymbol{\alpha}_B \times \mathbf{r} + \boldsymbol{\omega}_B \times (\boldsymbol{\omega}_B \times \mathbf{r})) + \mathbf{a}_0. \quad (6.4)$$

Equation (6.4) can be written in vector form as

$$\mathbf{a}_s = \mathbf{c}\mathbf{z} + \mathbf{a}_0, \quad (6.4)$$

where $\mathbf{z} = [a_{B,x}, a_{B,y}, a_{B,z}, \alpha_{B,x}, \alpha_{B,y}, \alpha_{B,z}, \omega_{B,x}^2, \omega_{B,y}^2, \omega_{B,z}^2, \omega_{B,x}\omega_{B,y}, \omega_{B,x}\omega_{B,z}, \omega_{B,y}\omega_{B,z}]^T$ and

$$\mathbf{c} = [s_x, s_y, s_z, s_z r_y - s_y r_z, s_x r_z - s_z r_x, s_y r_x - s_x r_y,$$

$$-(s_y r_y + s_z r_z), -(s_x r_x + s_z r_z), -(s_x r_x + s_y r_y), s_x r_y + s_y r_x, s_x r_z + s_z r_x, s_y r_z + s_z r_y]^T.$$

By using four sensors with totally twelve sensitive axes it is possible to directly compute the quadratic terms of $\boldsymbol{\alpha}_B$ as well as \mathbf{a}_B and $\boldsymbol{\omega}_B$. So the system becomes linear and can be written in matrix vector form as

$$\mathbf{y} = \mathbf{A} \mathbf{z} + \mathbf{a}_{0,S}, \quad (6.5)$$

where $\mathbf{y} = [\mathbf{a}_{S1}, \mathbf{a}_{S2}, \dots, \mathbf{a}_{S12}]^T$, $\mathbf{A} = [\mathbf{c}_{S1}, \mathbf{c}_{S2}, \dots, \mathbf{c}_{S12}]^T$ and $\mathbf{a}_{0,S} = [\mathbf{a}_{0,S1}, \mathbf{a}_{0,S2}, \dots, \mathbf{a}_{0,S12}]^T$.

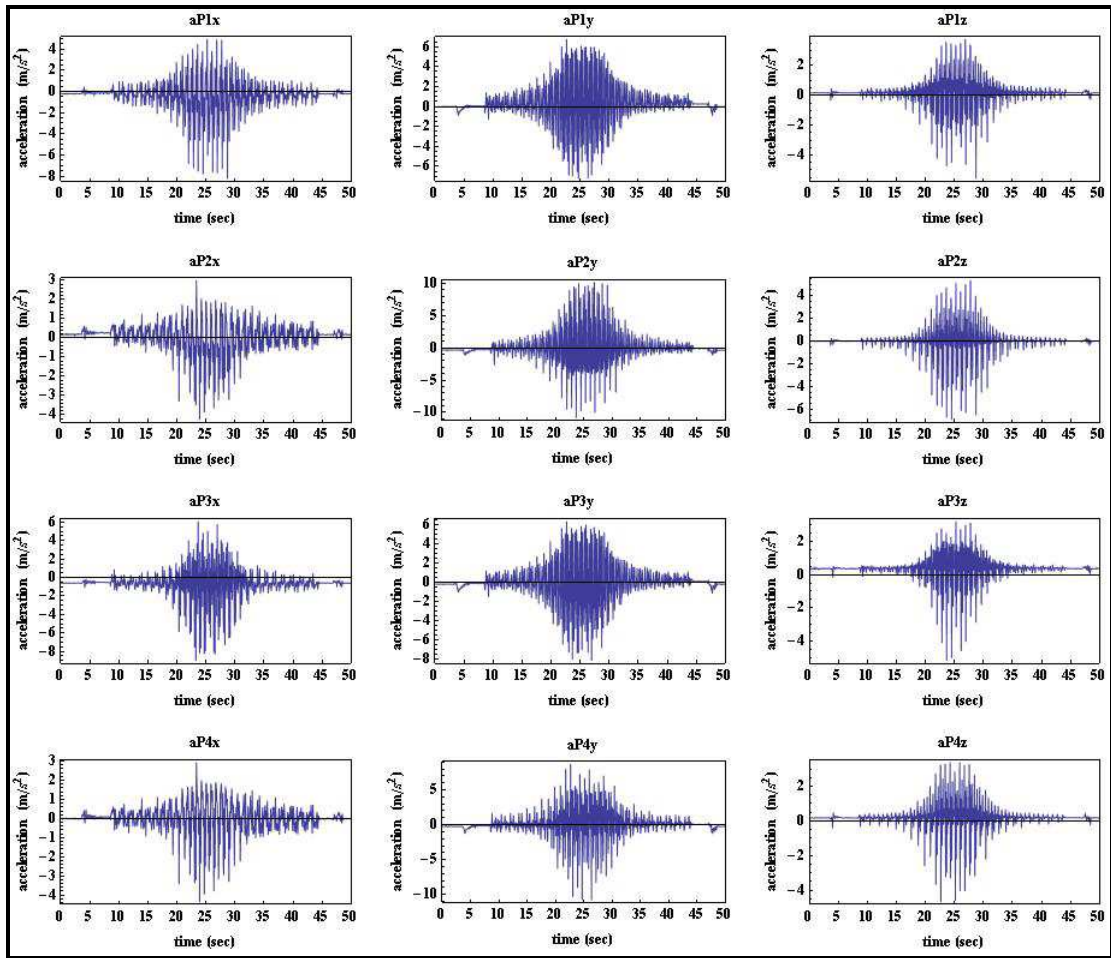


Figure 6.9. Accelerometer data during earthquake simulation.

By inverting \mathbf{A} it is possible to calculate characteristics of the relative body movement held by vector \mathbf{z} for a given measurement vector \mathbf{y} applying

$$\mathbf{z} = \mathbf{A}^{-1} (\mathbf{y} - \mathbf{a}_{0,S}). \quad (6.6)$$

By using Equation (6.6) the linear accelerations (\mathbf{a}_H), angular accelerations ($\boldsymbol{\alpha}_H$) and angular velocities ($\boldsymbol{\omega}_B$) around point H are calculated and shown in Figure 6.10.

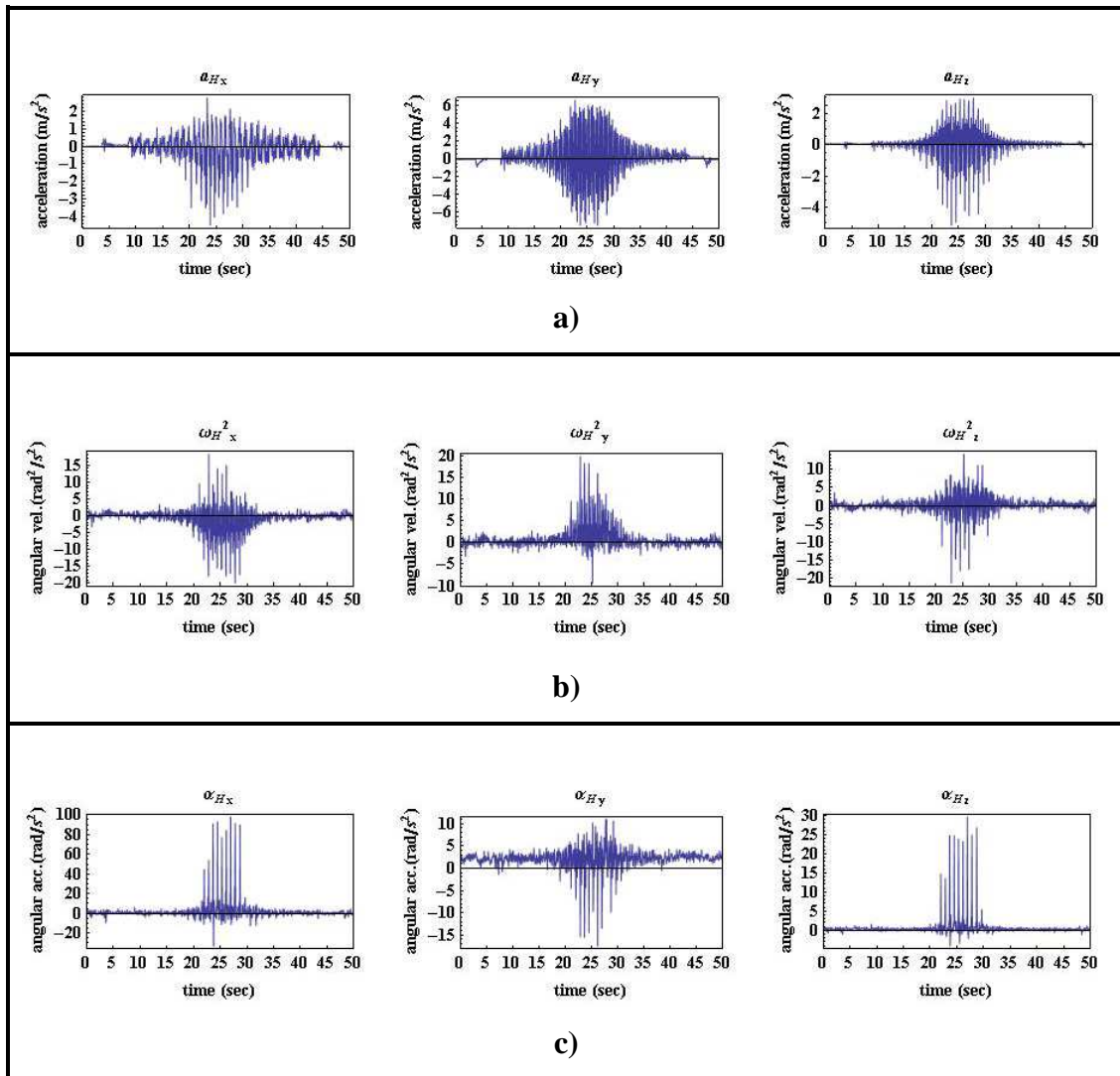


Figure 6.10. An example of acceleration data during earthquake simulation; a) For platform center H, b) Angular platform velocity, c) Angular platform acceleration.

6.4. Experimental Tests with Prototypes

Experimental tests have been carried out by using a slider-crank linkage with DC and servo motors, a robot leg linkage, a small car model, and LARM Hand as test-bed mechanisms with acceleration or force sensors.

6.4.1. Slider Crank Actuated with Dc Motor

An accelerometer is attached to the slider of the slider crank mechanism as shown in Figure 6.11.a and accelerometers sensing axes can be seen in Figure 6.11.b.

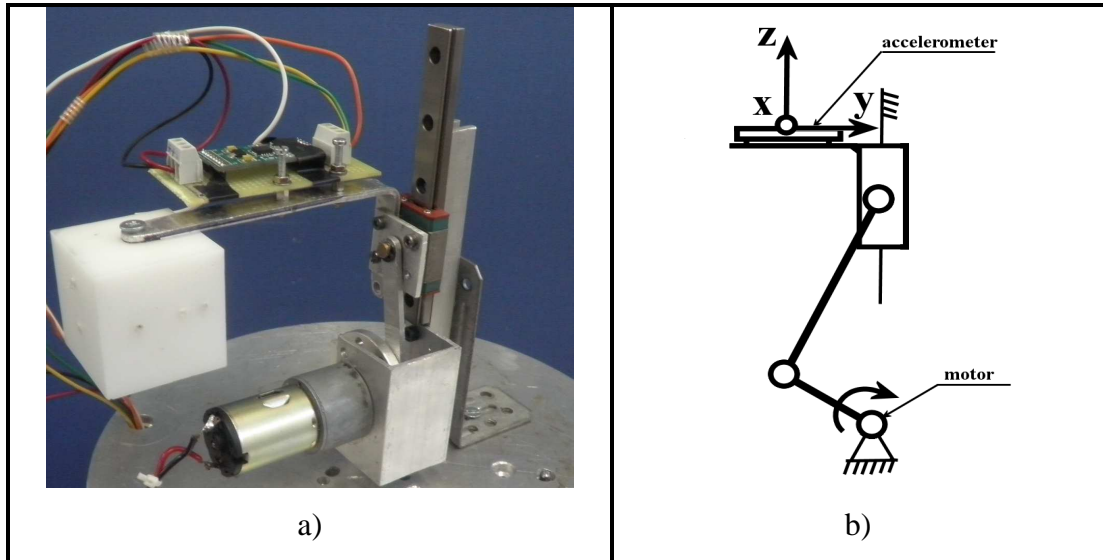


Figure 6.11. A test-bed slider-crank mechanism at LARM; a) An experimental set up with accelerometer and weight on the slider, b) Sensing axes of the accelerometer.

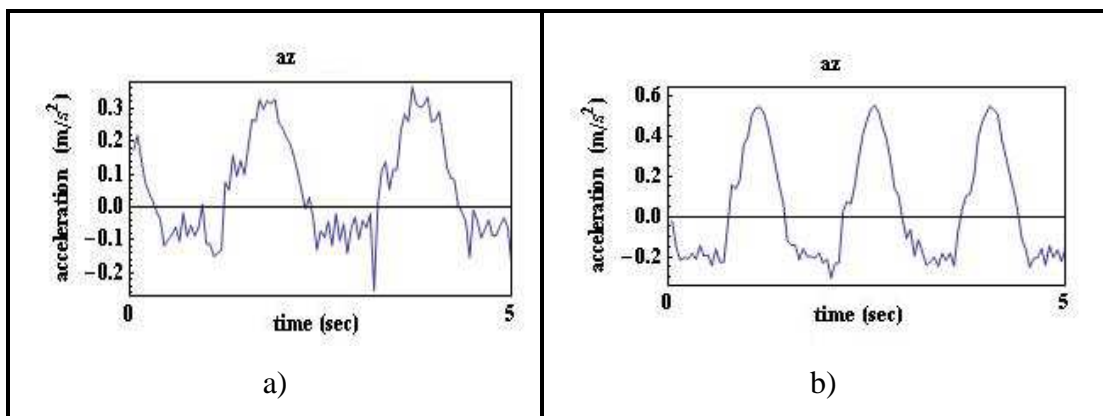


Figure 6.12. An experimental measure of the typical accelerations of the slider-crank with stationary frame; a) Crank rotation 32 rpm, b) Crank rotation 43 rpm.

Slider-crank mechanism with DC motor actuation is subjected to earthquake vibrations with different operating speeds. Figure 6.12 shows the filtered experimental measure of the acceleration of the slider as from the case in Figure 6.2.b. The noise in

the experimental measure is due to backlash of the components, flexibility of the links and design tolerances. Also some noise is caused by environmental waves into the frame link. Experiments are repeated with and without attached weight on the slider.

6.4.2. Slider Crank Actuated by Servo Motor

An accelerometer is attached to the slider of the slider crank mechanism as shown in 6.13.a and accelerometers sensing axes can be seen in Figure 6.13.b. Usage of servo motor gives the advantage to view torque data during operation. In Figure 6.14.a torque data of the motor and acceleration of the slider is given without earthquake disturbance with crank motion of 90 rpm. In Figure 6.14.b same type of data with crank rotation 180 rpm is given.

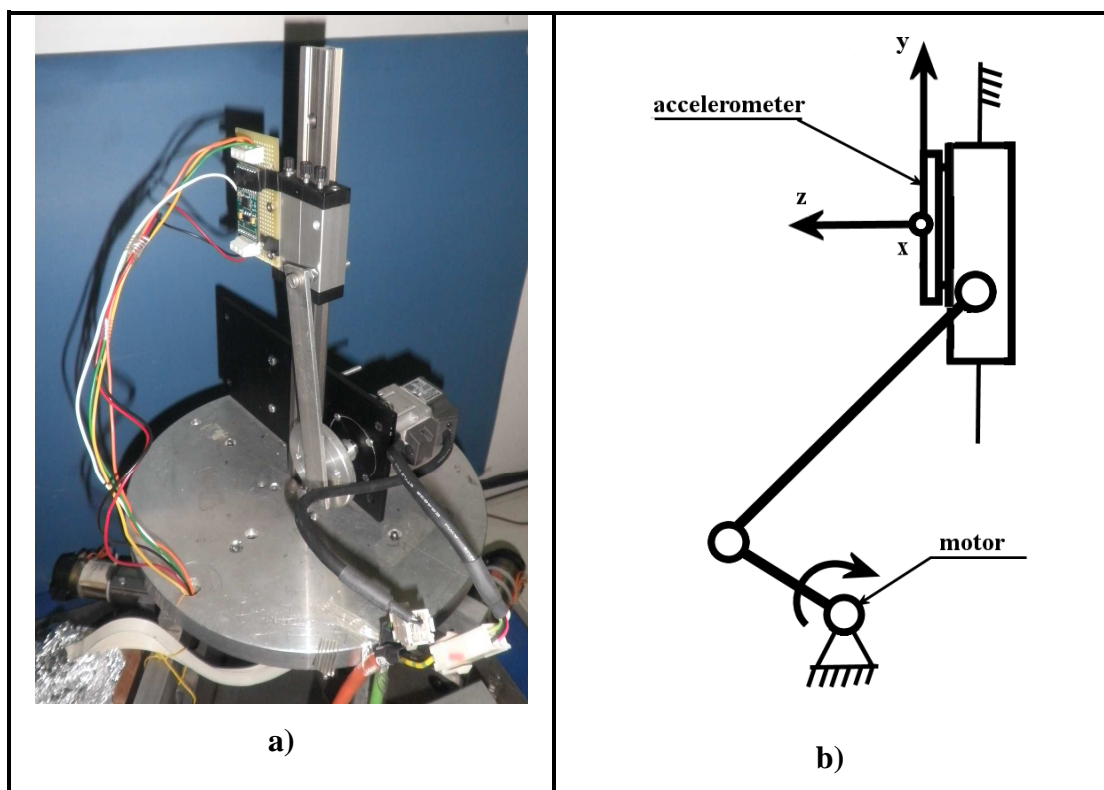


Figure 6.13. A test-bed slider-crank mechanism with servo motor at LARM; a) An experimental set up with accelerometer on the slider, b) Sensing axes of the accelerometer.

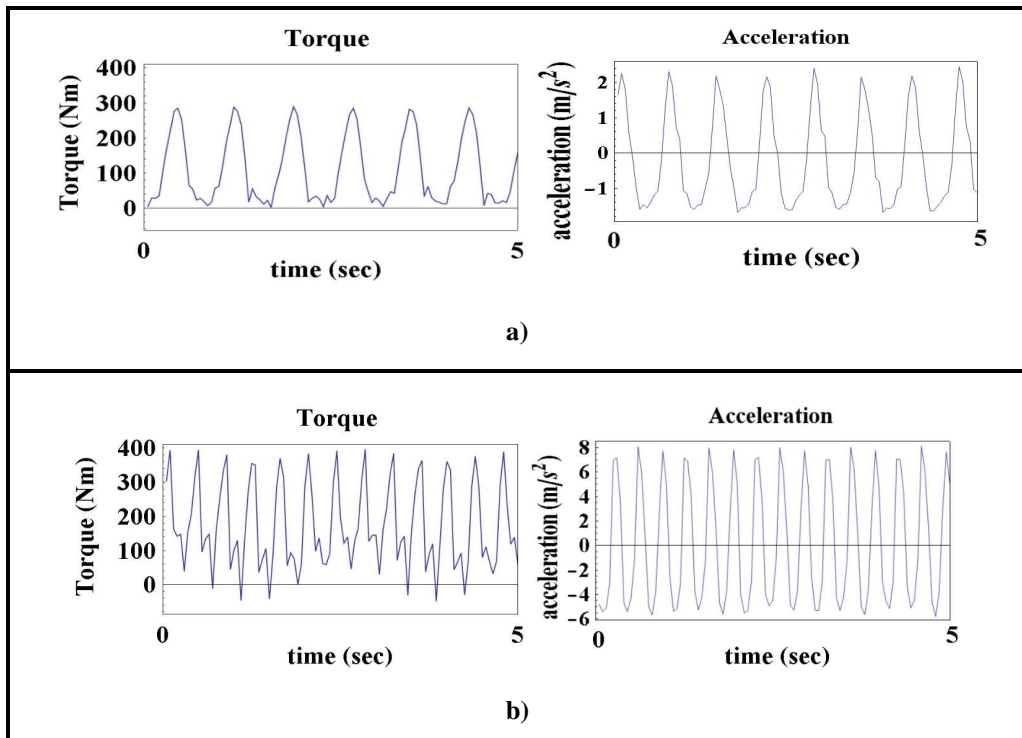


Figure 6.14. Experimental measures of slider crank with servo motor without earthquake effect, Torque data of the motor, acceleration of the slider with crank rotation; a) 90 rpm, b) 180rpm.

6.4.3. Leg Mechanism

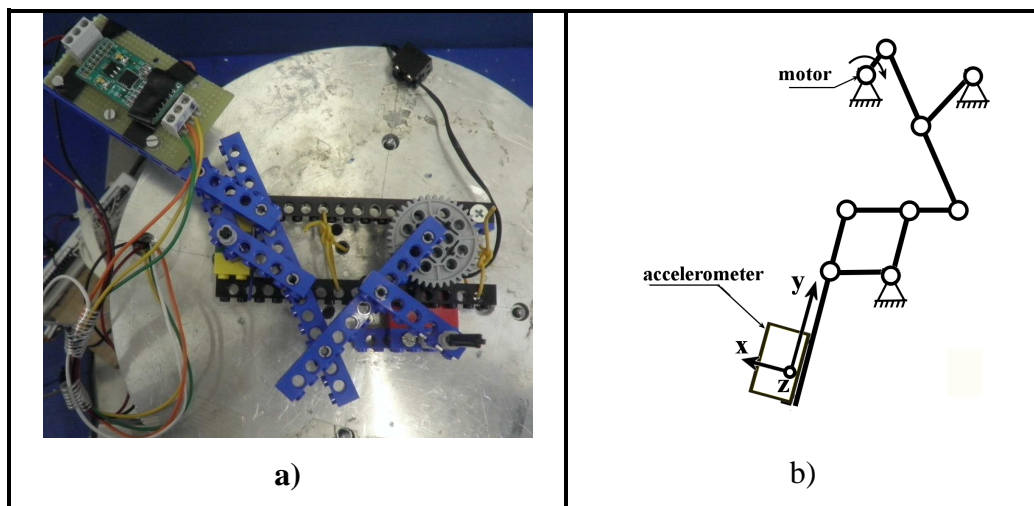


Figure 6.15. A test-bed pantograph-Chebyshev mechanism; a) An experimental set up with an accelerometer, b) Sensing axes of the accelerometer.

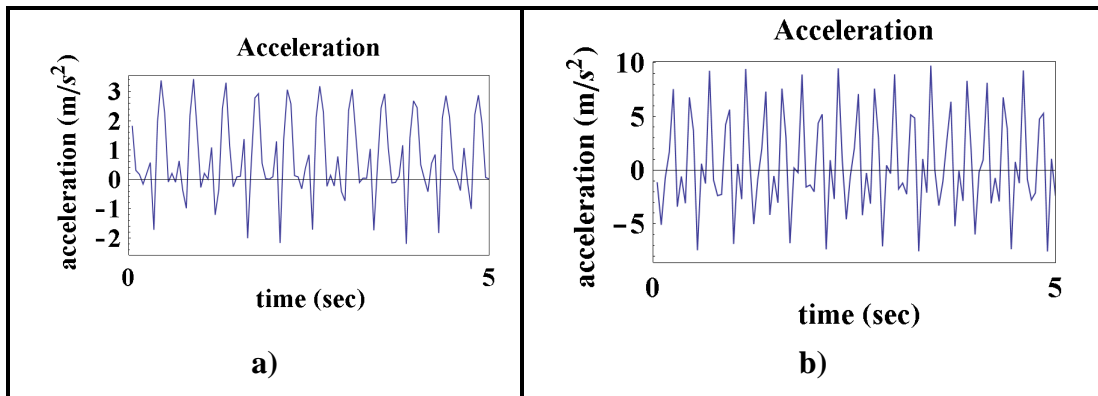


Figure 6.16. An experimental measure of the typical accelerations of the leg mechanism without earthquake effect; a) Crank rotation 150 rpm, b) Crank rotation 257 rpm.

An accelerometer is attached to the end link of the pantograph- Chebyshev linkage as shown in Figure 6.15.a and accelerometers sensing axes can be seen in Figure 6.15.b. In Figure 6.16.a Experimental measure of accelerations with different speeds of input motion are shown in Figure 6.16.a with 150 rpm in Figure 6.16.b with 257 rpm.

6.4.4. LARM Hand

Other peculiar mechanism operation can be considered from robotic systems. As test-bed mechanism LARM Hand prototype has been used in this work. The LARM Hand shown in Figure 6.17 is composed of three fingers. In particular, a human-like grasping is obtained by each finger with one DoF motion by using a suitable mechanism, whose design has been obtained through cross four-bar linkages to be fitted in the finger body as described in the study of Carbone and Ceccarelli (2008). Consequently the grasp can be regulated through a simple control by using force sensor signals and an industrial small PLC for operation. The LARM Hand can be used as a grasping end-effector in robots and automatic systems. Each finger of LARM Hand has three joints and one actuator. The range of motion for the prototype in Figure 6.17 is 40 degrees for finger inputs and 140 degrees for fingertip links. LARM Hand is equipped with four force sensors whose ranges of sensitivities are from 1N to 100 N. The dimensions of the finger are 1:1.2 of the human finger size and the hand is 110x240x120 mm and range of the grasp is between 10-100 mm.

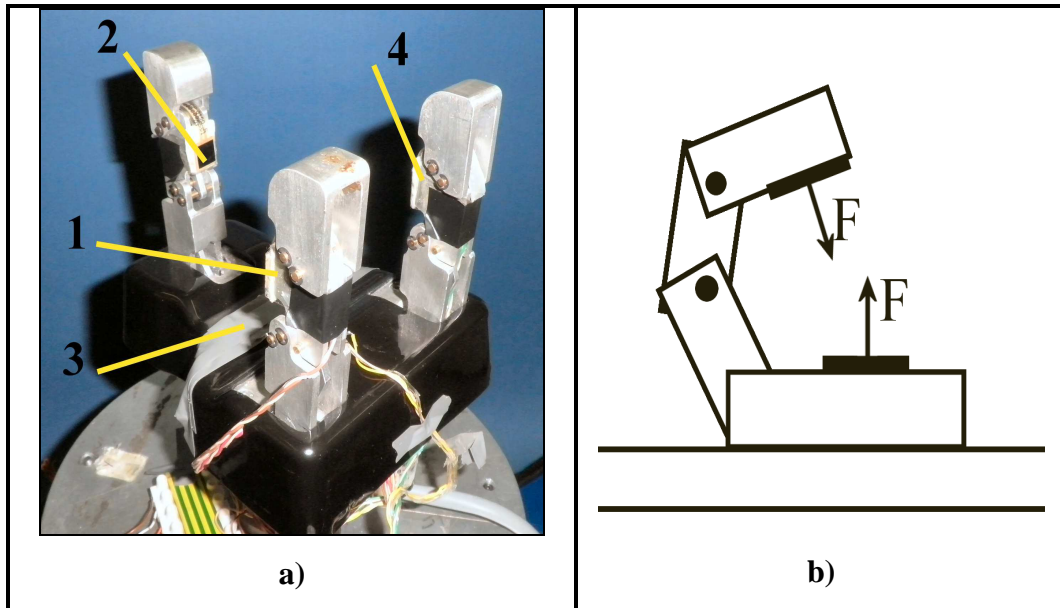


Figure 6.17. LARM Hand; a) Prototype, b) Sensor locations.

Both types of earthquakes are applied to LARM Hand during grasping a cylinder block. Earthquakes are repeated also just after implementation of the first one because of the difference between first assembly before no earthquake and after earthquake as shown in Table 6.2.

Table 6.2. Force data of the sensors on LARM hand while the platform is stable.

	F1(N)	F2(N)	F3(N)	F4(N)
Static	2.437	2.493	2.389	2.854

6.4.5. Vehicle Model

A vehicle model is designed for characterization of earthquake effects on machinery operation. The vehicle model has a dc motor and set on a rail as shown in Figure 6.18.a. A force sensor and a three axis accelerometer are attached as shown in Figure 6.18.b. Due to friction on the wheels when voltage is applied to dc motor a force is applied on the force sensor.

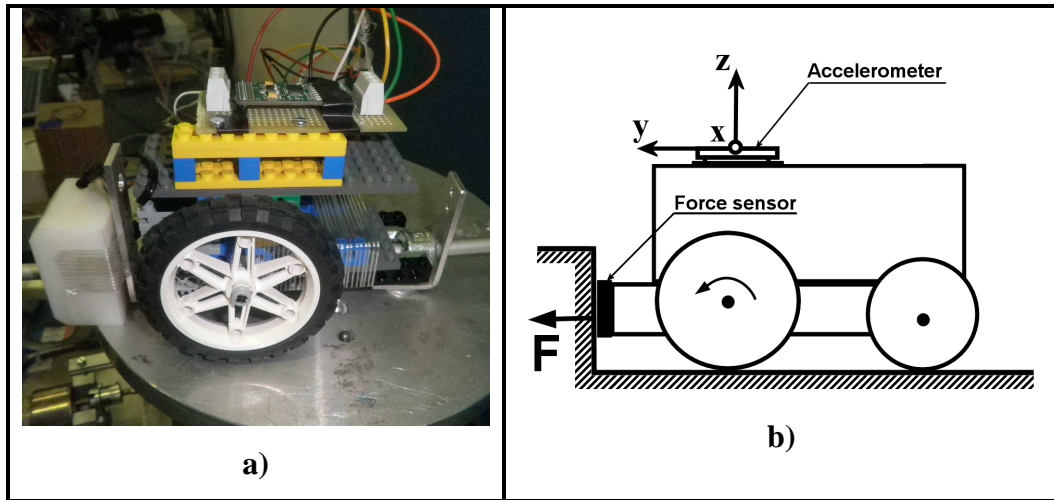


Figure 6.18. Model car with force and accelerometer sensors; a) Experimental setup with prototype b) Sensors and directions.

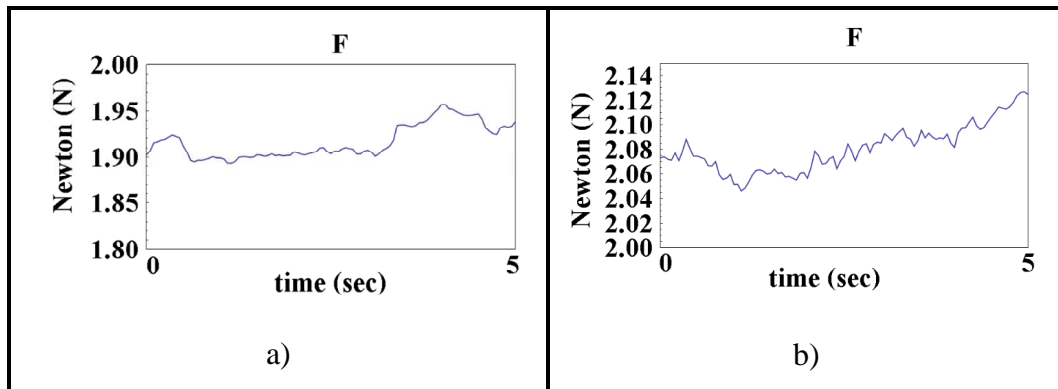


Figure 6.19. An experimental measure of the typical forces on the model car without earthquake effect; a) Applied voltage 7v, b) Applied voltage 9v.

6.5. Results of Tests and Considerations for Characterization

The results of simulated earthquakes can be summarized with the maximum acceleration values of center point H. For the earthquake type 1 maximum acceleration is $a_{h,max} = 8.4 \text{ m/s}^2$, and for earthquake type 2 max acceleration of point H is $a_{h,max} = 5.29 \text{ m/s}^2$. In Table 6.3 maximum acceleration data for the mechanisms are given for comparison. In each sub-section experimental data from mechanism sensors are shown during earthquake disturbance.

Table 6.3. Experimental data from experimental tests with test-bed mechanisms.

		Exp data	Earthquake type 1	Earthquake type 2	Stationary	
Slider crank With DC motor $a_{z_{max}}$ (m/s²)	Horizontal	24 volts 32rpm	8.575	9.160	0.452	
		32 volts 43rpm	5.664	5.267	0.531	
	weighted	24 volts 32rpm	9.023	8.006	0.316	
		32 volts 43rpm	6.235	6.223	0.574	
	Vertical	24 volts 32rpm	9.286	7.438	0.447	
		32 volts 43rpm	4.390	3.829	0.587	
	weighted	24 volts 32rpm	7.145	8.583	0.609	
		32 volts 43rpm	3.975	4.242	0.706	
New slider crank $a_{y_{max}}$ (m/s²)		15k-90rpm	7.530	4.15	2.508	
		30k-180rpm	11.64	10.81	8.211	
		60k-360 rpm	16.90	16.03	13.97	
Pantograph-Chebyshev leg $a_{x_{max}}$ (m/s²)		4v 150 rpm	15.446	11.172	3.452	
		7.5v 257 rpm	16.253	13.845	9.541	
Larm Hand Force (N)		Max	2.65, 2.65, 2.53, 2.99	2.23, 2.30, 2.37, 3.10	2.52, 2.57, 2.47, 2.97	
		Min	1.9, 1.99, 1.91, 2.25	1.64, 1.73, 1.77, 2.33	1.89, 1.94, 1.86, 2.23	
Car model Force (N)		7v	Max	2.086	2.121	1.980
			Min	1.189	1.604	1.839
		9v	Max	2.102	2.091	1.995
			Min	1.155	0.012	1.95

6.5.1. Slider Crank

6.5.1.1. Actuation by Dc Motor

When the slider-crank is subjected to an earthquake motion the acceleration of the slider is altered up to the measured acceleration shown in Figure 6.20 for slider position horizontal and Figure 6.21 for slider position vertical. Details of these changes are visible from Figure 6.20 to Figure 6.21 with views of slider acceleration between 25 and 30 seconds of earthquake motion, when the seismic accelerations are at maximum.

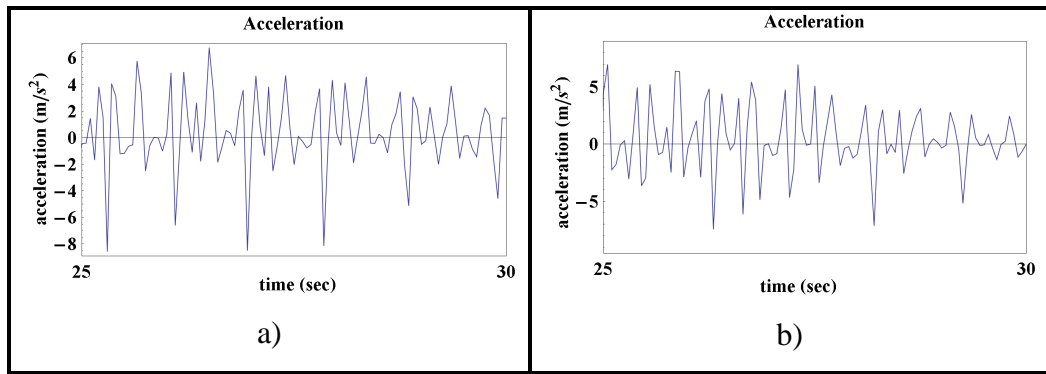


Figure 6.20. An experimental measure of the typical accelerations with horizontal slider under earthquake effect (type 1); a) Crank rotation 32 rpm, b) Crank rotation 43 rpm.

It is observed from the Figures 6.20 and 6.21 that the shape and amplitude of the acceleration of the slider during a simulated earthquake are strongly changed and oscillations of the slider acceleration are also vanished. It seems that the slider acceleration is fully disturbed by the earthquake effects. Considering the different speeds and different position of the mechanism the motion is affected more when crank speed is at lower speed or slider position is vertical.

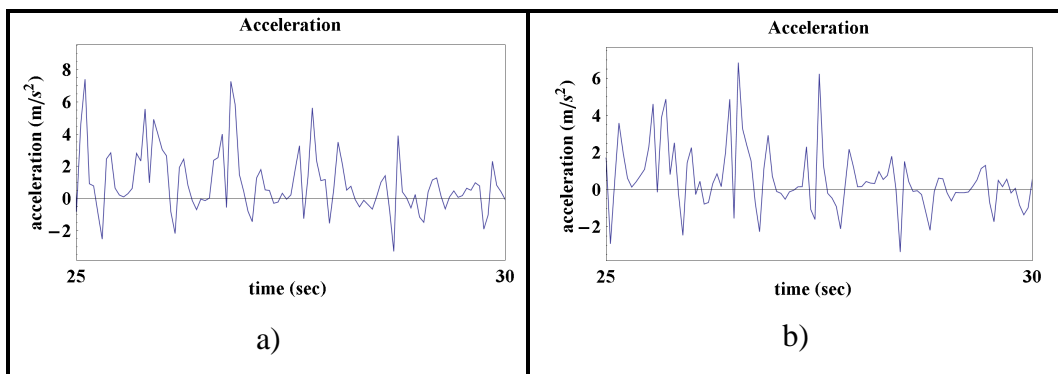


Figure 6.21. An experimental measure of the typical accelerations with vertical slider under earthquake effect (type 1); a) Crank rotation 32 rpm, b) Crank rotation 43 rpm.

6.5.1.2. Actuation by Servo Motor

In Figure 6.22.a and Figure 6.22.b experimental data of motor torque and slider acceleration during earthquake disturbance are shown for a crank rotation of 90 rpm and

180 rpm respectively. It is recognized from acceleration data of slider shown in Figure 6.20 that not only shape and amplitude of the acceleration of the slider during a simulated earthquake are strongly changed but also oscillations of the slider are vanished. Meanwhile torque data of the motor has some disturbances in the amplitude; shape and oscillation can be told to be similar with the static state.

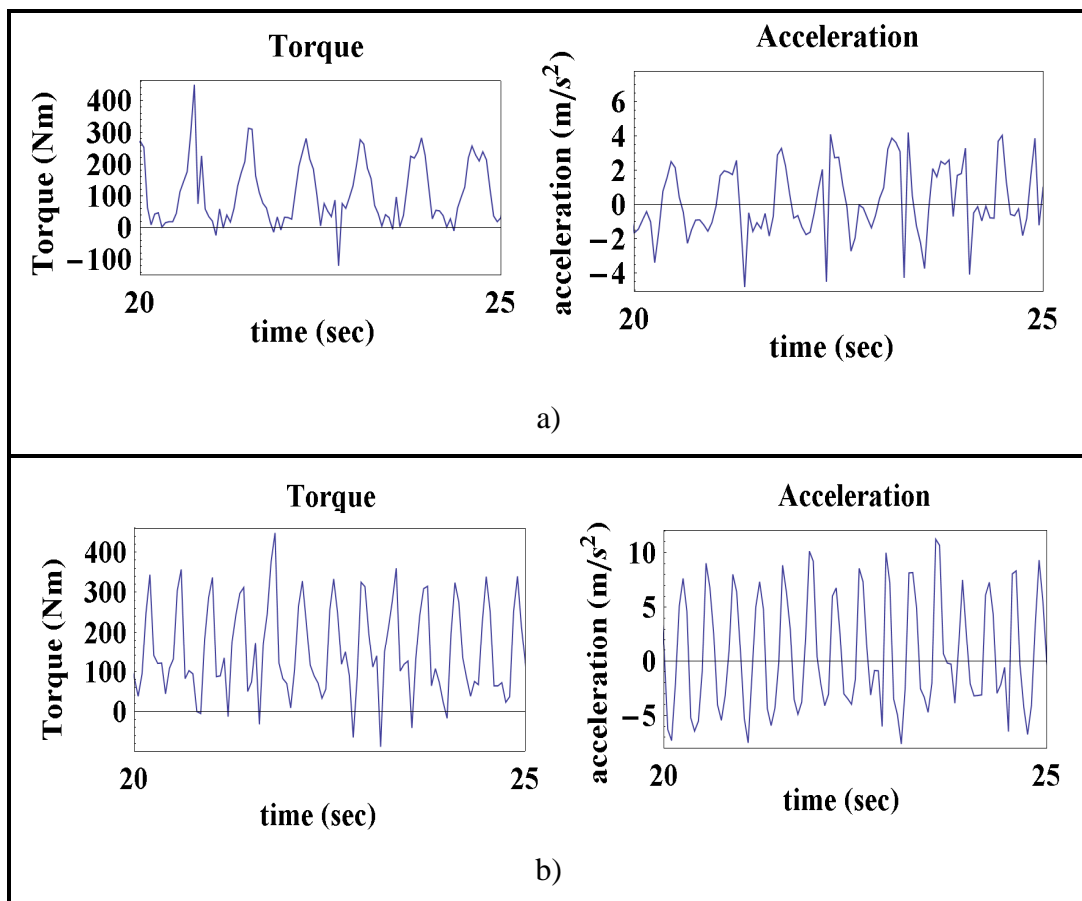


Figure 6.22. An experimental measure of slider crank with servo motor with earthquake effect (type 1), Torque data of the motor, acceleration of the slider with crank rotation a) 90 rpm, b) 180 rpm

6.5.2. LARM Hand

In Table 6.3 forces acting to object during static condition and during earthquake disturbance are given. In Figure 6.23 force data of the grippers and palm are shown during a simulated earthquake. From Table 6.3 and Figure 6.23 force on gripper fingers and palm have an oscillatory motion during the earthquake and there is an obvious change at the end. These results show that during an earthquake characteristic for the

manipulator such as output (force), repeatability of the operation frequency and efficiency, and the reliability of the process (precision accuracy) are affected. For the LARM Hand the holding force on the fingers decreases during the earthquake and if the force exceeds the force needed to handle object it can cause to the slipping of material. Amount of the applied force to the object is increased at the end of the experiment. Therefore, the object can be damaged.

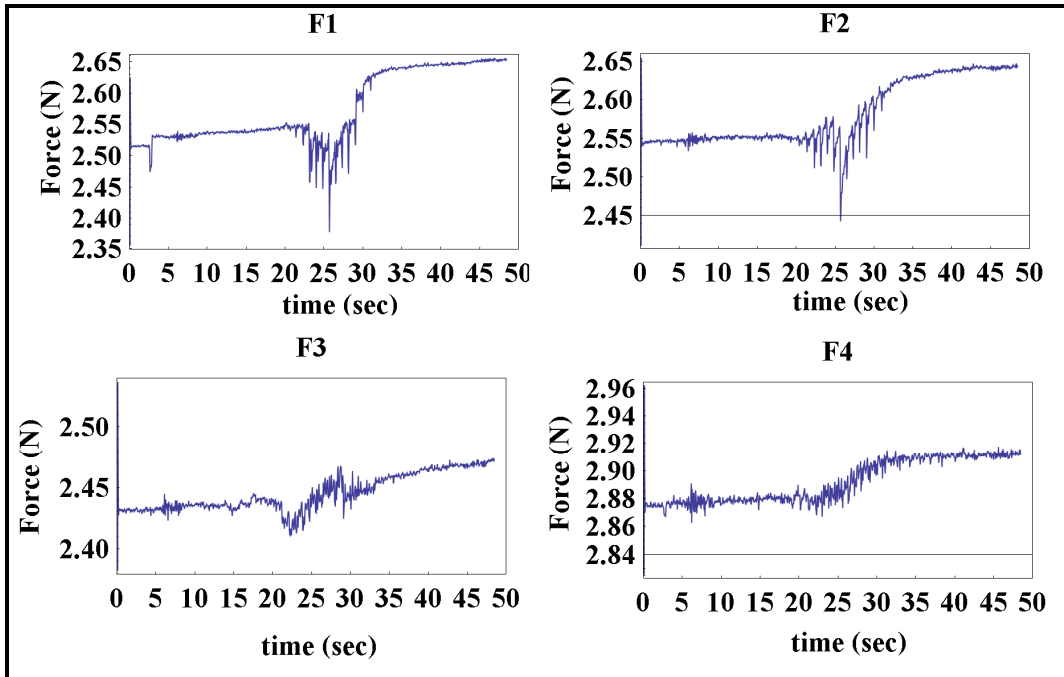


Figure. 6.23. Force data of LARM Hand during earthquake type 1.

6.5.3. Leg Mechanism

Detail of changes on the acceleration of leg mechanism can be seen in Figure 6.24 with views of slider acceleration between 25 and 30 seconds of earthquake motion when the seismic accelerations are at maximum. In contrast with static accelerations of leg mechanism shown in Figure 6.16 the amplitude and shape of accelerations do not represent the motion of the leg mechanism because of earthquake disturbance.

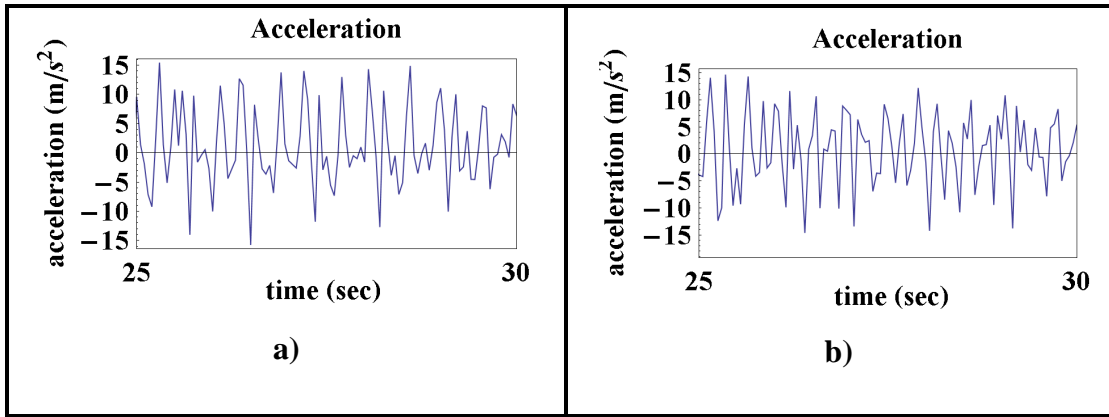


Figure 6.24. An experimental measure of the typical accelerations of the leg mechanism without earthquake effect; a) Crank rotation 150 rpm, b) Crank rotation 257 rpm.

6.5.4. Vehicle Model

Figure 6.25 shows force data on the vehicle model under earthquake disturbance. Comparing with static data shown in Figure 6.19 Force on the sensor has radically changed with oscillations. Details of these changes can be seen in Figure 6.26 with views of force data between 20 to 25 seconds of earthquake motion when the seismic accelerations are at maximum. Considering the different voltages applied to motor of the mechanism from Figures 6.25 and 6.26 earthquakes seems to be affecting same.

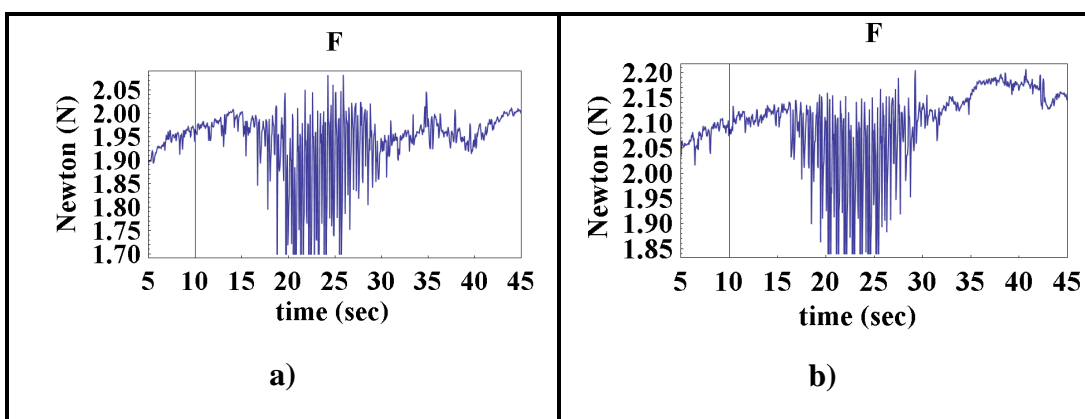


Figure 6.25. An experimental measure of forces on the model car with earthquake effect; a) Applied voltage 7v, b) Applied voltage 9v.

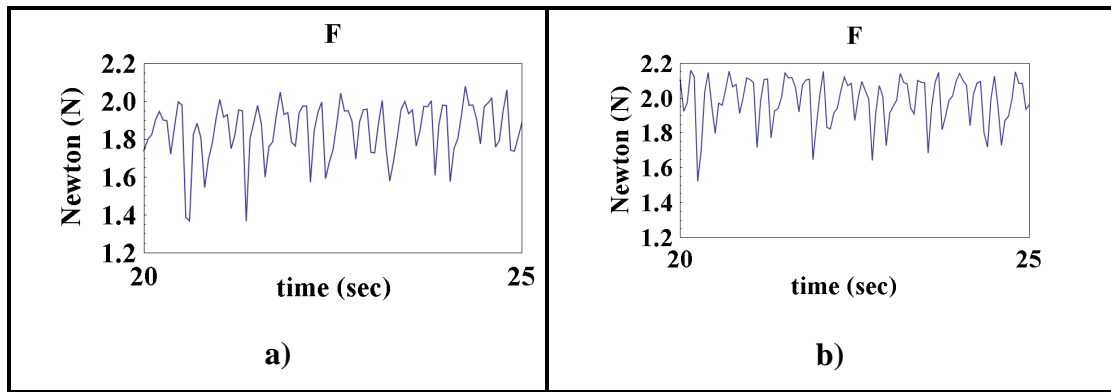


Figure 6.26. Detailed view of the experimental measure of forces on the model car with earthquake effect; a) Applied voltage 7v, b) Applied voltage 9v.

Summarizing, with the help of CaPaMan the effects of earthquakes on the operation of mechanical systems have been investigated by an analysis and reproduction of an earthquake motion. The sensitivity of the operation characteristics of machinery to earthquake disturbance is characterized in terms of acceleration response of output of machinery operation. Experimental tests have been carried out by using a slider-crank linkage with DC and servo motors, a robot leg linkage, a small car model, and LARM Hand as test-bed mechanisms with acceleration or force sensors. The results show that an earthquake will surely effect the acceleration of the mechanism operation both in shape and amplitude of the output motion. Also effect of earthquake is inverse proportional with the speed of the mechanism, in other words, the more we are approaching to the frequency of the earthquake the less mechanism is affected. Applied force is affected during earthquake and it is observed that it is increased after earthquake disturbance.

CHAPTER 7

CONCLUSION

In this thesis a generalized approach for structural synthesis and creation of new overconstrained manipulators is described and a potentially generalizable approach for function and motion generation synthesis of overconstrained mechanism is presented. Studies on these subjects are investigated and presented as a literature survey. Then an introduction is given with the definition of the problems and methods for solution of these problems. A novel method for calculation of screws is presented called “*Unit Transformation Screw Matrix*” and kinematic calculations for mechanisms is described for position, velocity, acceleration and force analyses. Methodology for structural analysis of parallel manipulators is described using reciprocity and virtual work and screw systems. Eleven overconstrained mechanism are represented for $\lambda= 2, 3, 4$ subspaces and a methodology for the generation of new overconstrained mechanisms is given by utilizing these mechanisms in lower subspaces. 4, 11 and 30 overconstrained mechanisms are generated for $\lambda=3, \lambda=4, \lambda=5$ subspaces respectively. Moreover, mathematical models for overconstrained subspaces are exemplified.

To describe structural synthesis initially degree of screw (Do\$) and mathematical models of kinematic pairs are described. Then novel mobility equations for manipulators are given. Using new formulas simple overconstrained structural groups with general constraint one and two are calculated and listed with examples. A procedure for the structural design of overconstrained parallel manipulators by using simple structural groups is given and illustrated with examples

Furthermore kinematic synthesis of overconstrained mechanisms is shown with a novel method for function generation of double spherical and planar spherical 6R linkages. Also motion generation for planar spherical 6R linkage for three positions is described which has a new approach for the motion synthesis of overconstrained mechanisms. Moreover, a synthesis method for a multi loop platform mechanism is shown with a numerical example. Finally to make an application on parallel robots an experimental setup is used to investigate the effects of earthquake motions on mechanisms.

REFERENCES

- Al-Widyan K., Angeles J. 2003. A robust solution to the spherical rigid body guidance problem. *Proceedings of DETC'03, ASME, Chicago, USA*, 1-8.
- Alizade R., Selvi O., Gezgin E. 2010. Structural design of parallel manipulators with general constraint one. *Mechanism and Machine Theory*, 45(1), 1-14.
- Alizade R., Bayram C., Gezgin E. 2007b. Structural synthesis of serial platform manipulators. *Mechanism and Machine Theory*, 42(5), 580-599.
- Alizade R.I., Can F.C., Gezgin E., Selvi O. 2007a. Structural Synthesis of New Parallel and Serial Platform Manipulators. *12th IFToMM World Congress, Besançon, France*.
- Alizade R.I. 1994. Synthesis of four-bar spherical mechanism on five parameters. *Journal of Mechanical Engineering Russian Academy of Science (ANR)*, 6 (in Russian).
- Alizade R.I., Kilit O. 2005. Analytic synthesis of function generating spherical four-bar mechanism for the five precision points. *Mechanism and Machine Theory*, 40(7), 863-878.
- Alizade R., Gezgin E. 2011. Synthesis of function generating spherical four bar mechanism for the six independent parameters. *Mechanism and Machine Theory*. 46, 1316-1326.
- Angeles J. 2002. The qualitative synthesis of parallel manipulators. *Proceedings of the workshop on Fundamental Issues and Future Research Directions for Parallel Mechanisms and Manipulators, Quebec, Canada*, 1-10.
- Bottema O., Roth B. 1979. *Theoretical Kinematics. Reprinted (1990)*, Dover, New York.
- Bodduluri R., McCarthy J.M. 1992. Finite position synthesis using the image curve of a spherical four-bar motion. *ASME Journal of Mechanical Design*, 114(1), 55-60.

- Bruneau M. et al. 2002. Versatile shake tables and large-scale high-performance testing facility towards real-time hybrid seismic testing. *Proceedings of ASCE Structures Congress, Denver*.
- Carbone G., Ceccarelli M. 2008. Design of LARM Hand: problems and solutions. *Journal of Control Engineering and Applied Informatics*, 10(2), 39-46.
- Carricato M. 2005. Fully-isotropic four degrees-of-freedom parallel mechanisms for Schönflies motion. *Int. J. Robotics Research*, 24 (5), 397-414.
- Carricato M., Castelli V.P. 2002. Singularity-free fully-isotropic translational parallel mechanisms. *Int. J. Robotics Research*, 21(2), 161-174.
- Carvalho J.C.M., Ceccarelli M. 2002. Seismic motion simulation based on CaPaMan simulation. *Journal of the Brazilian Society of Mechanical Sciences*, 25(3), 213-219.
- Ceccarelli M. 1997. A new 3 dof parallel spatial mechanism. *Mechanism and Machine Theory*, 32(8), 895-902.
- Ceccarelli M. et al. 1999. CaPaMan (Cassino Parallel Manipulator) as sensed earthquake simulator. *Proceedings of the IEEE/RSJ International Conference on Intelligent Robots and Systems, Kyongju*, 1501-1506.
- Ceccarelli M., Ottaviano E., Galvagno M. 2002. A 3-dof parallel manipulator as an earthquake motion simulator. *Seventh International Conference on Control, Automation, Robotics and Vision, Singapore*, 944-949.
- Cervantes-Sanchez J.J. et al. 2009. Some improvements on the exact kinematic synthesis of spherical 4R function generators. *Mechanism and Machine Theory*, 44, 103-121.
- Cervantes-Sánchez J.J. et al. 2011. Synthesis of a special RPSPR spatial linkage function generator for six precision points. *Mechanism and Machine Theory*, 46(2), 83-96.
- Conte J.P., Trombetti T.L. 2000. Linear dynamic modeling of a uni-axial servo-hydraulic shaking table system. *Earthquake Engineering and Structural Dynamics*, 29, 1375-1404.

- Courant R., Robbins H., Steward I. 1996. Euler's formula. *What is Mathematics*, 235-240.
- Crewe A.J., Severn R.T. 2001. The European collaborative programme on evaluating the performance of shaking tables. *Phil. Trans. Royal Soc. London, Series A*, 359(1786), 1671-1696.
- Di Gregori R., Castelli V.P. 1998. A Translational 3-dof parallel manipulator. *Advances in Robot Kinematics: Analysis and Control*, Lenarcic J, Husty ML (editors.), Kluwer Academic Publishers, 49-58.
- Di Gregori R., Castelli V.P. Mobility analysis of the 3-UPU parallel mechanism assembled for a pure translational motion. *Proc. of IEEE/ASME International Conference on Advanced Intelligent Mechatronics*, 520-525
- Dukkipati R.V. 2001. *Spatial Mechanisms: Analysis and Synthesis*, CRC Press.
- Fang Y., Tsai L.W. 2002. Structure synthesis of a class of 4-dof and 5-dof parallel manipulators with identical limb structures. *The International Journal of Robotic Research*, 21(9), 799-810.
- Fang Y., Tsai L.W. 2004a. Analytical identification of limb structures for translational parallel manipulators. *Journal of Robotic Systems*. 21(5), 209-218.
- Fang Y., Tsai L.W. 2004b. Structure synthesis of a class of 3-dof rotational parallel manipulators. *IEEE Transactions on Robotics and Automation*, 20(1), 117-121.
- Fang Y., Tsai L.W. 2004c. Enumeration of a class of overconstrained mechanisms using the theory of reciprocal screws. *Mechanism and Machine Theory*, 39, 1175-1187.
- Farhang K., Midha A., Bajaj A.K. 1988. Synthesis of harmonic motion generation linkages part-I, function generation. *ASME, J. Mech. Trans. Automat. Design*, 110(1), 16-21.
- Farhang K., Zargar Y.S. 1999. Design of spherical 4R mechanisms: function generation for the entire motion cycle. *ASME, J. Mech. Design*, 121, 521-528.

- Field P., Ziwet A. 1916. The accelerations of the points of a rigid body. *The American Mathematical Monthly*, (23/10), 371-381
- Freudenstein F. 1954. An analytical approach to the design of four-link mechanisms. *Trans. ASME*, 76, 483-492.
- Frisoli A. et al. 2000. Synthesis by screw algebra of translating in-parallel actuated mechanisms., *Advances in Robot Kinematics: Analysis and Control*, Lenarcic J, Husty ML (editors.), *Kluwer Academic Publishers*, 433-440.
- Gao F. et al. 2002. New kinematic structures for 2-,3-,4-, and 5-dof parallel manipulator designs. *Mechanism and Machine Theory*, 37, 1395-1411.
- Glazunov V. 2010. Design of decoupled parallel manipulators by means of the theory of screws. *Mechanism and Machine Theory*, 45, 239-250.
- Gogu G. 2008. *Structural Synthesis of Parallel Robots, Part 1: Methodology*. Springer.
- Gogu G. 2005. Fully-isotropic over-constrained parallel wrists with two degrees of freedom. *Proceedings of the 2005 IEEE International Conference on Robotics and Automation, Barcelona, Spain*, 4014-4019.
- Gupta K.C., Beloiu A.S. 1998. Branch and circuit defect elimination in spherical four-bar linkages. *Mechanism and Machine Theory*, 33(5), 491-504.
- Hartenberg R.S., Denavit J. 1964. *Kinematic Synthesis of Linkages*. McGraw-Hill.
- Hervé J.M., Sparacino F. 1991. Structural synthesis of parallel robots generating spatial translation. *Fifth International Conference on Advanced Robotics, Robots in Unstructured Environments*, 808-813.
- Hervé J.M., Sparacino F. 1993. Synthesis of parallel manipulators using Lie-groups: Y-STAR and H-ROBOT. *Proc. IEEE Intl. Workshop on Advanced Robotics, Tsukuba, Japan*, 75-80.
- Hervé J.M. 2003. The planar-spherical kinematic bond: Implementation in parallel mechanisms. "<http://www.parallemic.org/Reviews/review013.html>".

- Hervé J.M. 1999. The lie group of rigid body displacements: a fundamental tool for mechanism design. *Mechanism and Machine Theory*, 34(5), 719-730.
- Hervé J.M. 1994. New translational parallel manipulators with extensible parallelogram. *Proceedings of the 11th World Congress in Mechanism and Machine Science, China*, 4, 1599-1603.
- Huang Z., Li Q.C. 2002a. General methodology for type synthesis of symmetrical lower-mobility parallel manipulators and several novel manipulators. *The International Journal of Robotic Research*, 21(2), 31-145.
- Huang Z., Li Q.C. 2003a. Type synthesis of 4-dof parallel manipulators. *Proceedings of the IEEE International Conference on Robotics & Automation, Taipei, Taiwan*, 755-760.
- Huang Z., Li Q.C. 2003b. Li, Type synthesis of 5-dof parallel manipulators. *Proceedings of the IEEE International Conference on Robotics & Automation, Taipei, Taiwan*, 1203-1208
- Huang Z., Li Q.C. 2002b. On the type synthesis of lower-mobility parallel manipulators. *Proceedings of the workshop on Fundamental Issues and Future Research Directions for Parallel Mechanisms and Manipulators Quebec, Canada*, 272-283.
- Huang Z., Li Q.C. 2003c. Type synthesis of symmetrical lower-mobility parallel mechanisms using the constraint-synthesis method. *Int. J. Robotics Research*, 22(1), 59-79.
- Kazerounian K., Solecki R. 1993. Mobility analysis of general bi-modal four-bar linkages based on their transmission angle. *Mechanism and Machine Theory*, 28 (3), 437-445.
- Kuehn J.L., Epp D.S., Patten W.N. 1998. A high fidelity control for seismic shake tables. *Proc. 12th Engineering Mechanics Conference, LaJolla, CA*, 783-786.
- IFTToMM terminology /English 10.1. 2003. *Mechanism and Machine Theory*, 38-7-10, 859-879

- Jin Y., Chen I.M., Yang G. 2004. Structure synthesis and singularity analysis of a parallel manipulator based on selective actuation. *Proceedings of the IEEE International Conference on Robotics and Automation*, 4533-4538.
- Karouia M., Hervé J.M. 2004a. New parallel wrists: special limbs with motion dependency. *On advances in Robot Kinematics*, Kluwer Academic Publishers, 371-380
- Karouia M., Hervé J.M. 2004b. Asymmetrical 3-dof spherical parallel mechanisms. *Eur. J. Mech. A Solids*, 24. 47-57.
- Kong X., Gosselin C.M. 2004. Type synthesis of 3T1R 4-dof parallel manipulators based on screw theory. *IEEE Transactions on Robotics and Automation*, 20(2), 181-190.
- Kong X., Gosselin C.M. 2006. Type synthesis of 4-dof SP-equivalent parallel manipulators: A virtual chain approach. *Mechanism and Machine Theory*, 41, 1306-1319.
- Kong X., Gosselin C.M. 2001. Generation of parallel manipulators with three translational degrees of freedom based on screw theory. *Proceedings of CCToMM Symposium on Mechanisms, Machines and Mechatronics, Montreal, Canada*
- Kong X., Gosselin C.M. 2007. *Type Synthesis of Parallel Mechanisms*, Springer
- Larochelle P. et.al. 1993. SPHINX: Software for synthesizing spherical 4R mechanisms. *Proceeding of NSFD and MSC, Univ.of North Carolina at Charlotte, NC*, 1, 607-611.
- Larochelle P.M. 2003. Approximate motion synthesis of open and closed chains via parametric constraint manifold fitting: preliminary results. *Proceedings of DETC'03, ASME, DETC-CIEC, Chicago, IL, USA*, 1-9.
- Lee W.T. et al. 2009. On adjustable spherical four-bar motion generation for expanded prescribed positions. *Mechanism and Machine Theory*, 44, 247-254.
- Lee C-C., Hervé J.M. 2009. Type synthesis of Schönflies motion generators. *Mechanism and Machine Theory*, 44(10), 1980-1997.

- Lee C-C., Hervé J.M. 2006. Translational parallel manipulators with doubly planar limbs. *Mechanism and Machine Theory*, 41(4), 433-455.
- Levitskii N. I. 1946. *Synthesis of Mechanisms by Chebyshev*, USSR Academy of Science.
- Meng J., Liu G.F., Li Z. 2005. A geometric theory for synthesis and analysis of sub-6 dof parallel manipulators. *Proceedings of the 2005 IEEE International Conference on Robotics and Automation, Barcelona, Spain*. 2938-2943.
- McCarthy J. M., Bodduluri R. M. 2000. Avoiding singular configurations in finite position synthesis of spherical 4R linkages. *Mechanism and Machine Theory*, 35. 451-462.
- Murray A.P., McCarthy J.M. 1995. A linkage map for spherical four position synthesis. *ASME Tech. Conf. Boston. MA*, 833-844.
- Ogawa N. et al. 2001. Construction of a three-dimensional large scale shaking table and development of core technology. *Phil. Trans. Royal Soc. London, Series A*, (359-1786), 1725-1751.
- Ottaviano E., Ceccarelli M. 2006. Application of a 3- DOF parallel manipulator for earthquake simulations. *IEEE Transactions on Mechatronics*, 11(2), 140-146.
- Ottaviano E., Grande S., Ceccarelli M. 2010. A biped walking mechanism for a Rickshaw robot. *Mechanics Based Design of Structures and Machines*, 38(2), 227-242.
- Rao A.V.M. et al. 1973. Closed form synthesis of spatial function generating mechanism for the maximum number of precision points. *J. Eng. Industry*, 95, 725-736.
- Ravani B., Roth B. 1983/ Motion synthesis using kinematic mappings. *ASME J. Trans. and Autom. in Design*, 105(1), 460-467.
- Refaat S. et al. 2006. Asymmetrical three-dofs rotational-translational parallel-kinematics mechanisms based on Lie group theory. *European Journal of Mechanics, A Solids*, 25(3). 550-558

- Rico J.M. et.al. 2006. A comprehensive theory of type synthesis of fully parallel platforms. *ASME Conf. Proc.*, 1067-1078
- Ruth D.A., McCarthy J.M. 1999. The design of spherical 4R linkages for four specified orientations. *Mechanism and Machine Theory*, 34. 677-692.
- Sancibrian R. et al. 2007. Optimal synthesis of function generating spherical and RSSR mechanisms. *12th IFToMM World Congress, Besançon France*,
- Schopp P. et al. 2009. Sensor fusion algorithm and calibration for a gyroscope free IMU. *Proc. Eurosensors XXIII Conference*, 1323-1326.
- Selvi O., Ceccarelli M. 2010. An experimental evaluation of earthquake effects on mechanism operation. *Proceedings of the International Symposium of Mechanism and Machine Science, AzCIFTToMM, Izmir, Turkey*, 408-416
- Shortreed J.S. et al. 2001. Characterization and testing of the Caltrans Seismic Response Modification Device Test System. *Phil. Trans. Royal Soc. London, Series A*, (359-1786), 1829-1850.
- Tse D.M., Laroche P.M. 2000. Approximating spatial locations with spherical orientations for spherical mechanism design. *ASME J. Mech. Design*, 122(4), 457-463.
- Wu T.M., Chen C.K. 1997. Closed form synthesis of planar and spatial linkages function generation with symbolic representation. *Mathematics and Computers in Simulation*, 44(2), 155-162.
- Zhao T.S., Dai J.S., Huang Z. 2002a. Geometric analysis of overconstrained parallel manipulators with three and four degrees of freedom. *JSME International Journal Series C*, 45(3), 730-740.
- Zhao T.S., Dai J.S., Huang Z. 2002b. Geometric synthesis of spatial parallel manipulators with fewer than six degrees of freedom. *Journal of Mechanical Engineering Science, Proc. IMechE*, 216(C12), 1175-1186.
- Zimmerman J. R. 1967. Four-precision synthesis of the spherical four-bar function generator. *Mechanism and Machine Theory*, 2, 133-139.

VITA

Personal Information

Surname, Name : SELVİ, Özgün
Nationality : Turkish (T.C.)
Date and Place of Birth : 20.03.1982, ÇANKIRI
E-mail : ozgonselvi@yahoo.com

Education

Degree	Institution	Year of Graduation
MS	Izmir Institute of Technology	2005
BS	Izmir Institute of Technology	2008

Work Experience

Year	Place	Enrollment
November 2005-Present	Izmir Institute of Technology	Research Assistant
2003	İzeltaş, Izmir	Trainee
2004	Çanakkale Seramik, Çanakkale	Trainee

Publications:

Journal Papers

- Alizade R., **Selvi O.**, Gezgin, E. 2010. *Structural design of parallel manipulators with general constraint one*. Mechanism and Machine Theory, 45, pp. 1-14,
- **Selvi O.**, Sevil H.E., Ozdemir S. (2007). *Synthesis of mechanisms with adjustable links using least squares optimization*. IFToMM Journal of Problem of Mechanics, 2(27), pp. 21-25.

Conference Papers

- Carbone G., Gómez-Bravo F., **Selvi O.** (2011). *An experimental validation of collision free trajectories for parallel manipulators*, 4th International Symposium on Multibody Systems And Mechatronics, Musme, Valencia, Spain ,pp. 239-257
- Alizade R., **Selvi O.**, Gezgin E. 2010. *Structural synthesis of multiloop manipulators with general constraint one*. Proc. of the Int. Symposium of Mechanism and Machine Science, AzCIFTtoMM 5-8 October, Izmir, Turkey, pp. 11-32
- **Selvi O.**, Ceccarelli M. 2010. *An experimental evaluation of earthquake effects on mechanism operation*. Proc. of the Int. Symposium of Mechanism and Machine Science, AzCIFTtoMM, 5-8 October, Izmir, Turkey, pp. 408-416.
- Dede M.I.C., **Selvi O.**, Bilginçan T., Kant Y. 2009. *Design of a haptic device for precision operations*. Systems, Man and Cybernetics, SMC. IEEE International Conference on, 11-14 Oct., San Antonio, TX, pp. 3623-3628.
- Bilginçan T. **Selvi O.**, Kant Y., Dede M.I.C. 2009. *Novel structural design of a robotic device for use in virtual reality simulators*. Proceeding of the National Machine Theory Symposium UMTS, Guzelyurt, Turkish Republic of Northern Cyprus, July 2-4, pp. 535-542.
- **Selvi O.**, Bilginçan T., Kant Y.; Dede M.I.C. 2009. *Novel structural design of a haptic device for medical applications*. Proceeding of the 14th National Biomedical Engineering Meeting, BIYOMUT 2009, Izmir, Turkey, May 20-22,
- Alizade R.I., Can F.C., Gezgin E., **Selvi O.** 2007. *Structural synthesis of new parallel and serial platform manipulators*, presented in 12th IFToMM World Congress, Besancon, France, June 18-21, (A-853).